## الجمهورية الجزائرية الديمقراطية الشعبية

République Algérienne Démocratique et Populaire Ministère de L'Enseignement Supérieur et de la Recherche Scientifique



## UNIVERSITÉ FERHAT ABBAS - SETIF1 FACULTÉ DE TECHNOLOGIE

## **THÈSE**

Présentée au Département de Génie Civil

Pour l'obtention du diplôme de

## **DOCTORAT 3<sup>ème</sup> Cycle LMD**

**Domaine: Sciences et Technologie** 

Filière: Génie Civil Option: Géotechnique

## Par BENREBOUH Imed

## **THÈME**

# Comportement des sols salés (sols sebkha) traités par un liant hydraulique

## Soutenue le 08/07/205 devant le Jury:

RIHEB Hadji	Professeur	Univ. Ferhat Abbas Sétif 1	President
MERDAS Abdelghani	Professeur	Univ. Ferhat Abbas Sétif 1	Directeur de thèse
<b>HAFHOUF Ilyas</b>	M.C.B.	Univ. Ferhat Abbas Sétif 1	Co-Directeur
<b>BENZAID Riad</b>	Professeur	Univ. Jijel	Examiner
BELKADI Ahmed Abderraouf	M.C.A	Univ. Bordj Bou Arreridj	Examiner
<b>BELEBCHOUCHE</b> Cherif	Professeur	Univ. Ferhat Abbas Sétif 1	Examiner
HEBBACHE Kamel	M.C.A	Univ. Ferhat Abbas Sétif 1	Invited

## الجمهورية الجزائرية الديمقراطية الشعبية

# Democratic Republic Of Algeria Ministry Of Higher Education and Scientific Research



# FERHAT ABBAS UNIVESITY – SETIF 1 FACULTY OF TECHNOLOGY

## **THESIS**

# Presented to the Department of Civil Engineering For the award of the degree of DOCTORATE 3<sup>rd</sup> Cycle LMD

**Program: Science and Technology** 

Field of Study: Civil Engineering Specialization: Geotechnics

## Presented by BENREBOUH Imed

## **TITLE**

# Behaviour of saline soils (sebkha soils) treated with a hydraulic binder

## Defended on 08/07/205 in front of the jury:

RIHEB Hadji	Professor	Univ. Ferhat Abbas Sétif 1	President
MERDAS Abdelghani	Professor	Univ. Ferhat Abbas Sétif 1	Supervisor
<b>HAFHOUF Ilyas</b>	M.C.B.	Univ. Ferhat Abbas Sétif 1	Co-Supervisor
BENZAID Riad	Professor	Univ. Jijel	Examiner
BELKADI Ahmed Abderraouf	M.C.A	Univ. Bordj Bou Arreridj	Examiner
BELEBCHOUCHE Cherif	Professor	Univ. Ferhat Abbas Sétif 1	Examiner
HEBBACHE Kamel	M.C.A	Univ. Ferhat Abbas Sétif 1	Invited

## **Contents**

Abstract	1
List of figures	5
List of tables	7
General introduction	8
Chapter 1. Literature review on saline soils (Sebkha soils).	
1.1. Introduction	12
1.2. Generality about saline soils	12
1.2.1. Definition of saline soil	12
1.2.2. Definition of salinization and salinity	12
1.2.3. Salinization, sodicity and alkalinity	13
1.2.5. Classification of saline soils	15
1.2.6. Water-soluble salts	16
1.3. Generality about Sebkha soils	17
1.3.1. Definition of Sebkha	17
1.3.2. Types of Sebkha	17
1.3.3. Distribution of Sebkha	20
1.3.4. Factors affecting Sebkha formation	22
1.3.5. Geotechnical characteristics of Sebkha	23
1.3.6. Problems bounded to Sebkha	25
1.4. Conclusion	26
Chapter 2. Literature review on the treatment of saline soils (Sebkha soils) wibinders.	ith hydraulic
2.1. Introduction	32
2.2. Cement and lime treatment	32
2.2.1. Soil stabilization.	32
2.2.2. Mechanisms of lime and cement treatment	33
2.2.3. Determination of optimum lime and cement content	35
2.3. Geotechnical properties of treated saline (Sebkha) soils	36
2.4. Physicochemical and mineralogical properties of treated saline (Sebkha) soils	39

0.41.37	
2.4.1. X-ray diffraction analysis	
2.4.2. Fourier transform infrared spectroscopy characterization	
2.4.3. Thermogravimetric-differential thermal analysis	
2.4.4. pH & Electrical Conductivity (dS/m)	
2.5. Salinity effect on the physic-chemical and geotechnical properties of treated saline (Sebkl	•
2.6. Conclusion.	49
Chapter 3. Salinity effects on the physicochemical and mechanical behaviour of and lime-treated saline soils (Sebkha soils).	untreated
3.1. Introduction	60
3.2. Materials and Methods	64
3.2.1. Materials	64
3.2.1.1. Study area	
3.2.1.2. Soil and lime characteristics.	
3.2.2. Methods	
3.2.2.1. Soil sampling and preparation	
3.2.2.2. Chemical, mineralogical and geotechnical tests	
3.2.2.3. Unconfined Compressive Strength test	
3.3. Results and Discussion	
3.3.1. Effect of salinity on carbonation content of untreated Sebkha soil	
3.3.2. Effect of salinity on the granulometry and mineralogy of the untreated Sebkha soil	
3.3.3. Effect of salinity on untreated Sebkha soil UCS	
3.3.4. Effect of salinity and curing time on carbonation content of Sebkha soil	
3.3.5. Effect of salinity and curing time on Sebkha soil UCS	
3.3.6. Effect of salinity on the mineralogy of cured soils	
3.4. Conclusions	85
Chapter 4. Effect of sulfate-resistance-cement treatment on saline soil (Sebkl subgrades.	na soil)
4.1. Introduction	9
4.2. Materials and methods	90

4.2.1. Materials	96
4.2.2. Methods	100
4.2.2.1. Samples preparation	100
4.2.2.2. Unconfined Compressive Strength test	101
4.2.2.3. Chemical and mineralogical tests	102
4.3. Results and discussion	103
4.3.1. UCS	103
4.3.1.1. Effect of curing time and SRC addition on stress-strain curves	103
4.3.2. Effect of curing time on the physic-chemical behavior	109
4.3.2.1. XRD of SRC-treated Sebkha at different curing conditions	109
4.3.2.2. TGA and FTIR of SRC-treated Sebkha at different curing conditions	111
4.3.2.3. pH value and Electrical Conductivity (mS/cm)	113
4.3.3. Application of Stabilized Sebkha Soil in Pavement Design	115
4.3.3.1. Design of Flexible Pavement	
3.3.2. Assessment of raw material and construction costs	117
4.4. Conclusion	119
General conclusion	127

#### ملخص

يعتبر التثبيت الكيميائي من خلال المعالجة بالأسمنت والجير تقنية شائعة لمعالجة الأتربة ذات أحمال ضعيفة. من بين هذه الأتربة ، تربة السبخة ، التي توجد عادةً في المناطق شبه الجافة والجافة ، تمثل تحديات هندسية كبيرة بسبب ضعف قوة تحملها وقابليتها العالية للانضغاط. تتكون هذه التربة بشكل أساسي من جزيئات دقيقة ، بما في ذلك رمل الكوارتز والطمي ، مع محتوى طيني بسيط ، متماسكة بشكل طبيعي بواسطة معادن الملح مثل الهاليت والجبس والكالسيت. في الطبيعة ، يؤدي تسرب المياه والفيضانات إلى انحلال و هجرة المعادن الملحية من تربة السبخة مما يقلل من ملوحتها ويضعف الروابط الإسمنتية بين الجسيمات. و هذا يؤدي إلى تدهور الخصائص الفيزيائية والميكانيكية للتربة. ولذلك ، فإن قياس تأثير الملوحة على الخواص الجيوتقنية لتربة السبخة غير المعالجة والمعالجة أمر مهم.

في هذه الدراسة، تم فحص تربة السبخة الواقعة بعين مليلة التي تتميز بملوحة عالية تبلغ ECe3=23.2 dS/m وتصنف كتربة كلوريد الكبريتات. خُصمص الجزء الأول من هذه الدراسة لدراسة تأثير المعالجة بالجير الحي على الخصائص الفيزيائية الكيميائية و الميكانيكية لسبخة عين مليلة بمستويات ملوحة مختلفة من ECe3= 23.2 dS/m، و ECe2= 8.3 dS/m، و ECe1= 2.32 dS/m. خُصص الجزء الثاني لدر اسة إمكانية تحسين السبخة عند الملوحة العالية باستخدام الأسمنت المقاوم للكبريتات (SRC). أجريت اختبارات قياس قوة الضغط غير المحصورة (UCS) والكربنة (CaCO<sub>3</sub>) وقياس التغيير الحجمي للحبيبات لتقييم الخصائص الفيزيائية والكيميائية والميكانيكية للتربة. بعد ذلك، تم إجراء فحوصات الأشعة السينية (XRD)، و تحويل فورييه للأشعة تحت الحمراء (FTIR)، و التحليل الحراري الوزني (TGA)، ودرجة الحموضة (pH) و الموصلية الكهربائية (ECe) لفهم تطور التفاعل الكيميائي بشكل أفضل وتفاعلاتها المحتملة مع معادن الملح القابلة للذوبان في الماء. أظهرت النتائج أن الملوحة أثرت بشكل كبير على خصائص التربة. قبل معالجة التربة ، أدى انخفاض الملوحة إلى زيادة قيمة UCS وترسيب CaCO3، بينما أدى في التربة المعالجة بالجير إلى زيادة UCS ولكن انخفض محتوى CaCO3. وفي حين لم يُظهر XRD أي تغيرات في طور المعادن، إلا أن TGA كشف عن تكوين مادة البورتلاندايت بكمية أقل في التربة ECe3 مقارنة بالتربة ECe1، مما يشير إلى أن التركيز العالى لأيونات -Cl و-SO4<sup>2</sup> من الأملاح الذائبة غطت الجسيمات الدقيقة وبالتالي أعاقت التفاعل البوزولاني في التربة ECe3، مما يشير إلى أن معالجة التربة ستكون أكثر فعالية في التربة منخفضة الملوحة. أثبتت المعالجة بـ SRC فعاليتها العالية، حيث أظهرت زيادة في القوة بمقدار 11.56 مرة عند 14يوم من المعالجة مع نسبة 8% من محتواها بسبب تكوين أملاح فريدل و سيليكات الكالسيوم رطبة (CSH) . على الرغم من الانخفاض الطفيف في القوة عند 28 يوم من المعالجة، حققت المعالجة بـ SRC انخفاضًا بنسبة 30% في سُمك طبقة الأساس وانخفاض تكاليف المواد بمقدار 5.7 مرة، مما يثبت قابليتها للتطبيق العملي.

الكلمات المفتاحية: تربة السبخة؛ تربة كلوريد الكبريتات؛ الملوحة؛ قوة الانضغاط غير المحصورة؛ الخواص الفيزيائية الكيميائية؛ إضافة الجير والأسمنت

#### **Abstract**

Chemical stabilization through cement and lime treatment is a common technique for improving weak soils. Among these, Sebkha soil, usually found in arid and semi-arid regions, presents significant engineering challenges due to its low bearing capacity and high compressibility. This soil consists mainly of fine particles, including quartz sand and silt, with minor clay content, naturally cemented by salt minerals such as halite, gypsum, and calcite. In nature, water infiltration and flooding cause the dissolution and migration of salt minerals in Sebkha soil, reducing its salinity and weakening the cementing bonds between particles. This deteriorates the soil's physical and mechanical properties. Therefore, quantifying the salinity effect on the geotechnical properties of untreated and treated Sebkha soil is of interest.

In this study, Ain M'lila Sebkha soil, characterized by high salinity of ECe3=23.2 dS/m and classified as chloride-sulfate soil, was investigated. The first part of this study was devoted to investigating the quick lime treatment effect of the physicochemical and mechanical properties of Sebkha with different salinity levels of ECe3= 23.2 dS/m, ECe2=8.3 dS/m, and ECe1= 2.32 dS/m. The second part was devoted to studying the potential stabilization of Sebkha at high salinity with sulfate-resistance cement (SRC). UCS, carbonation, and granulometry tests were carried out to assess the soil's physico-chemical and mechanical properties. Subsequently, XRD, FTIR, TGA, pH, and EC measurement tests were performed to understand better chemical reaction development and their potential interactions with water-soluble salt minerals. Results showed that salinity significantly affected soil's properties. In untreated soil, decreasing salinity led to increased UCS and CaCO<sub>3</sub> precipitation, while in lime-treated soil, it increased UCS but decreased CaCO<sub>3</sub> content. While XRD showed no minerals phase variations, TGA revealed portlandite formation with a lower quantity in ECe3 soil compared to ECe1 soil, which indicates that high concentration of Cl<sup>-</sup> and SO<sub>4</sub><sup>2-</sup> ions from dissolved salts coated finer particles and thus hindered the pozzolanic reaction in ECe3 soil, suggesting that soil treatment would be more effective in low saline soil, SRC treatment proved highly effective, showing an 11.56-fold strength increase at 14d curing with 8% content due to CSH and Friedel's salt formation. Despite minor strength reduction at 28d curing, SRC stabilization achieved a 30% reduction in pavement thickness and 5.7 times lower material costs, establishing its viability for practical applications.

**Keywords:** Sebkha soil; Chloride-sulfate soil; Salinity; Unconfined compressive strength; Physicochemical properties; Lime and cement addition

## Résumé

La stabilization chimique par le traitement au ciment et à la chaux est une technique largement utilisée pour améliorer les sols faibles. Parmi ceux-ci, le sol de Sebkha, que l'on trouve généralement dans les régions arides et semi-arides, présente des difficultés techniques importantes en raison de sa faible capacité portante et de sa grande compressibilité. Ce sol se compose principalement de particules fines, notamment de sable quartzeux et de limon, avec une teneur faible en argile, naturellement cimentées par des sels tels que l'halite, le gypse et la calcite. Dans la nature, l'infiltration de l'eau et les inondations provoquent la dissolution et la migration des sels minéraux dans le sol de Sebkha, ce qui diminue sa teneur en sel et fragilise les liens de cimentation entre les particules. Les propriétés physiques et mécaniques du sol sont donc détériorées. Par conséquent, il est important de quantifier l'effet de la salinité sur les propriétés géotechniques du sol de la Sebkha, traité ou non traité.

Dans cette étude, le sol Sebkha d'Ain M'lila, caractérisé par une salinité élevée ECe3=23,2 dS/m et classé comme sol chlorure-sulfate, a été étudié. La première partie de cette étude a été consacrée à l'étude de l'effet du traitement à la chaux vive sur les propriétés physicochimiques et mécaniques de la Sebkha avec différents niveaux de salinité ECe3= 23.2 dS/m, ECe2=8.3 dS/m, et ECe1= 2.32 dS/m. La deuxième partie a été consacrée à l'étude de la stabilisation potentielle de la Sebkha à une salinité élevée avec du ciment résistant au sulfate (SRC). Des essais UCS, de carbonatation et de granulométrie ont été réalisés pour évaluer les propriétés physico-chimiques et mécaniques du sol. Ensuite, des tests de XRD, FTIR, TGA, pH et EC ont été effectués pour mieux comprendre le développement des réactions chimiques et leurs interactions potentielles avec les minéraux salins solubles dans l'eau. Les résultats ont montré que la salinité affecte de manière significative les propriétés du sol. Dans le sol non traité, la diminution de la salinité a conduit à une augmentation de l'UCS et de la teneur de CaCO3 précipitée, tandis que dans le sol traité à la chaux vive, l'UCS augmente mais la teneur de CaCO3 diminue. Tandis que la XRD n'a montré aucune variation de phase minérale, la TGA a révélé la formation de portlandite avec une quantité plus faible dans le sol ECe3 par rapport au sol ECe1, ce qui indique que la concentration élevée d'ions Cl<sup>-</sup> et SO<sub>4</sub><sup>2-</sup> provenant des sels dissous a enrobé les particules plus fines et a donc empêché la réaction pouzzolanique dans le sol ECe3, ce qui indique que le traitement du sol serait plus efficace dans un sol faiblement salé. Le traitement à base de SRC a montré une grande efficacité, montrant une augmentation de la résistance de 11,56 fois à une teneur de 8 % en raison de la formation de CSH et de sels de Friedel. Même si la résistance a légèrement diminué après 28 jours de durcissement, la stabilisation du SRC a permis de réduire de 30 % l'épaisseur de la chaussée et de diminuer de 5,7 fois le coût des matériaux, établissant ainsi sa faisabilité pour des applications pratiques.

**Mots-clés** : Sol Sebkha ; Sol chlorure-sulfate ; Salinité ; Résistance à la compression non confinée ; Propriétés physico-chimiques ; Ajout de chaux et de ciment

## List of figures

## Chapter 1. Literature review on saline soils (Sebkha soils).

Fig 1-1. Global distribution of salt-affected soils (1980-2018): (a) Surface salinity potential, (b)
Continental distribution, (c-d) Latitudinal and longitudinal distribution at 1km resolution (excluding frigingly)
zones (Hassani et al., 2020).
Fig 1-2. Solubility degrees of soils' main minerals/salts (Lide, 2004)
Fig 1-3. Typical profile type of coastal Sebkha
Fig 1-4. Hydrological and geological map of the largest Sebkha in Oran, Algeria (Benkesmia et al.,
2023)
Fig 1-5. Typical profile type of continental Sebkha
Fig 1-6. Continental Ain M'lila Sebkha (Ez Zemoul Sebkha), Oum El Bouaghi, Algeria (Benrebouh et al.
2025)
Fig 1-7. Active and potential locations of Sebkha/wetlands: (a) in Earht's lands and (b) in North-Eastern
of Algeria (Bougoffa et al., 2023).
Fig 1-8. Mechanism of salt precipitations: (a) by evaporation and saturated concentration and (b) types of
salts precipitation via evaporation
Suits proofpitation via ovaporation
Chapter 2. Literature review on the treatment of saline soils (Sebkha soils) with hydraulic
binders.
biliters.
Fig 2-1. Variations of USC, plastic limit and pH with lime content (Ciancio et al., 2014)
Fig 2-2. XRD patterns of the soil specimens: (a) after 28-day curing (b) and after 90-day soaking4
Fig 2-3. Thermogravimetric analysis of untreated and lime treated smectite (Sm) soil
Fig 2-4. Relationship between: (a) EC of modified soil and curing period and (b) UCS of modified soil
and curing period
Fig 2-5. Effects of gypsum and lime contents on the pH of treated soil for different cured period (Aldaood
et al., 2021).
Fig 2-6. Effects of gypsum and lime contents on the EC of treated soil for different cured period (Aldaoo
et al., 2021)
Ct al., 2021)
Chapter 3. Salinity effects on the physicochemical and mechanical behavior of untreated
- ·
and lime-treated saline soils (Sebkha soils).
Fig 3-1. Ain M'illa Sebkha soil location.
· ·
Fig 3-2. Ain M'lila Sebkha soil: (a) white layer on Sebkha's surface; (b) sky survey state; (c) Sebkha
profile; (d) mineralogy of soluble salts
Fig 3-3. Chemical composition by XRF (a) and mineralogical composition by XRD (b) of Sebkha soil
ECe3
Fig 3-4. Samples preparation: (a) soil crystals and aggregates; (b) washing process
Fig 3-5. Lime and salinity impact on the pH of solution
Fig 3-6. Dietrich-Frühling calcimeter.
Fig 3-7. CaCO <sub>3</sub> content of ECe1, ECe2, and ECe3 soil by calcimeter
Fig 3-8. Grain distribution curves of ECe1, ECe2, and ECe3 soils (a), mineralogic composition of ECe1
and ECe3 soils by XRD (b), chemical composition of ECe1 and ECe3 soils by XRF (c)75

Fig 3-9. Stress-strain curves of ECe1, ECe2, and ECe3 soils (a), UCS at different salinity levels (b	). 76
Fig 3-10. Damage caused on Sebkha surface by track's wheels.	78
Fig 3-11. CaCO3 content of untreated and ECe1, ECe2, and ECe3-treated soil by calcimeter	79
Fig 3-12. Salinity effects on the stress-strain curves of untreated and lime treated soils at different	curing
periods (0 d, 3 d, 7 d, 14 d, and 28 d): (a) ECe1 soil, (b) ECe2 soil and (c) ECe3 soil	80
Fig 3-13. Mineralogy composition by XRD of untreated and treated soil samples: (a) ECe3 soil an	
ECel soil.	82
Fig 3-14. Loss of mass by TGA of untreated ECe3 and ECe1 soils (a), dehydration of gypsum (b),	
decomposition of calcite (c) and melting of halite (d).	83
Fig 3-15. Loss of mass by TGA of untreated and treated ECe3 (a) and ECe1 (b) soils and dehydrat	ion of
portlandite (c)	84
Chapter 4. Effect of sulfate-resistance-cement treatment on saline soil (Sebkha soil)	
•	
subgrades.	
Fig 4-1. Sebkha soil study area location.	
Fig 4-1. Sebkha soil study area location.  Fig 4-2. Sebkha profile (a), mineralogical phases of salt crystals within the sebkha profile (b), and	
Fig 4-1. Sebkha soil study area location	97
Fig 4-1. Sebkha soil study area location.  Fig 4-2. Sebkha profile (a), mineralogical phases of salt crystals within the sebkha profile (b), and theoretical diagram of salt precipitation during seawater evaporation (c).  Fig 4-3. TGA curve of pure sebkha soil.	97 99
Fig 4-1. Sebkha soil study area location.  Fig 4-2. Sebkha profile (a), mineralogical phases of salt crystals within the sebkha profile (b), and theoretical diagram of salt precipitation during seawater evaporation (c).  Fig 4-3. TGA curve of pure sebkha soil.  Fig 4-4. The Glimpses of Soil Sample Preparation.	97 99
Fig 4-1. Sebkha soil study area location.  Fig 4-2. Sebkha profile (a), mineralogical phases of salt crystals within the sebkha profile (b), and theoretical diagram of salt precipitation during seawater evaporation (c).  Fig 4-3. TGA curve of pure sebkha soil.	97 99
Fig 4-1. Sebkha soil study area location.  Fig 4-2. Sebkha profile (a), mineralogical phases of salt crystals within the sebkha profile (b), and theoretical diagram of salt precipitation during seawater evaporation (c).  Fig 4-3. TGA curve of pure sebkha soil.  Fig 4-4. The Glimpses of Soil Sample Preparation.	97 99 102
Fig 4-1. Sebkha soil study area location.  Fig 4-2. Sebkha profile (a), mineralogical phases of salt crystals within the sebkha profile (b), and theoretical diagram of salt precipitation during seawater evaporation (c).  Fig 4-3. TGA curve of pure sebkha soil.  Fig 4-4. The Glimpses of Soil Sample Preparation.  Fig 4-5. Glimpses of Strength and Microstructure Experimentations.	97 99 102 103
Fig 4-1. Sebkha soil study area location.  Fig 4-2. Sebkha profile (a), mineralogical phases of salt crystals within the sebkha profile (b), and theoretical diagram of salt precipitation during seawater evaporation (c).  Fig 4-3. TGA curve of pure sebkha soil.  Fig 4-4. The Glimpses of Soil Sample Preparation.  Fig 4-5. Glimpses of Strength and Microstructure Experimentations.  Fig 4-6. Stress-strain curves of treated sebkha soil: 2% SRC (a), 5% SRC (b), and 8% SRC (c)	9799102103105 % SRC-
Fig 4-1. Sebkha soil study area location.  Fig 4-2. Sebkha profile (a), mineralogical phases of salt crystals within the sebkha profile (b), and theoretical diagram of salt precipitation during seawater evaporation (c).  Fig 4-3. TGA curve of pure sebkha soil.  Fig 4-4. The Glimpses of Soil Sample Preparation.  Fig 4-5. Glimpses of Strength and Microstructure Experimentations.  Fig 4-6. Stress-strain curves of treated sebkha soil: 2% SRC (a), 5% SRC (b), and 8% SRC (c)  Fig 4-7. Failure patterns of sebkha soil: untreated soil before (a) and after peak strength (b), and 8%	9799102103105 % SRC107
Fig 4-1. Sebkha soil study area location.  Fig 4-2. Sebkha profile (a), mineralogical phases of salt crystals within the sebkha profile (b), and theoretical diagram of salt precipitation during seawater evaporation (c).  Fig 4-3. TGA curve of pure sebkha soil.  Fig 4-4. The Glimpses of Soil Sample Preparation.  Fig 4-5. Glimpses of Strength and Microstructure Experimentations.  Fig 4-6. Stress-strain curves of treated sebkha soil: 2% SRC (a), 5% SRC (b), and 8% SRC (c)  Fig 4-7. Failure patterns of sebkha soil: untreated soil before (a) and after peak strength (b), and 8% treated soil before (c) and after peak strength (d).	97102103105 % SRC107
Fig 4-1. Sebkha soil study area location.  Fig 4-2. Sebkha profile (a), mineralogical phases of salt crystals within the sebkha profile (b), and theoretical diagram of salt precipitation during seawater evaporation (c).  Fig 4-3. TGA curve of pure sebkha soil.  Fig 4-4. The Glimpses of Soil Sample Preparation.  Fig 4-5. Glimpses of Strength and Microstructure Experimentations.  Fig 4-6. Stress-strain curves of treated sebkha soil: 2% SRC (a), 5% SRC (b), and 8% SRC (c)  Fig 4-7. Failure patterns of sebkha soil: untreated soil before (a) and after peak strength (b), and 8% treated soil before (c) and after peak strength (d).  Fig 4-8. UCS histograms of treated Sebkha soil.  Fig 4-9. XRD diagrams of untreated and treated Sebkha soil.  Fig 4-10. TGA curves of untreated and treated Sebkha soil.	97102103105 % SRC107108110
Fig 4-1. Sebkha soil study area location.  Fig 4-2. Sebkha profile (a), mineralogical phases of salt crystals within the sebkha profile (b), and theoretical diagram of salt precipitation during seawater evaporation (c).  Fig 4-3. TGA curve of pure sebkha soil.  Fig 4-4. The Glimpses of Soil Sample Preparation.  Fig 4-5. Glimpses of Strength and Microstructure Experimentations.  Fig 4-6. Stress-strain curves of treated sebkha soil: 2% SRC (a), 5% SRC (b), and 8% SRC (c)  Fig 4-7. Failure patterns of sebkha soil: untreated soil before (a) and after peak strength (b), and 8% treated soil before (c) and after peak strength (d).  Fig 4-8. UCS histograms of treated Sebkha soil.  Fig 4-9. XRD diagrams of untreated and treated Sebkha soil.  Fig 4-10. TGA curves of untreated and treated Sebkha soil.	97102103105 % SRC107108110
Fig 4-1. Sebkha soil study area location.  Fig 4-2. Sebkha profile (a), mineralogical phases of salt crystals within the sebkha profile (b), and theoretical diagram of salt precipitation during seawater evaporation (c).  Fig 4-3. TGA curve of pure sebkha soil.  Fig 4-4. The Glimpses of Soil Sample Preparation.  Fig 4-5. Glimpses of Strength and Microstructure Experimentations.  Fig 4-6. Stress-strain curves of treated sebkha soil: 2% SRC (a), 5% SRC (b), and 8% SRC (c)  Fig 4-7. Failure patterns of sebkha soil: untreated soil before (a) and after peak strength (b), and 8% treated soil before (c) and after peak strength (d).  Fig 4-8. UCS histograms of treated Sebkha soil.  Fig 4-9. XRD diagrams of untreated and treated Sebkha soil.	9799102103105 % SRC107108110112

## List of tables

Chapter 1. Literature review on saline soils (Sebkha soils).	
Table 1-1. Soil classification based on the ECe values (Richards, 1954).	
Table 1-2. Saline soil categories based on ECe, SAR and pH (Rengasamy, 2016)	
Chapter 2. Literature review on the treatment of saline soils (Sebkha soils) with hydr binders.	aulic
Chapter 3. Salinity effects of the physicochemical and mechanical behavior of untrea and lime-treated saline soils (Sebkha soils).	ted
Table 3-1. Geotechnical characteristics of Sebkha soil.	
Table 3-2. The chemical compositions obtained based on the saturated soil past extract: salinity, saccentration, pH and soluble salt content.	
Table 3-3. Chemical composition of lime.	
Chapter 4. Effect of sulfate-resistance-cement treatment on saline soil (Sebkha soil) subgrades.	
Table 4-1. The chemical compositions obtained based on the saturated soil paste extract	
Table 4-3. The chemical compositions and mineralogical phases of CEM I 42.5N SR3.	
Table 4-4. Compaction characteristics of SRC treated sebkha soil	
Table 4-5. Traffic class (TPLi) for the principal network (RP1) and subgrade bearing capacity clas	` /
Table 4-6. Material thickness of capping layer for low subgrade bearing (i.e., S4 and S3)	
Table 4-7. Pavement structure design as per the Algerian catalog	11′
Table 4-8. Raw materials and constructions costs.	118

## **General introduction**

Sustainability of nations economic highly depends on the durability and stability of their engineering infrastructures. In this regard, the development of Algeria's road networks that present the main transport lines encounters significant geotechnical challenges, particularly in semi-arid and arid regions with saline soils, which are known as Sebkha soils. Recently, in Algeria, many projects have been severed from Sebkha soil degradation, such as a construction project of a road embankment crosses a section of about 11 km on the Sebkha of Chott El Hodna, Algeria, posed significant challenges during the investigation of the subsurface soil and the construction of the first embankment layers (Benmebarek et al., 2015). Furthermore, the foundation layer of the Es-Senia Oran airport near the extensive Sebkha of Oran in western Algeria has been affected by natural cavities formed by water containing carbon dioxide, posing a long-term risk of collapse (Chikhaoui et al., 2015). A study focusing on the national road RN03 has found various types of road damage on pavement surface between the regions of Batna and Ain M'lila, especially near Sebkha (Hafhouf et al., 2022; Hafhouf and Abbeche, 2023). Moreover, the government has recently initiated a project to link the RN100 to the Batna-Chelghoum Laid highway via a 45 km, 2x2 lane road. This highway intersects the RN03 near the Sebkha of Ain M'lila. Consequently, building on or near these problematic soils can cause unexpected changes in the structure over time, affecting both short-term and long-term development in semi-arid areas. Therefore, Sebkha soil was chosen for this study not only because it presents unique challenges in foundation design with significant economic impact, but also because it is commonly found in Algeria.

Sebkha soil is a complicated system that occurs due to the interaction of one or more of the following factors: climatic, biological, hydrological, geochemical and geomorphological. This soil consists generally of quartz sand and silt, with small amounts of mud and clay, naturally cemented by salt minerals and has a hard, crusty surface (Al-Amoudi, 2002). Sebkha soil formed as the precipitation of salt minerals in its profile where two types of precipitated salts can be identified: salt precipitation above ground water level by evaporation and salt precipitation within groundwater level by an increase in salt concentration beyond its saturation point (Al-Amoudi, 2002, 1995). Sebkha soil is a heterogeneous material that usually consists of a combination of cemented and uncemented layers, as well as pieces of quartz and/or carbonate sand. In the cemented layers, the main cementing materials are halite (NaCl), anhydrite (CaSO<sub>4</sub>), gypsum

(CaSO<sub>4.2</sub>H<sub>2</sub>O), aragonite and calcite (CaCO<sub>3</sub>) (Abduljauwad and Al-Amoudi, 1995a; Al-Amoudi, 2002; Al-Homidy et al., 2017; Mohamedzein and Al-Rawas, 2011; Nasr, 2015). Sebkha is a weak soil associated with many geotechnical problems, such as low natural strength, high salinity, and high compressibility (Abduljauwad and Al-Amoudi, 1995b; Babar et al., 2023; Elsawy and Lakhouit, 2023; Hafhouf, 2022; Hamid and Alnuaim, 2023). Moreover, Sebkha is considered collapsible soil, and its use as a foundation under structures can result in unpredictable problems (Elsawy and Lakhouit, 2023; Hafhouf, 2022). Indeed, with water flow movement in soil profile such as precipitation or flooding actions, some natural cementing materials (i.e., salt minerals) dissolved rapidly in water, breaking down cohesion and bonding between soil particles, resulting in high volume reduction and thus strength failure. This negative effect of water-soluble salts on the strength of soil is salts type and salt content-dependent (Garakani et al., 2018; Li and Yang, 2024; Li et al., 2016; Shen et al., 2024; Xing et al., 2009). Several researchers have investigated the physical and mechanical properties of saline soils with different salinity levels (Hafhouf et al., 2022; Li and Yang, 2024; Li et al., 2016; Liu and Zhang, 2014; Shen et al., 2024), with controversial results were founded. On the one hand, Hafhouf et al. (2022) found that Sebkha strength was highly affected by salt contents under the effect of drying-wetting (D-W) cycles. When D-W increases salinity, the unconfined compressive strength (UCS) of compacted Sebkha samples decreases. This was confirmed by Liu and Zhang (2014), where it was found that an increase in salt contents provides higher cementation of soil particles, and thus, higher saline soil's UCS were obtained. On the other hand, Li and Yang (2024) showed that an increase in NaCl content led to the formation of more particle agglomerates in the soil. However, an excess of salt content changed the soil structure and reduced its resistance. Shen et al. (2024) demonstrated that increased NaHCO<sub>3</sub> content led to higher liquidity and plasticity limits but reduced mechanical properties. This adverse impact was also supported by Nu et al. (2020), who found that higher salinity in soft soil resulted in lower shear strength and increased liquid limit. Zhang et al. (2020) also showed that higher salinity decreased resistance. Therefore, the salt amounts and salt types are highly affected by the physical and mechanical characteristics such as granulometry and UCS; however, this effect is not well understood, and studies on the effect of salinity on Sebkha soil behavior are scarce.

Given the poor geotechnical properties of Sebkha soils, other researchers have tried to improve these soils using different modification/stabilization techniques, such as physical stabilization (e.g., geotextile) (Abduljauwad et al., 1994; Aiban et al., 2006, 1998), mechanical stabilization (e.g., vibroflotation, dynamic compaction and stone columns) (Al-Shamrani and Dhowian, 1997; **Dhowian**, 2017), and chemical stabilization (e.g., cement kiln dust [CKD], ordinary Portland cement [OPC], and lime) (Al-Amoudi, 2002, 1994; Al-Homidy et al., 2017; Elsawy and Lakhouit, 2023). However, the latter method provides high strength, easy application and costeffective (Moayed et al., 2012; Pei and Shouxi, 2011). Chemical stabilization of Sebkha soils has been used by several researchers during the last 30 years (Elsawy and Lakhouit, 2023). However, although Sebkha soils exhibited alternation in their salt minerals contents under water effects, in literature, less attention had been paid to the salinity effects on the physicochemical and mechanical behavior of modified Sebkha soils. Moreover, each Sebkha presents a unique salinity system, including varying salt types and concentrations. Therefore, it is of interest to investigate salinity effects on the physical and mechanical behavior of untreated and treated Sebkha soils to ensure the stability, serviceability and durability of infrastructures constructed near those areas. In this study, it was focused on the effect of salinity on the strength of untreated and lime-treated Ain M'lila Sebkha, considering their physicochemical properties. For this purpose, based on the electrical conductivity measurement (ECe), three soil salinity levels (ECe3=23.2 dS/m, ECe2=8.3 dS/m and ECe1= 2.32 dS/m) were chosen, and the optimum lime content for each one was determined based on pH method (Eades and Grim, 1966), and samples were cured for different curing periods (i.e., 3d, 7d, 14d and 28d). This study involves physical tests using granulometric analysis, mechanical tests including UCS, chemical tests via calcimeter and X-ray fluorescence (XRF), and mineralogical tests including X-ray diffraction (XRD) and thermos-gravimetric analysis (TGA). In addition, the potential stabilization of Ain M'lila Sebkha using sulfateresistance-cement (SRC) to be used as a flexible pavement subgrade was investigated. Where after sampling and preparing the soil, UCS tests were conducted to assess the soil's strength for different curing periods (3d, 7d, 14d and 28d) and distinct SRC contents (i.e., 2%, 5% and 8% by dry mass). Subsequently, XRD, Fourier transform infrared spectroscopy (FTIR), TGA, pH and EC measurement tests were conducted.

The thesis is divided into four chapters.

The first chapter is a review of the literature on saline soils and Sebkha soils. In the first part, this chapter presents saline soils definition with difference between salinity, sodicity and alkalinity, followed by their classifications and techniques to measure the salinity. In the second part, Sebkha

soils definition, describing their types, distributions, and influencing factors. After that, the main geotechnical properties of Sebkha and their problems associated with the presence of soluble salt minerals are discussed.

The second chapter is devoted to a bibliographical study of saline soils and Sebkha soils treated with hydraulic binders, where the mechanism of lime and cement treatment are first presented. After this, a literature review of the geotechnical, physicochemical and mineralogical of treated saline soils and Sebkha soils is discussed. Lastly, a comprehensive review of the salinity effects on the salinity effect on the chemical, mineralogical, and mechanical behavior of saline soils and Sebkha soils is presented.

The third chapter presents salinity effects on the physicochemical and mechanical behavior of untreated and lime-treated Sebkha soils where literature review is first presented and then soil sampling, soil and lime characterization and samples preparation are described, followed by chemical, mineralogical and geotechnical tests. Finally, the part of results is discussed.

The fourth chapter is devoted to studying the potential stabilization of Sebkha soils with SRC addition, in which, firstly, a literature review is presented, followed by soil sampling, soil and SRC characterization and sample preparation. After that, UCS, chemical and mineralogical tests are conducted, and their results are discussed. Finally, a comparative analysis of untreated and treated Sebkha subgrades using a local Algerian flexible pavement design framework is discussed.

# CHAPTER 1. LITERATURE REVIEW ON SALINE SOILS (SEBKHA SOILS)

## 1.1. Introduction

Salt-affected areas represent a global concern, particularly in Algeria, where salt-rich soils known as Sebkha are prevalent. This chapter examines saline and Sebkha soils in detail.

Section 1.2 discusses the causes of salinization and the differences between salinity, sodicity, and alkalinity. After that, the classification of saline soils is presented using different chemical techniques to measure salinity degree and identify salinity type. Section 1.3 focuses on Sebkha soils, detailing their types, distributions, and influencing factors. After that, the main geotechnical properties of Sebkha and their problems associated with the presence of soluble salt minerals are discussed. Understanding these aspects is essential for addressing issues related to salt-affected areas and promoting sustainable infrastructures constructed on these saline lands.

## 1.2. Generality about saline soils

## 1.2.1. Definition of saline soil

Saline soil is a kind of soil that contains a significant amount of water-soluble salt, with a minimum salt content of 0.3% by mass (Nan et al., 2022) and solubility higher than gypsum (HAFHOUF, 2022).

## 1.2.2. Definition of salinization and salinity

The process of water-soluble salt accumulation in the upper soil surface is denoted by soil salinization. This latter adversely affects crop production and soil structure (Shokri et al., 2024). On the other hand, soil salinity is the quantity of total salt dissolved in soil pore water and is usually measured in grams of salt per kilogram (g/kg) or liter of water (g/L). Besides, the electrical conductivity (EC) technique is one of the most rapid and reliable measurements of soil salinity (Laboratory (US), 1954; Shokri et al., 2024). This method measures the salt concentration based on the saturated soil paste extract in mmhos/cm (mS/cm) at 25 °C, referred to by ECe (Laboratory (US), 1954). ECe can be converted into total soluble salt concertation or salt quantity through the following equation:

$$mS/cm = dS/m = 640 \,mg/l \tag{1}$$

Table 1-1 gives saline soil classification considering their salinity levels (Richards, 1954).

Table 1-1. Soil classification based on the ECe values (Richards, 1954).

ECe (dS/m)	Soil classification
ECe <4	non-saline
$4 \le ECe < 8$	moderately saline
$8 \le ECe \le 16$	strongly saline
ECe > 16	very strongly saline

## 1.2.3. Salinization, sodicity and alkalinity

Salinization—Salinization is a critical issue affecting around 1 billion hectares of land globally, or nearly 7% of Earth's surface (Khan and Weber, 2006; Metternicht and Zinck, 2003), which is more than four times the size of Algeria. Currently, about 20% of croplands are salinized, and projections indicate this could rise to 50% by 2050, threatening global food production (Nachshon, 2018). Two main factors generally drive soil salinization: they are either natural (primary salinization) or man-made (secondary salinization) (DING et al., 2011).

Primary salinization— In field conditions, the interaction of one or all climatic, geologic, and hydrogeologic factors generally determines salt-affected area distribution. In inland regions, weathering of hard and crystalline rocks induced the breaking down of their main minerals that contained. Where water dissolved ions such as magnesium, calcium, sodium, and potassium are formed by weathering. After which, surface and subsurface water flow strongly affected their movement within the soil fabric. Finally, with time, these redistributed/movable salts interact with other materials, forming unconsolidated sedimentary deposits (e.g., clay and silt) and sedimentary rocks (e.g., limestone) (Zinck and Metternicht, 2009). On the other hand, in coastal areas, the movement of seawater has generally influenced soil salinization through the high potential for saltwater intrusion and the flooding of shallow areas (HAFHOUF, 2022).

Secondary salinization— Soil salinization by humans involved two practices: (i) Industrial material waste such as salt added to road surfaces in order to lower the freezing point of water and oil extraction and (ii) nonsustainable agricultural processes such as flooding over drip irrigation, brackish water and much water that cause the water table to rise (Shokri et al., 2024).

To this end, secondary and primary salinization interact with each other. The former is intensified by later ones that act faster and, sometimes, denser. Fig 1-1 presents the global distribution of saline soils, apart from the frigid zones (Hassani et al., 2020). Africa is classified as the second most salt-affected continental region, with the highest contribution of Algerian lands.

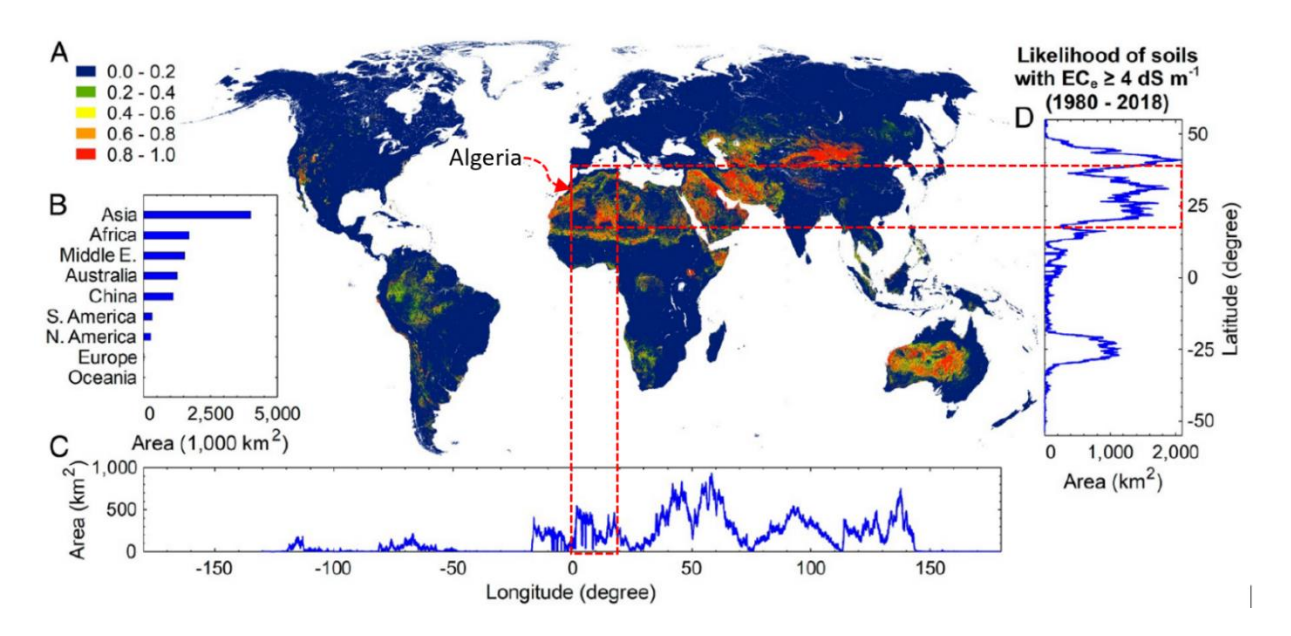


Fig 1-1. Global distribution of salt-affected soils (1980-2018): (a) Surface salinity potential, (b) Continental distribution, (c-d) Latitudinal and longitudinal distribution at 1km resolution (excluding frigid zones (Hassani et al., 2020).

Sodicity—Soil sodicity is a type of saline soil associated with higher sodium (Na<sup>+</sup>) ions than other cations. When the leaching process takes place in the soil, certain Na<sup>+</sup> ions remain connected to clay particles and shift to other cations. As soon as the quantity of these ions achieves a certain level that affects structural soil properties, it is viewed as sodic soil. Sodicity adversely affects soil characteristics by lowering the bond between soil particles. Specifically, Na<sup>+</sup> ions bonded to clay particles by electrostatic forces (i.e., Coulomb force). This increases the repulsive forces of soil particles as these monovalent ions (i.e., Na<sup>+</sup>) have a higher hydration ratio than bivalent ones (e.g., Mg<sup>2+</sup> and Ca<sup>2+</sup>), inducing dispersion. While sodicity increases the hazard of wind and water erosion (De La Paix et al., 2013), it also degrades soil infiltration (Wong et al., 2010). The following equation gives the proportion of cation exchange sites occupied by sodium (i.e., sodicity):

$$ESP = \left(\frac{Na^{+}}{CEC}\right) * 100 \tag{2}$$

Where ESP: exchangeable sodium percentage, CEC: cation exchange capacity

Akalinity—On the other hand, soil alkalinity is another form of soil salinity characterized by high pH levels. When the pH level reaches 8, it is considered "alkaline" soil (Sposito, 2008). The pH rises due to higher HCO<sub>3</sub>- and CO<sub>3</sub><sup>2</sup>- ions concentrations compared to Mg<sup>2+</sup> and Ca<sup>2+</sup>ones (Rengasamy et al., 2022). A good example of this to confirm this is that the pH in calcareous (calcite) soil is between 8 and 8.5, and it remains around this value regardless of the amount of calcite (CaCO<sub>3</sub>) being added. However, Na<sup>+</sup> is abundant in soil solution, and with increasing salinity, protons released by NaCl dissolution react with calcite, forming HCO<sub>3</sub>- and CO<sub>3</sub><sup>2</sup>- that increase pH. It should be noted that a high concentration of Na<sup>+</sup> (i.e., high ESP) did not increase environment alkalinity, which is confirmed by Jobbagy Gampel et al (2017), who suggest that although seawater contains high NaCl and low CaCO<sub>3</sub>, it is classified as saline soils and not as alkaline-sodic soils. From this point of view, alkalinity is caused by high concentrations of HCO<sub>3</sub>- and CO<sub>3</sub><sup>2</sup>- ions, while high concentrations of Na<sup>+</sup> ones cause sodicity.

#### 1.2.5. Classification of saline soils

Several soil classification systems have been proposed, such as the Brazilian Soil Classification System (Ribeiro et al., 2010), WRB (World Reference Base for Soil Resources; (Group, 2014)), and the US Salinity Laboratory (Richards, 1954). However, a more detailed and recent classification has been proposed by Rengasamy (2016). Twelve (12) categories of salt-affected soils are presented (Table 1-2), taking into account three factors: salinity level (ECe), alkalinity (pH), and sodium adsorption ratio (SAS).

$$SAR = Na^{+} / \sqrt{(Ca^{2+} + Mg^{2+})/2}$$
 (3)

Table 1-2. Saline soil categories based on ECe, SAR and pH (Rengasamy, 201	Ί	lable	1-2.	Sal	ine so	I cat	egories	based	lon	ECe.	, SAR	and	pН	(Ren	gasam	y,	20	116	),
----------------------------------------------------------------------------	---	-------	------	-----	--------	-------	---------	-------	-----	------	-------	-----	----	------	-------	----	----	-----	----

Nº	Saline soil category	Criteria
01	Acidic-saline soil	ECe > 4; SAR < 6; pH < 6
02	Neutral saline soil	ECe > 4; SAR < 6; pH 6–8
03	Alkaline-saline soil	ECe > 4; SAR < 6; pH 8–9
04	Highly alkaline soil	ECe > 4; $SAR < 6$ ; $pH > 9$
05	Acidic-saline-sodic soil	ECe > 4; $SAR > 6$ ; $pH < 6$
06	Neutral saline-sodic soil	ECe > 4; SAR > 6; pH 6–8

07	Alkaline-saline-sodic soil	ECe > 4; SAR > 6; pH 8–9
08	Highly acidic-saline-sodic soil	ECe > 4; $SAR > 6$ ; $pH > 9$
09	Acidic-sodic soil	ECe < 4; $SAR > 6$ ; $pH < 6$
10	Neutral sodic soil	ECe < 4; SAR > 6; pH 6–8
11	Alkaline-sodic soil	ECe < 4; SAR > 6; pH 8–9
12	Highly alkaline-sodic soil	ECe < 4; $SAR > 6$ ; $pH > 9$

In order to get a general idea of saline soil behavior, the main problematic properties of salt-affected soils are given in Table 1-3 (Rengasamy et al., 2022).

Table 1-3. Problematic behavior of saline soils considering their category (Rengasamy et al., 2022).

Category	Problematic encountered
Saline	The primary effect of salinity is osmotic stress caused by high salt concentration
Alkalinity (pH>8)	Soil pH influences both ion toxicity and nutrient deficiency in crops, while
	salinity can also compromise soil structural stability
Sodic (dispersive)	At low electrical conductivity (EC), clay particles undergo swelling and
	dispersion, degrading soil physical structure

#### 1.2.6. Water-soluble salts

In order to measure soil salinity, the primarily dissolved inorganic ions in water that are considered are involved Ca<sup>2+</sup>, Mg<sup>2+</sup>, Na<sup>+</sup>, K<sup>+</sup>, CO<sub>3</sub><sup>2-</sup>, HCO<sub>3</sub><sup>-</sup>, SO<sub>4</sub> <sup>2-</sup>, and Cl<sup>-</sup>. From this point of view, chlorides, sulfates and carbonates species are considered the main readily soluble minerals or soluble salts. Based on the degree of solubility in water, these soluble minerals can be classified as weakly soluble, moderately soluble, and readily soluble (James, 1992). Salts with the lowest solubility degrees are carbonates such as calcite (CaCO<sub>3</sub>), magnesite (MgCO<sub>3</sub>), and dolomite (CaMg (CO<sub>3</sub>)<sub>2</sub>). It should be noted that except for calcite, other carbonate minerals are virtually insoluble (Petrukhin, n.d.). Chloride minerals are considered readily soluble salts, such as potassium chloride (KCl), sodium chloride (NaCl), magnesium chloride (MgCl<sub>2</sub>), and also magnesium sulfate (MgSO<sub>4</sub>). Besides, sodium carbonate (Na<sub>2</sub>CO<sub>3</sub>), sodium sulfate (Na<sub>2</sub>SO<sub>4</sub>), and sodium bicarbonate (NaHCO<sub>3</sub>) remain bound to this category. However, calcium sulfate (CaSO<sub>4</sub>.2H<sub>2</sub>O) has moderate solubility. Fig 1-2 shows primarily soluble minerals in soils (Lide, 2004).

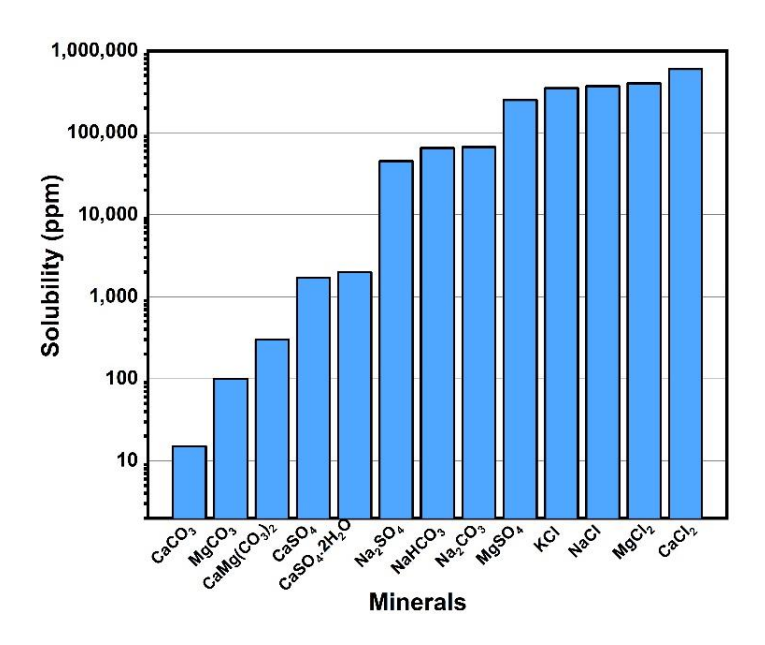


Fig 1-2. Solubility degrees of soils' main minerals/salts (Lide, 2004).

## 1.3. Generality about Sebkha soils

In arid environments, where precipitation rates are much lower than evaporation, saline soils are named "Sebkha "soils. Sebkha is a complicated saline system characterized by high salinity levels due to the solubility of one or more types of salt minerals. Therefore, this system should be investigated, considering its specific constituents.

#### 1.3.1. Definition of Sebkha

The salt-bearing soils are known in Arabic as "Sabkha" or "Sebkha"; they are generally sediments in arid and semi-arid regions. Sebkha had a unique formation resulting from historical sea level drops and subsequent evaporation (Abduljauwad and Al-Amoudi, 1995; Akili, 1981; Nasr, 2015). Al-Amoudi (1992) defined Sebkha as areas characterized by extremely flat, saline, and shallow groundwater associated with evaporative conditions, distinguishing them from normal soil environments.

#### 1.3.2. Types of Sebkha

Sebkha can be classified as continental when situated inland and coastal when located at sea (Abduljauwad and Al-Amoudi, 1995; Akili, 1981).

Coastal Sebkha— Coastal Sebkha refers to a supratidal flat with a minimal slope towards the sea, with elevation typically ranging from 0 to 2 m above high tide (Abduljauwad and Al-Amoudi, 1995). The accumulation of sediments in this area results from the sea advancing over a billion years ago. Dunes have developed on the seaward side, while aeolian sand migrates from the landward side due to wind effects (Nasr, 2015). The typical profile of a coastal Sebkha is illustrated in Fig 1-3, and Fig 1-4 presents the hydrological and geological map of the largest Sebkha in Oran, Algeria (Benkesmia et al., 2023).

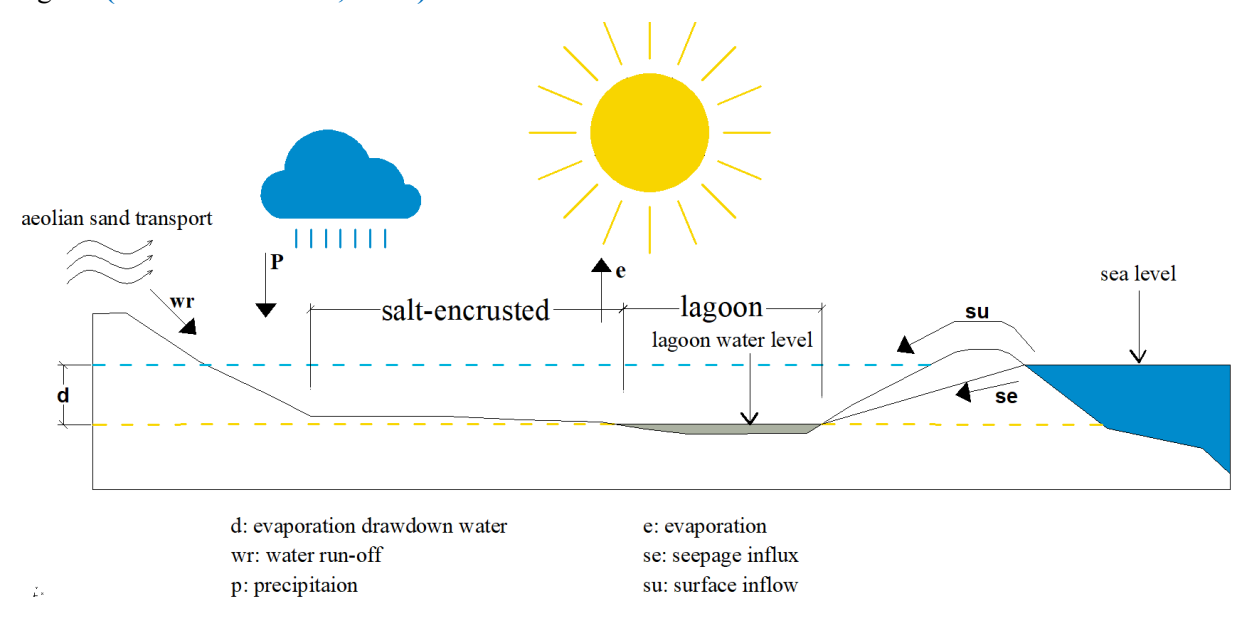


Fig 1-3. Typical profile type of coastal Sebkha

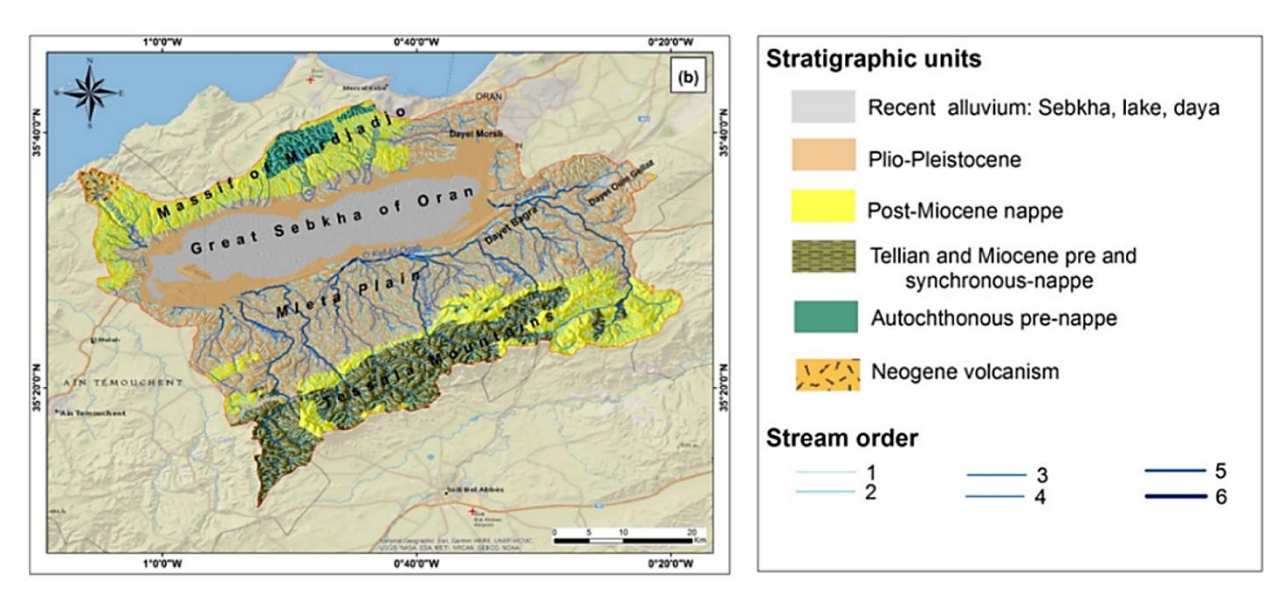


Fig 1-4. Hydrological and geological map of the largest Sebkha in Oran, Algeria (Benkesmia et al., 2023).

Continental Sebkha— Continental Sebkha refers to an inland soil type formed without marine sediment's influence. Unlike the supratidal flats of coastal sabkha, continental sabkhas are formed by wind erosion, which creates a surface parallel to the water table as the wind removes dry sediment (deflated surface) (Abduljauwad and Al-Amoudi, 1995). This erosion effect leads to the generation of shallow groundwater that rises through capillary action due to evaporation, increasing soil salinity and causing evaporates to form in the topsoil. The typical continental profile of Sebkha is presented in Fig 1-5, while Fig 1-6 shows the Sebkha of Ain M'lila (Benrebouh et al., 2025).

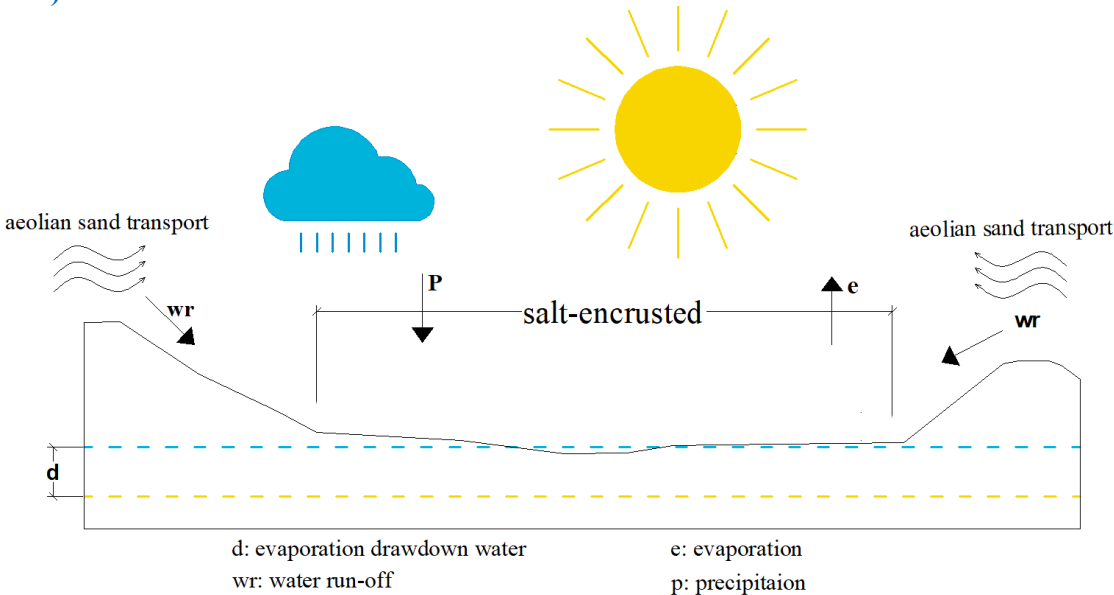


Fig 1-5. Typical profile type of continental Sebkha

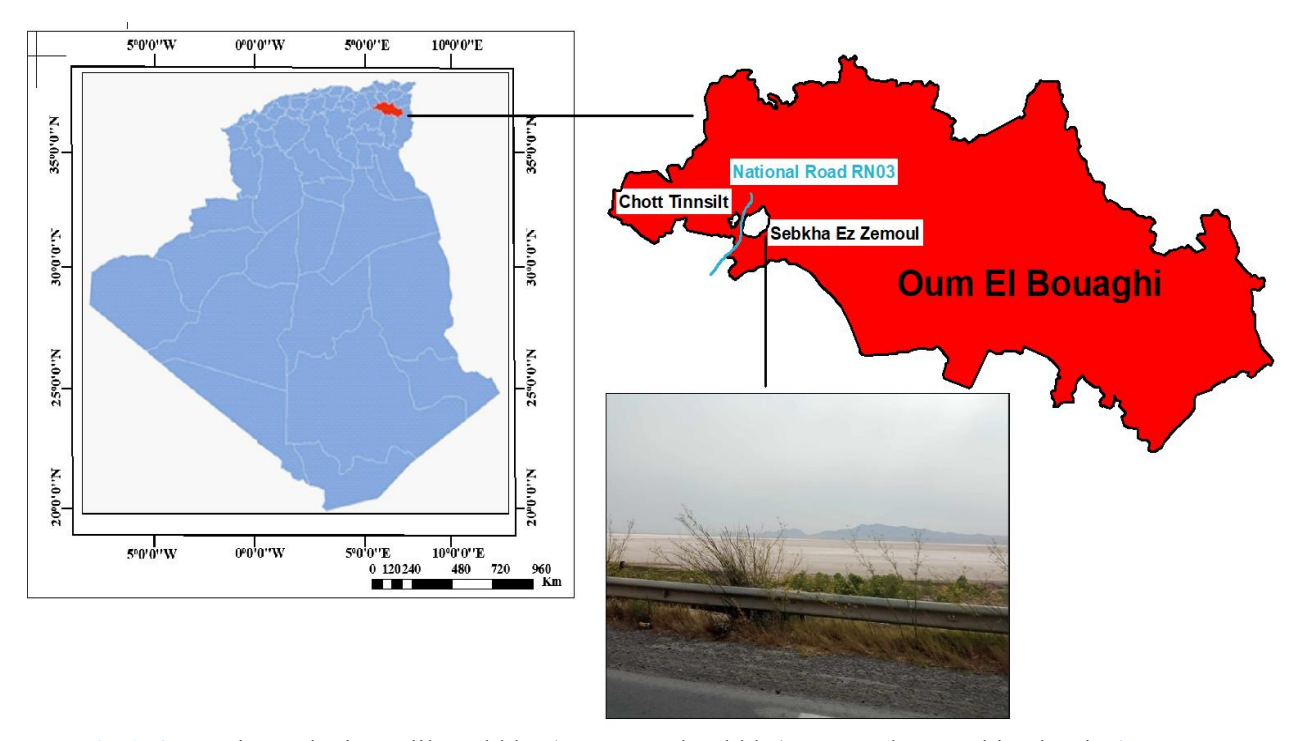


Fig 1-6. Continental Ain M'lila Sebkha (Ez Zemoul Sebkha), Oum El Bouaghi, Algeria (Benrebouh et al., 2025).

#### 1.3.3. Distribution of Sebkha

The interaction between harsh, hot, and arid environments and shallow standing water will most likely produce a Sebkha system. In these regions, evaporation exceeds precipitation, forming salt crystals within the soil profile through capillary action as water evaporates. These salt crystals can also dissolve due to precipitation from rainwater, flooding, and storms, resulting in the concentration of solutions within the groundwater. Thus, the processes of salt precipitation and dissolution occur repeatedly.

About 30% of the world's land surface is located in arid climatic areas, which promotes the global distribution of Sebkha systems. Sebkha can be found in various countries (Fig 1-7a), including Saudi Arabia, India, and China in Asia; Tunisia, Algeria, and Libya in Northern Africa; as well as in Australia and the United States (Arifuzzaman et al., 2016). The arid and semi-arid climate is prevalent in Algeria, making it a typical site for Sebkha originating (Fig 1-7b).

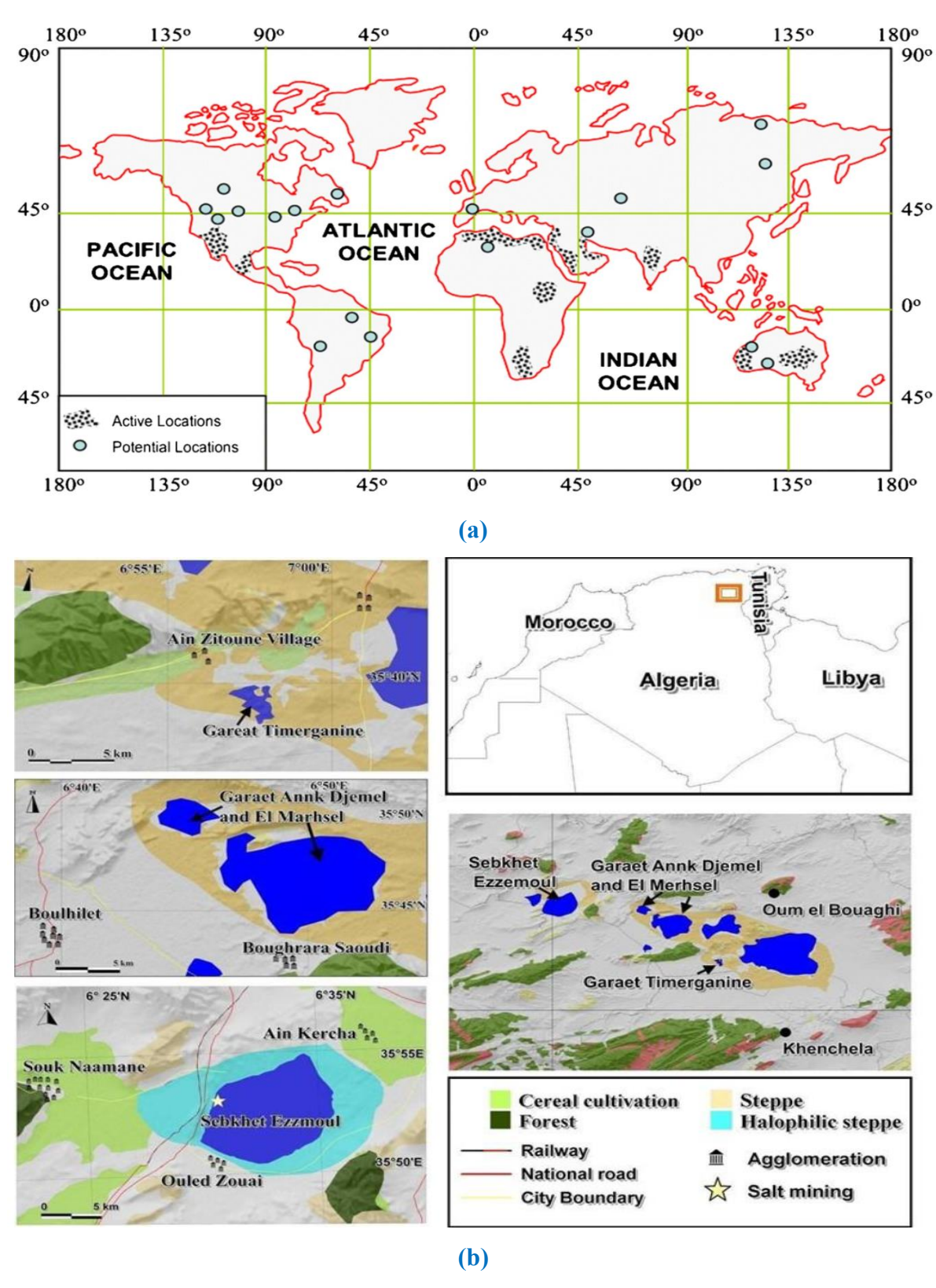


Fig 1-7. Active and potential locations of Sebkha/wetlands: (a) in Earth's lands and (b) in North-Eastern of Algeria (Bougoffa et al., 2023).

## 1.3.4. Factors affecting Sebkha formation

Generally, Sebkha formation system is a complicated process, drawn by five predominant conditions, which are as follows:

Climatic—Changes in external climatic conditions, such as temperature and water content, can significantly affect the Sebkha system. When it rains, the saline solid phases dissolve, causing the saline solution to move gravity, decreasing the salinity of the Sebkha profile (Abduljauwad and Al-Amoudi, 1995). Conversely, when the temperature rises, the rate of evaporation increases, causing the concentrated saline solution to precipitate at the surface due to capillary action. Therefore, the interaction between temperature and water content can result in continuous variations in the quantity (increase or decrease) and the state (solid or liquid) saline phase, consequently changing the soil Sebkha composition.

*Geochemical*— Sebkha soil is a conductive system in which water moves through the soil, saline solution ions (negative or positive) enter porous media and then interact with charged soil particle surfaces, which affects soil properties (Koniorczyk, 2012).

*Geomorphological*— The lower the inclined Sebkha surface, the closer the groundwater (Sebkha brine) is to the surface, and the higher the evaporation rate. Therefore, the geomorphological features associated with evaporation are known to be highly correlated with Sebkha characteristics.

*Hydrological*— Hydraulic conductivity (permeability) and porosity are crucial in the diagenesis of Sebkha (**Abduljauwad and Al-Amoudi**, 1995). For example, the processes of brine seepage and evaporative rise rely on adequate permeability (**Al-Shayea**, 2000).

Biological factors—Some of the sediments in the lagoon area were situated intertidally instead of subtidally (Bush, 1973). These areas were then highly colonized by algal mats, which grew over the sediments pushed to the margins of lagoons. This has led to a change in the composition of the soil Sebkha.

It should be noted that, the degree to which any of these factors affects the formation of Sebkha depends on the type of Sebkha. For example, biological factors have a significant impact on the formation of coastal Sebkha, while climatic factors have a major influence on the formation of continental Sebkha.

#### 1.3.5. Geotechnical characteristics of Sebkha

The Sabkha is primarily formed of quartz sand and silt, with small amounts of mud and clay, and has a hard, crusty surface (Al-Amoudi, 2002). Diagenetic salts and shallow groundwater are the main characteristics of Sebkha, which are caused by high evaporation rates and the sand erosion effect on this land. There are two types of precipitated salt in the Sebkha profile: salt deposition in the surface layers (above groundwater level) is due to the evaporation of moisture drawn into the upper layers by capillary action, while salt precipitation below the water table is caused by an increase in salt concentration beyond its saturation point (Al-Amoudi, 2002, 1995). The evaporation process reveals that after 50% of seawater has evaporated, carbonate (aragonite) begins to deposit, followed by gypsum, halite, and highly saline potassium and magnesium salts as the volume decreases to 19%, 9.5%, and 4%, respectively (Al-Amoudi, 2002). Fig 1-8a displays the types of precipitated salts, while Fig 1-8b illustrates the mechanisms involved. Crucially, the salinity in Sebkha is five times higher than seawater, due to elevated levels of diagenetic salts like CaCO<sub>3</sub> and CaSO<sub>4.2</sub>H<sub>2</sub>O. Additionally, harsh conditions in such areas (temperature, humidity, and pressure) and the complicated process formation (chemical, hydrological, and biological) render Sebkha an abnormal soil associated with the sharp deviation potential of evaporation seawater results. These evaporates can be present by calcite and aragonite (CaCO<sub>3</sub>), along with anhydrite (CaSO<sub>4</sub>) and gypsum (CaSO<sub>4</sub>, 2H<sub>2</sub>O) in the coastal Sebkha whereas in the continental Sebkha consist of gypsum (CaSO<sub>4</sub>, 2H<sub>2</sub>O), quartz (SiO<sub>2</sub>), and calcite (CaCO<sub>3</sub>), with halite (NaCl) found on flat surfaces (Al-Amoudi, 2002). These salts serve a natural cementing function for mineral soil particles, significantly influencing the geotechnical characteristics of sabkha soils (Nasr, 2015).

In the 1970s, Ellis (1973) and Fookes (1976) began exploring the potential of Sebkha for road construction in Saudi Arabia. However, a significant gap persists in understanding Sebkha sediments, highlighting the urgent need for further studies on their geotechnical properties and associated construction challenges. As economic development accelerates, the demand for utilizing these untouched areas has led to the construction of military facilities, industrial zones, and residential complexes, along with various associated difficulties. Comprehensive data on the geotechnical properties of these salt-encrusted flats is crucial for assessing their viability as construction sites. The work of Akili and Torrance (1981) emphasized the heterogeneous nature of Sebkha, influenced by factors such as diagenetic minerals and layering. They noted that horizontal variations depend on proximity to the shoreline, while vertical variations relate to the deposition environment and subsequent changes. Taylor and Illing's (1969) study in Qatar found that the Sabkha features

alternating cemented layers, ranging from 5 cm to 1 m in thickness, separated by uncemented layers. To fully realize the construction potential of Sebkha, prioritizing additional research and data collection is essential to facilitate sustainable development in the region.

When Sebkha is dry in situ, it forms a hard crust due to natural cementing agents from diagenetic salts. However, when it comes into contact with water from rain or storms, the cementing agents dissolve, causing Sebkha to lose its hardness and become soft (Akili and Ahmed, 1983; Ellis, 1973; Fookes, 1976; Nasr, 2015). In other words, Sebkha can support light construction loads when dry, but when wet, it can cause trucks' wheels to get stuck easily (Hafhouf et al., 2022). Therefore, the geotechnical properties of salt-bearing soils are mainly affected by their salt constituents. From this aspect, several researchers have studied the effect of deionized water and brine (highly saline water) on the geotechnical properties of Sebkha soils (Akili, 1981; Al-Amoudi et al., 1992; Hafhouf et al., 2022; Nasr, 2015). Their findings indicate that the percolation of distilled water (rainwater) through a Sebkha causes the destruction of natural cementation and leads to collapse, increased permeability, reduced resistance, and increased settlement. At the same time, Al-Amoudi et al. (1992) and Abduljauwad and Al-Amoudi (1995) showed in their studies that Sebkha soils in the natural state have a low resistance to simple compression, about 20 kPa, which is also confirmed by (Hafhouf et al., 2022) with a value of about 35 kPa.

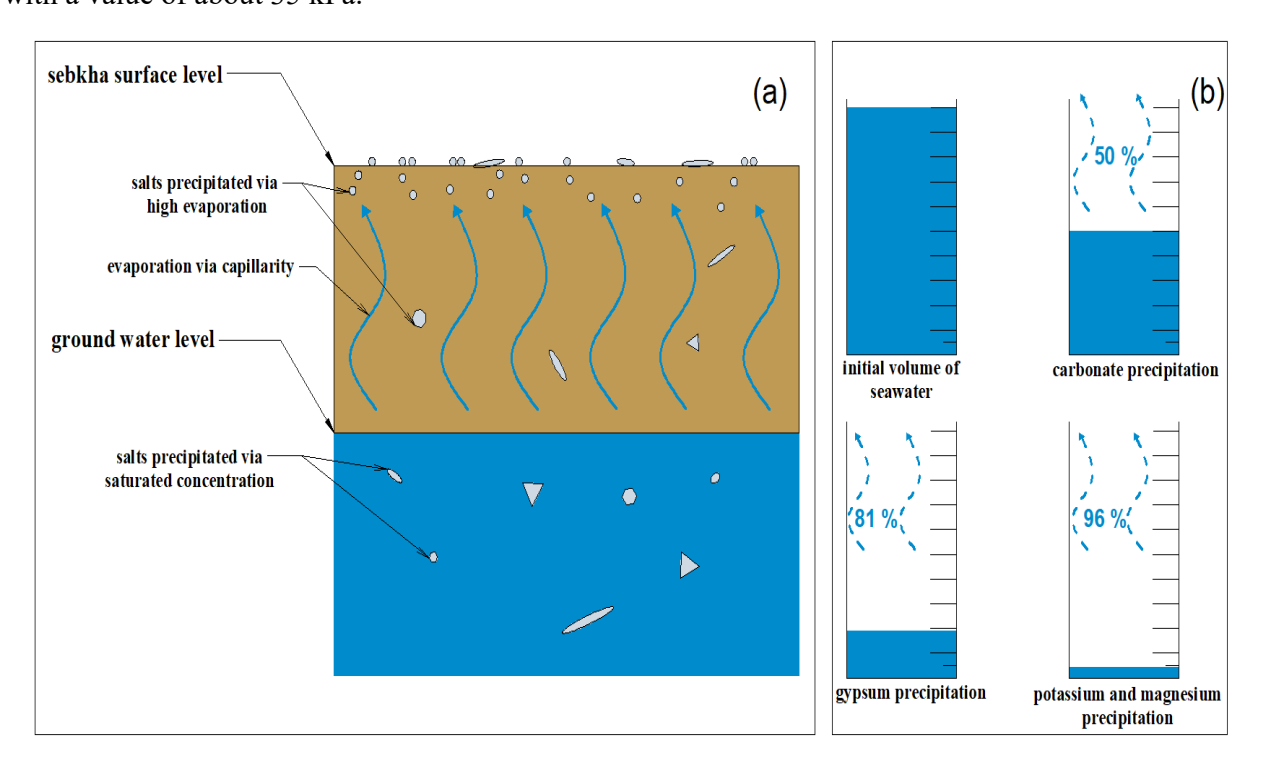


Fig 1-8. Mechanism of salt precipitations: (a) by evaporation and saturated concentration and (b) types of salts precipitation via evaporation

## 1.3.6. Problems bounded to Sebkha

Since Sebkha's geotechnical behavior is influenced mainly by its diagenetic salts, most geotechnical issues are salt-related. Additionally, problems associated with the heterogeneity of Sebkha sediments are also considered.

*Problems relates to diagenetic salts*—Regarding diagenetic salts, three main salt activities cause soil problems: dissolution, crystallization/recrystallization, and corrosive effects.

Salts Dissolution—The solubility of diagenetic salts due to runoff from the sewerage system, rainwater, floods, or storms adversely affects the surface crust of Sebkha that is in direct contact, causing a loss of strength in the upper surface layer and resulting in impassable surfaces (Ellis, 1973; Fookes, 1976). The solubility of salts depends on factors such as salt crystallization (Bednarska et al., 2022), temperature (Yin et al., 2024), humidity (Shen et al., 2017), and the type of salt (Katz et al., 1981). Among the different salt types, halite (NaCl) is the most soluble, followed by gypsum (CaSO<sub>4</sub>,2H<sub>2</sub>O) and calcite (CaCO<sub>3</sub>) (Doner and Grossl, 2018). Furthermore, as the surface crust is primarily associated with halite, damage to the Sebkha surface intensifies rapidly.

Salts crystallization/recrystallization—The soluble salts move upwards through capillary action due to the effects of evaporation and then precipitate in a crystalline form (Abduljauwad and Al-Amoudi, 1995; Jafarzadeh and Burnham, 1992). These salt crystals typically cause blisters and surface cracking in porous materials, especially on pavement surfaces (Al-Amoudi, 1994; Fookes, 1976). Additionally, gypsum is known for its high-volume change during the hydration/dehydration cycle (Chikhaoui et al., 2017). This significant volume variation leads to construction swelling during hydration and construction collapse during dehydration, resulting in significant soil deformation that often exceeds permissible limits (Chikhaoui et al., 2017). Depending on the climatic conditions, this deformation can have short-term and long-term adverse effects, leading to high financial costs such as pavement cracking and raveling (Hafhouf et al., 2022; Tang et al., 2024). Therefore, the problem of salt crystallization is one of the most serious challenges in geotechnical engineering and requires careful attention.

Salts corrosion effects— Salts can cause corrosion when they move upward through evaporation, posing a structure risk (Casey et al., 2014; Elsawy and Lakhouit, 2020; Ismail and

El-Shamy, 2009; Valdez et al., 2016). For instance, if a facility such as a military, civilian, or industrial building is constructed with reinforced concrete over a sabkha surface, gypsum and halite can corrode the concrete and steel in those areas, respectively. Hence, due to the continual upward movement of salts and their continuous contact with construction materials, this potential damage should be considered before constructing anything over or near a Sabkha.

Problems relates to Sebkha heterogeneity— The low geotechnical properties of Sebkha result from its heterogeneity drive to the densification of the loose upper portion of Sebkha through conventional methods, leading to an increase in density and bearing capacity and reducing settlement of this superficial part. However, breaking down the cementing agents in the subsequent cement layers is highly expected to exacerbate the situation (Akili and Torrance, 1981). In addition, the compressibility characteristics of Sebkha are expected to vary significantly, especially in the uncemented layers. For example, the sediments of Sebkha near Jubail and Dhahran, Saudi Arabia, are known to transition from a very loose state to a dense state within a distance of about 100 m (James and Little, 1994). This variation could result in significant differential settlement.

#### 1.4. Conclusion

This chapiter firstly presents an overview about saline soils with focusing on their water-soluble salts such their origins, their types, and their degree of solubilities, ...etc. After which, the second part introduces an overview about Sebkha soils considering their types, their geotechnical properties, and their relates problems, ...etc. the following conclusions can be drawn:

- (1) In addition to widespread of saline soils, their rate of increasing due to lands salinization is rapid and high and thus serious concern should be done to those areas. In which, pH, ECe, and SAR/ESP can be good, rapid and reliable techniques to classify such soils and identify some of their characteristics.
- (2) Due to higher evaporation rate compared to precipitation one, Sebkha soils are typically found in arid or semi-arid regions. These soils have been exhibited highly variable geotechnical characteristics, which can obstruct and/or inhibit the serviceability and stability of future earth ground infrastructure such as dams, slopes, and embankment, ...etc. In fact, Sebkha properties are humidity dependent, in which, the number of soluble salts and their types in profile highly control

and shape Sebkha geotechnical properties. Where halite (NaCl), gypsum (CaSO<sub>4</sub>.2H<sub>2</sub>O), and calcium carbonate (CaCO<sub>3</sub>) are common soluble minerals in Sebkha.

## References

- Abduljauwad, S.N., Al-Amoudi, O.S.B., 1995. Geotechnical behaviour of saline sabkha soils.

  Géotechnique 45, 425-445. https://doi.org/10.1680/geot.1995.45.3.425
- Akili, W., 1981. On sabkha sands of eastern Saudi Arabia, in: Proceedings of the Geotechnical Problems in Saudi Arabia Symposium. pp. 775–793.
- Akili, W., Ahmed, N., 1983. The sabkhas of eastern Saudi Arabia: geotechnical considerations, in: Proceedings, First Saudi Engineering Conference. pp. 300-322.
- Akili, W., Torrance, J.K., 1981. The development and geotechnical problems of sabkha, with preliminary experiments on the static penetration resistance of cemented sands. QJEGH 14, 59–73. https://doi.org/10.1144/GSL.QJEG.1981.014.01.05
- Al-Amoudi, O.S.B., 2002. Characterization and Chemical Stabilization of Al-Qurayyah Sabkha Soil. J. Mater. Civ. Eng. 14, 478-484. https://doi.org/10.1061/(ASCE)0899-1561(2002)14:6(478)
- Al-Amoudi, O.S.B., 1995. Soil stabilization and durability of reinforced concrete in sabkha environments.
- Al-Amoudi, O.S.B., 1994. Chemical stabilization of sabkha soils at high moisture contents. Engineering geology 36, 279–291.
- Al-Amoudi, O.S.B., 1992. Studies on soil-foundation interaction in the sabkha environment of eastern province of Saudi Arabia (PhD Thesis). King Fahd University of Petroleum and Minerals (Saudi Arabia).
- Al-Amoudi, O.S.B., Abduljauwad, S.N., El-Naggar, Z.R., 1992. Response of sabkha to laboratory tests: a case study. Engineering Geology 33, 111-125.
- Al-Shayea, N.A., 2000. Inherent heterogeneity of sediments in Dhahran, Saudi Arabia—a case study. Engineering geology 56, 305–323.
- Arifuzzaman, M.D., Habib, M.A., Al-Turki, M.K., Khan, M.I., Ali, M.M., 2016. Improvement and characterization of sabkha soil of Saudi Arabia: A review. Jurnal Teknologi 78.
- Bednarska, D., Koniorczyk, M., Steiger, M., 2022. Identification of various salt crystallization and water freezing patterns induced by temperature variation from Na2SO4-H2O system confined in porous materials. Construction and Building Materials 347, 128540.

- Benkesmia, Y., Hassani, M.I., Kessar, C., 2023. Variation of surface water extent in the great Sebkha of Oran (NW of Algeria), using Landsat data 1987–2019: interaction of natural factors and anthropogenic impacts. Remote Sensing Applications: Society and Environment 30, 100953.
- Benrebouh, I., Hafhouf, I., Douadi, A., Merdas, A., Marathe, S., 2025. Effect of sulfate resistance cement treatment on saline soil (Sebkha) subgrades. Indian Geotechnical Journal 1–19.
- Bush, P., 1973. Some Aspects of the Diagenetic History of the Sabkha in Abu Dhabi, Persian Gulf, in: Purser, B.H. (Ed.), The Persian Gulf. Springer Berlin Heidelberg, Berlin, Heidelberg, pp. 395–407. https://doi.org/10.1007/978-3-642-65545-6-19
- Casey, P.C., Alwan, C.W., Kline, C.F., Landgraf, G.K., Linsenmayer, K.R., 2014. Impacts of using salt and salt brine for roadway deicing.
- Chikhaoui, M., Belayachi, N., Nechnech, A., Hoxha, D., 2017. Experimental characterization of the hydromechanical properties of the gypsum soil of Sebkha of Oran. Periodica Polytechnica Civil Engineering 61, 706–717.
- De La Paix, M.J., Lanhai, L., Xi, C., Varenyam, A., Nyongesah, M.J., Habiyaremye, G., 2013.
  PHYSICOCHEMICAL PROPERTIES OF SALINE SOILS AND AEOLIAN DUST. Land
  Degrad Dev 24, 539–547. https://doi.org/10.1002/ldr.1148
- DING, J., WU, M., Tiyip, T., 2011. Study on soil salinization information in arid region using remote sensing technique. Agricultural sciences in China 10, 404–411.
- Doner, H.E., Grossl, P.R., 2018. Carbonates and Evaporites, in: Dixon, J.B., Schulze, D.G. (Eds.), SSSA Book Series. Soil Science Society of America, Madison, WI, USA, pp. 199–228. https://doi.org/10.2136/sssabookser7.c6
- Ellis, C.I., 1973. Arabian salt-bearing soil (sabkha) as an engineering material.
- Elsawy, M.B., Lakhouit, A., 2020. A review on the impact of salinity on foundation soil of coastal infrastructures and its implications to north of Red Sea coastal constructions. Arabian Journal of Geosciences 13, 1–12.
- Fookes, P.G., 1976. Road geotechnics in hot deserts.
- Group, I.W., 2014. World reference base for soil resources 2014. International soil classification system for naming soils and creating legends for soil maps. (No Title).
- HAFHOUF, I., 2022. Étude de l'endommagement des sols salés soumis à des sollicitations d'humidification Séchage (température-humidité). (PhD Thesis). Université de Batna 2.
- Hafhouf, I., Bahloul, O., Abbeche, K., 2022. Effects of drying-wetting cycles on the salinity and the mechanical behavior of sebkha soils. A case study from Ain M'Lila, Algeria. Catena 212, 106099.

- Hassani, A., Azapagic, A., D'Odorico, P., Keshmiri, A., Shokri, N., 2020. Desiccation crisis of saline lakes: A new decision-support framework for building resilience to climate change. Science of The Total Environment 703, 134718.
- Ismail, A.I.M., El-Shamy, A.M., 2009. Engineering behaviour of soil materials on the corrosion of mild steel. Applied clay science 42, 356–362.
- Jafarzadeh, A.A., Burnham, C.P., 1992. Gypsum crystals in soils. Journal of Soil Science 43, 409-420. https://doi.org/10.1111/j.1365-2389.1992.tb00147.x
- James, A.N., 1992. Soluble materials in civil engineering. (No Title).
- James, A.N., Little, A.L., 1994. Geotechnical aspects of sabkha at Jubail, Saudi Arabia. QJEGH 27, 83– 121. https://doi.org/10.1144/GSL.QJEGH.1994.027.P2.03
- Jobbagy Gampel, E.G., Tóth, T., Nosetto, M.D., Earman, S., 2017. On the Fundamental Causes of High Environmental Alkalinity (pH≥ 9): An Assessment of Its Drivers and Global Distribution.
- Katz, A., Starinsky, A., Taitel-Goldman, N., Beyth, M., 1981. Solubilities of gypsum and halite in the Dead Sea and in its mixtures with seawater1. Limnology & Oceanography 26, 709–716. https://doi.org/10.4319/lo.1981.26.4.0709
- Khan, M.A., Weber, D.J. (Eds.), 2006. Ecophysiology of High Salinity Tolerant Plants, Tasks for Vegetation Science. Springer Netherlands, Dordrecht. https://doi.org/10.1007/1-4020-4018-0
- Koniorczyk, M., 2012. Salt transport and crystallization in non-isothermal, partially saturated porous materials considering ions interaction model. International Journal of Heat and Mass Transfer 55, 665–679.
- Laboratory (US), R.S., 1954. Diagnosis and improvement of saline and alkali soils. US Department of Agriculture.
- Lide, D.R., 2004. CRC handbook of chemistry and physics. CRC press.
- Metternicht, G.I., Zinck, J.A., 2003. Remote sensing of soil salinity: potentials and constraints. Remote sensing of environment 85, 1-20.
- Nachshon, U., 2018. Cropland soil salinization and associated hydrology: Trends, processes and examples. Water 10, 1030.
- Nan, J., Liu, J., Chang, D., Li, X., 2022. Mechanical characteristics and microstructure study of saline soil stabilized by quicklime after curing and freeze-thaw cycle. Cold Regions Science and Technology 201, 103625.
- Nasr, A.M.A., 2015. Geotechnical Characteristics of Stabilized Sabkha Soils from the Egyptian–Libyan Coast. Geotech Geol Eng 33, 893–911. https://doi.org/10.1007/s10706-015-9872-x
- Petrukhin, V., n.d. Construction of structures on saline soils.

- Rengasamy, P., 2016. Soil chemistry factors confounding crop salinity tolerance—a review. Agronomy 6, 53.
- Rengasamy, P., De Lacerda, C.F., Gheyi, H.R., 2022. Salinity, Sodicity and Alkalinity, in: Oliveira, T.S.D., Bell, R.W. (Eds.), Subsoil Constraints for Crop Production. Springer International Publishing, Cham, pp. 83-107. https://doi.org/10.1007/978-3-031-00317-2\_4
- Ribeiro, M.R., Ribeiro Filho, M.R., Jacomine, P.K.T., 2010. Origem e classificação dos solos afetados por sais. Manejo da salinidade na agricultura: estudos básicos e aplicados. Fortaleza: INCTSal 12–19.
- Richards, L.A., 1954. Diagnosis and improvement of saline and alkali soils. US Government Printing Office.
- Shen, Y., Chen, W., Kuang, J., Du, W., 2017. Effect of salts on earthen materials deterioration after humidity cycling. Journal of Central South University 24, 796–806.
- Shokri, N., Hassani, A., Sahimi, M., 2024. Multi-Scale Soil Salinization Dynamics From Global to Pore Scale: A Review. Reviews of Geophysics 62, e2023RG000804. https://doi.org/10.1029/2023RG000804
- Tang, Y., Fu, Z., Zhao, P., Ma, F., Hou, Y., 2024. Damage on asphalt surfaces caused by ionic solution erosion and salt crystallization at molecular scale. Applied Surface Science 643, 158718.
- Taylor, J.C.M., Illing, L.V., 1969. HOLOCENE INTERTIDAL CALCIUM CARBONATE CEMENTATION, QATAR, PERSIAN GULF. Sedimentology 12, 69–107. https://doi.org/10.1111/j.1365-3091.1969.tb00165.x
- Valdez, B., Ramirez, J., Eliezer, A., Schorr, M., Ramos, R., Salinas, R., 2016. Corrosion assessment of infrastructure assets in coastal seas. Journal of Marine Engineering & Technology 15, 124–134. https://doi.org/10.1080/20464177.2016.1247635
- Wong, V.N.L., Greene, R.S.B., Dalal, R.C., Murphy, B.W., 2010. Soil carbon dynamics in saline and sodic soils: a review: Soil carbon dynamics in saline and sodic soils. Soil Use and Management 26, 2–11. https://doi.org/10.1111/j.1475-2743.2009.00251.x
- Yin, W., Tang, Y., Wang, G., Wang, X., Cheng, W., Zhu, S., Liu, Y., Zhang, K., 2024. Salinization and salt expansion mechanism of soda residue soil at subgrade. Case Studies in Construction Materials 21, e04000.
- Zinck, J.A., Metternicht, G., 2009. Soil salinity and salinization hazard. Remote sensing of soil salinization 3–18.

#### **CHAPTER 2.**

## LITERATURE REVIEW ON SALINE SOILS (SEBKHA SOILS) TREATMENT WITH HYDRAULIC BINDERS

#### 2.1. Introduction

Hydraulic binder treatment is a widely applied technique in saline (Sebkha) soils, which are known for their poor geotechnical characteristics under water fluctuations. Among stabilization techniques, lime and cement (traditional binders) have been commonly used in soil treatment. This chapter first discusses the mechanism of lime and cement treatment in Section 2.2. A comprehensive review of the geotechnical properties of treated saline (Sebkha) soils is described in Section 2.3. Afterward, the physicochemical and mineralogical properties of treated saline (Sebkha) soils are presented in Section 2.4. Finally, the salinity effect on the chemical, mineralogical, and mechanical behavior of saline (Sebkha) soils is described in Section 2.5.

#### 2.2. Cement and lime treatment

#### 2.2.1. Soil stabilization

Using local soils for earth constructions, such as dikes, slopes, and embankments, offers significant socio-economic benefits. However, these local soils often have poor geotechnical properties that prevent their direct use, which makes soil stabilization techniques necessary.

Soil stabilization is crucial for enhancing soil mechanical properties and meeting structural strength requirements. Various binders such as fly ash, pozzolana, and polymers can be used (Consoli et al., 2019; Li et al., 2022; Pai and Patel, 2019). However, cement and lime are the preferred choices due to their ease of application, cost-effectiveness, and proven reliability (Benrebouh et al., 2025; Consoli et al., 2009; Liu et al., 2018, 2019). Incorporating these materials not only strengthens construction but also promotes sustainability.

Lime-based stabilization typically involves three primary forms: hydrated lime slurry, hydrated lime (calcium hydroxide, Ca(OH)<sub>2</sub>), and quicklime (calcium oxide, CaO). Quicklime shows superior performance characteristics, offering two key advantages: (i) enhanced pozzolanic reactions due to a higher free calcium content per unit mass and (ii) the generation of heat during hydration, which reduces soil water content and accelerates strength development (Ying, 2021). Based on Ordinary Portland Cement (OPC) constituents, different types are identified, such as CEM I, CEM II, and sulfate resistance cement (SRC) (Consoli et al., 2009). Construction

sites should choose cement types based on project type and environmental conditions. For saline soils (sulfate-rich soils), the addition of OPC promotes the formation of expansive minerals due to the reaction between sulfate minerals, aluminate ions, and calcium ions (Al-Dakheeli et al., 2021; Cabane, 2004). This expansive phase implies strength instability over time. Therefore, for saline soils (sulfate-rich soils), CRS (with low aluminate amount) presents an advantage.

#### 2.2.2. Mechanisms of lime and cement treatment

The physical and mechanical behavior of soils can be improved through lime treatment via a series of physicochemical reactions, including lime hydration, cation exchange, pozzolanic reaction, and carbonation.

#### (1) Quick lime hydration

Hydration process takes place rapidly when lime is mixed with soil and water, consuming large amounts of water and releasing heat.

$$CaO + H_2O = Ca(OH)_2 + heat \uparrow \Delta H = -57.86 \text{ kj/mol}$$
 (1)

This rapid reaction followed by ionization of calcium hydroxide (Ca(OH)<sub>2</sub>) which result in large amount of calcium ions (Ca<sup>2+</sup>) and hydroxide ions (OH<sup>-</sup>):

$$Ca(OH)_2 = Ca^{2+} + 2OH^-$$
 (2)

#### (2) Cation exchange

Free calcium ions (Ca<sup>2+</sup>) in soil pore water are vital as they adsorb onto clay particles, replacing monovalent ions (e.g., K<sup>+</sup> and Na<sup>+</sup>), reducing the thickness of the diffuse double layer, leading to soil particle flocculation and the formation of coarser aggregates (Liu et al., 2019; Tran et al., 2014). This process enhanced soil workability by reducing swell, shrinkage and plasticity (Al-Mukhtar et al., 2012; Bell, 1996; Ying et al., 2022a).

#### (3) Pozzolanic reaction

In soil pore water, the highly alkaline environment induced by OH<sup>-</sup> released from Ca (OH)<sub>2</sub> with a pH value around 12.4 caused the dissolution of silicon ions (Si<sup>2+</sup>) and aluminum ions (Al<sup>3+</sup>) from clay minerals, feldspar, and quartz. Si<sup>2+</sup> and Al<sup>3+</sup> react with Ca<sup>2+</sup> to produce cementitious

compounds, such as calcium silicate hydrate (CSH), calcium aluminate hydrate (CAH), and calcium aluminate silicate hydrate (CASH):

$$Ca^{2+} + 2OH^{-} + Al_2O_3 \rightarrow Calcium aluminum hydrate (CAH)$$
 (3)

$$Ca^{2+} + 2OH^{-} + SiO_2 \rightarrow Calcium silicate hydrate (CSH)$$
 (4)

$$Ca^{2+} + 2OH^{-} + Al_2O_3 + SiO_2 \rightarrow Calcium aluminate silicate hydrate (CASH)$$
 (5)

This process is known as the pozzolanic reaction, which is continuous as long as Al<sup>3+</sup>, Si<sup>2+</sup>, and Ca<sup>2+</sup> are available and a high pH level is maintained in soil pore water. The mechanical behavior of modified soils is highly enhanced by the pozzolanic reaction as the latter increases the bonding bridge between soil particles and coats the surface of the aggregate (Liu et al., 2019; Tran et al., 2014). Thus, strength properties of the soil significantly improved, such as unconfined compressive strength (Liu et al., 2019), shear strength (Liu et al., 2012) and stiffness (Tang et al., 2011).

#### (4) Carbonation

Combination of carbon dioxide (CO<sub>2</sub>) in water and Ca<sup>2+</sup> from dissolution of Ca (OH)<sub>2</sub> results in the precipitation of calcium carbonate (CaCO<sub>3</sub>):

$$Ca(OH)_2 + CO_2 \rightarrow CaCO_3 + H_2O$$
 (6)

This reaction consumes more Ca<sup>2+</sup> needed to produce cementitious compounds, such as CAH, CSH, and CASH, and thus, carbonation of lime inhibits the strength development of the modified soils.

Cement and lime provide similar chemical reactions with soils, in which a soil-cement-water mixture results in a cement hydration reaction that provides cementitious compounds such as CSH, CAH, and portlandite (Bouras et al., 2022). Generally, cement is preferred over lime in soil stabilization because cement induces higher strength and presents good durability. However, due to its higher embodied energy (higher temperature of produced clinker) (Santos et al., 2020), higher CO<sub>2</sub> emissions (Hebbache et al., 2024; Santos et al., 2020) and weak strength stability with sulfate soils (Aldaood et al., 2014a, 2014b), lime can be an advantage.

#### 2.2.3. Determination of optimum lime and cement content

From a socioeconomic standpoint, the minimum amount of binder corresponding to the maximum strength performance should be the first step in any soil treatment project.

After lime is added to the soil-water mixture, the released Ca<sup>2+</sup> is absorbed on the clay minerals surface, and after that, it's involved in producing CAH, CSH, and CASH compounds. Based on this, the quantity of lime needed strongly depends on the cation exchange capacity of each clay mineral (short-term) and the pozzolanic reaction (long-term). **Hilt and Davidson** (1960) denoted the amount of lime absorbed on the surface of clay particles as the initial consumption of lime (ICL). Where ICL later can be calculated based on the fraction of clay-size particles as follows:

$$ICL = \frac{Clay fraction (\%)}{35} + 1.25 \tag{7}$$

However, this equation did not consider the cation exchange capacity of each clay minerals, where smectite has the higher cation exchange capacity. In contrast, kaolinite has the lower (80-150 meq/100g Vs. 3-15 meq/100g) (Mitchell and Soga, 2005). Thus, this equation could not be representative of different clay minerals.

According to Eades and Grim (1966), the optimum lime content (OLC) (by dry weight) is the minimum amount of lime that provides sufficient Ca<sup>2+</sup> for cation exchange and pozzolanic reaction, which could achieve the maximum strength performance. The OLC can be determined based on the pH method, where the pH value of the lime-soil-water mixture should be equal to that of the lime-saturated solution, which is a value of around 12.4. This method is quickest and easy to apply. It should be noted that a deionized water-based solution is used; however, in-situ water should be used if soil pore water is highly basic (pH>9) or highly acidic (pH<6). It is well known that pH level is dependent on pore water ions. However, most studies focused on the effects of ions from lime and soil, while the research on the influence of soluble soil ions on pH values is still limited. In this respect, Emarah and Seleem (2018) found that adding hydrated lime to soil treated with Red Sea water raised the suspension's pH linearly, stabilizing at 3%–4% lime content. Beyond this point, the pH continued to increase with additional lime content. On the other hand, a strong correlation between OLC and salinity was observed in a study conducted by Ying et al. (2022b). The OLC levels were 1.5%, 3%, and 4% by dry weight for the deionized water–quick lime, synthetic seawater–quick lime, and mixed salt solution–quick lime suspensions.

According to Nelson and Miller (1997), the ICL can be obtained by soil consistency limits. The quantity of lime added after no further modification in soil plasticity should be considered as ICL. Thus, it is also known as the lime modification optimum of soil (Bhuvaneshwari et al., 2014; Marks and Haliburton, 1972).

Ciancio et al. (2014) measured the unconfined compressive strength (UCS) of lime-treated rammed earth materials to determine that the minimum lime content provides the maximum strength considered optimum (i.e., OLC). Their findings indicates that all different methods, such as pH, plastic limits, and USC testing, are coherent and provide almost the same OLC which is 4% lime content (Fig 2-1).

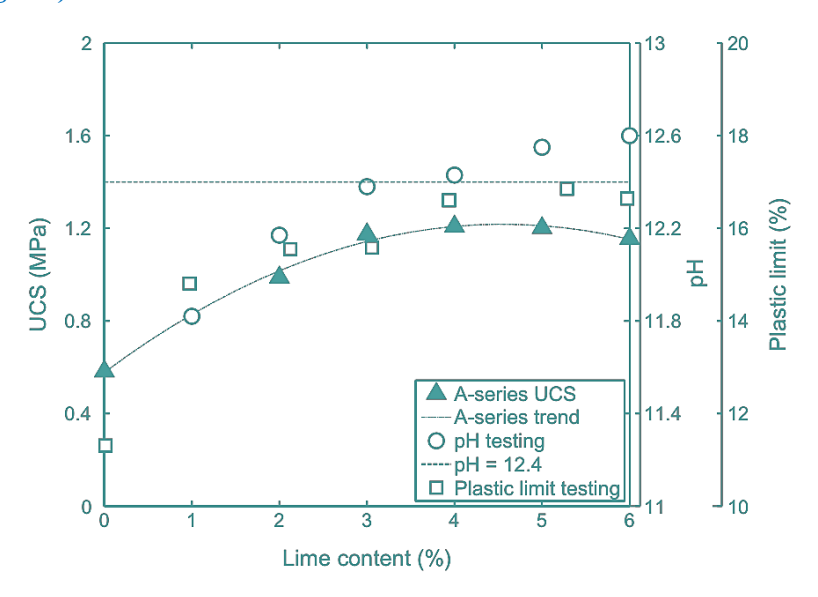


Fig 2-1. Variations of USC, plastic limit and pH with lime content (Ciancio et al., 2014).

For soil treatment with cement addition, identifying the optimum cement content (OCC) is more similar to lime, where the plasticity limits and UCS tests were widely applied in order to obtain OCC (Pongsivasathit et al., 2019; Sariosseiri and Muhunthan, 2009; Shooshpasha and Shirvani, 2015).

#### 2.3. Geotechnical properties of treated saline (Sebkha) soils

In field conditions, Sebkha is generally found in humid conditions associated with a certain solubility of their natural cementitious bonds (i.e., salt crystals) (Al-Amoudi, 2002, 1994). Solubility of some salt crystals led to a decrease in solid parts within the soil fabric and a decrease in the bonding bridge between soil particles, which highly change the physical and mechanical

properties of these types of soils with these climatic conditions (Al-Amoudi, 2002). In their natural state, sebkha has low unconfined compressive strength (UCS) of around 20 kPa (Abduljauwad and Al-Amoudi, 1995; Al-Amoudi et al., 1992). However, for samples prepared in the laboratory, the UCS reached a value of at least 200 kPa (Al-Amoudi, 2002; Benrebouh et al., 2024a; Hafhouf et al., 2022) which indicates the poor strength of sebkha and its high heterogeneity. Therefore, to maintain the stability of these soils and/or increase their strength, several researchers carried out soil chemical stabilization techniques through addition of hydraulic binders since the beginning of 1990s with a different success level achieved (Aiban et al., 2006; Al-Amoudi, 2008, 2002; Al-Amoudi et al., 1995, 1992; Al-Ayedi, 1996; Al-Homidy et al., 2017; Al-Otaibi, 2006; Benrebouh et al., 2024b; Hussain and Awn, 2015; Shabel, 2006).

**Al-Amoudi** (1994) studied the feasibility of stabilizing Sebkha at its natural moisture level (i.e., high moisture content) with a value between 16% and 22%. The sebkha strength increased significantly with cement addition at high moisture content. While with lime addition, the strength development of Sebkha was hindered. The optimum moisture content (i.e., 8.5%) provides an ideal environment for lime treatment, which is much lower than the natural moisture content. Therefore, adding lime to lower moisture content can not be favorable for practical reasons.

Al-Amoudi et al. (1995) investigated the effect of five stabilizing binders, namely emulsified asphalt, marl, limestone dust, cement, and lime, on the strength of Sebkha from the site of Ras Al-Ghar, eastern Saudi. With the three former binders, there is no significant effect on soil strength. However, with cement and lime addition in the range of 2.5% to 10% by dry weight of soil, the UCS increased between 21/2 and 22-fold. These results are also confirmed by the findings of Al-Amoudi (2002) and Al-Ayedi (1996). The engineering properties of Sebkha were treated with cement and lime at different dosages varying from 0 to 10%. Cement enhanced the performance of Sebkha more than lime, in which the addition of 7% cement can achieve the minimum strength requirement for the Sebkha soil to be used as a subbase in flexible pavements and as a base course in rigid pavements.

**Mubaraki** (2019) studied the feasibility of using hydraulic lime to enhance the properties of Sebkha soil, such as maximum dry density and strength. It was found that after lime incorporation into Sebkha with dosages of 0%, 3%, 6%, 9%, and 12% by dry weight, dry density and strength increase. However, water drainage should be the first concern when using lime-stabilized Sebkha as road construction materials.

**Mohamedzein and Al-Rawas (2011)** conducted an experimental study of the effectiveness of cement addition on the strength of sandy Sebkha obtained from the coastal plains at Al-Auzayba, Oman. After 14-d of curing, the UCS increased from 0.12 MPa with 0% cement to approximately 0.8 MPa, 1.4 MPa, 1.8 MPa, and 3.2 MPa with 2.5%, 5%, 7.5%, and 10% cement, indicating a significant effect of cement addition in Sebkha.

Al-Homidy et al. (2017) studied the feasibility of stabilizing Sebkha from the site at Ras Al-Ghar, eastern Saudi, using a combination of cement and cement kiln dust (CKD). After 7 curing days and with 5% cement, the UCS reached a value of around 1 MPa, approximately the same as 2% cement + 20% CKD. While with 2% cement + 30% CKD, the UCS increased to 1.6 MPa, rendering this Sebkha suitable for use as a subbase in rigid pavement as the minimum strength required is 1.38 MPa (ACI Committee, 1990). However, regarding quantity availability, providing such a quantity of CKD for road projects that need large quantities is unsuitable.

Recently, Hammad et al. (2024) treated Sebkha from the Al-Seeb site, Oman, with Ordinary Portland Cement (OPC) and marble powder (MP). After 28 days of curing, the modified Sebkha showed good strength and durability resistance. Where with 70% OPC and 30% MP, the UCS reached a value of 5.2 MPa. However, the UCS reached a value of around 5 MPa with 100% OPC, indicating that adding MP can be considered ineffective.

From the above-mentioned studies, the heterogeneity of the Sebkha system from the same location and different places is highly anticipated, which renders each Sebkha a unique system that should be investigated. In addition, although many new binders were incorporated in such soils, cement, and lime have been preferred over other new binders because they can provide high strength (Firoozi et al., 2017), are most commonly used (**Bhattacharja and Bhatty, 2003**) and abundant availability high (Aziz et al., 2021).

Many researchers studied the influence of particle size distribution on the strength behavior of soils (Cho et al., 2007; Hatefi et al., 2024; Li, 2013; Prakasha and Chandrasekaran, 2005). Li 2013 carried out an experimental study on the effects of particle shape and size distribution on the shear strength behavior of soils. The study results indicated that shear strength is proportional to particle size distribution. In other words, the higher the coarser fraction, the higher the shear strength was obtained. Fattahpour et al. (2014) found that higher strength can be achieved with better gradation since the well-graded specimens tend to lower porosity, and thus, higher UCS was provided. However, this effect on the strength of saline soils was less pronounced in the literature,

although decreasing salinity under climatic conditions (which is a repeated process) leads directly to a change in the grain size distribution curve due to two main reasons: (i) decrease in solid portion for a specific mass unit where some crystals transform to fluid. (ii) a decrease in coarser aggregates due to the solubility of the bonding bridge between soil particles. Only a few studies were focused on this subject. A study conducted by **Li and Yang (2024)** found that increased chlorine salt content was associated with a significantly higher number of agglomerates in the soil. **Li et al. (2016)** observed that increasing chlorine salt content in lime treated- inshore soil increases the number of coarse particles. These tendencies were coherent on different curing days, which can be related to the salt crystallization and flocculation induced by the salt solution (**Zhang et al., 2012**).

#### 2.4. Physicochemical and mineralogical properties of treated saline (Sebkha) soils

After cement and lime addition, the chemical reactions can be classified into two different processes: a fast reaction, which is cation exchange and flocculation, and a time-dependent reaction, which are pozzolanic reaction and hydration effects, in which the results of these chemical reactions are cementitious products such as CAH, CSH, CASH and Ca(OH)<sub>2</sub> (Bhattacharja and Bhatty, 2003). It is well known that the soil's macro behavior, such as strength, is highly related to its micro behavior (Al-Mukhtar et al., 2012; Li et al., 2023; Verbrugge et al., 2011). Therefore, it is of interest to investigate the micro-scale level by monitoring these cementitious compounds using physicochemical and mineralogical tests such as X-ray diffraction, X-ray fluorescence, Thermogravimetric-differential thermal, pH and electrical conductivity, and Fourier transform infrared spectroscopy.

#### 2.4.1. X-ray diffraction analysis

X-ray diffraction (XRD) is a semi-quantitative technique generally used for identifying crystalline phases in materials (Talero et al., 2011). Besides, it is a common method that is used for monitoring the development of cementitious products, which is generally associated with a variation in mineralogical phases (Akula and Little, 2020; Wang et al., 2017).

In their experimental study, **Modmoltin and Voottipruex (2009)** investigated salts' effect on cemented-treated clay's strength. Their findings indicated that sodium chloride (NaCl) and calcium chloride (CaCl<sub>2</sub>) addition raise the dissolution of aluminate and silicate in clay minerals, leading

to more production of CSH in cemented-treated clay. However, compared to NaCl, CaCl<sub>2</sub> provided greater CSH production.

Xing et al. (2009) pointed out that although the Ca<sup>2+</sup> and Al<sup>3+</sup> ions in cement-treated saline soil promoted the formation of cementitious compounds, the Cl<sup>-</sup>, Mg<sup>2+</sup>, and SO<sub>4</sub><sup>2-</sup> ions obstructed such formation. They observed that the Cl<sup>-</sup> ions first interacted with Ca<sup>2+</sup> and Al<sup>3+</sup> ions in pore water to form Ca<sub>2</sub>Al(OH)<sub>6</sub>Cl(H<sub>2</sub>O)<sub>2</sub>, which deposited on the surface of clays, preventing the clay mineral from being combined with Ca(OH)<sub>2</sub>; Mg<sup>2+</sup> ions could replace the Ca<sup>2+</sup> ions to produce low strength MgSH in place of the formation of CSH; SO<sub>4</sub><sup>2-</sup> ions were combined with 3CaO.Al<sub>3</sub>O<sub>3</sub> to form an expansive phase.

**Aldaood et al. (2014)** investigated the behavior of gypseous soil stabilized with 3% lime and cured for 28 days and 90 days. The mineralogical analysis confirmed the appearance of the cementitious phase, such as CSH and CAH (**Fig 2-2**).

In the study of Li et al. (2016), in lime-treated halite-rich soil, the salt content remains stable during the curing process. where this salt does not participate in the chemical reaction within the soil-lime mixture, but is only precipitated into soil pores or adsorbed onto the soil surface.

Nan et al. (2022) investigated the mechanical behavior and microstructure of saline soil stabilized by quicklime. Their findings show that natural saline soil contains calcite, albite, dolomite, kaolinite, albite, illite, chlorite, calcite, and quartz. After the addition of 3% quick lime and at 7 days of curing, the CSH gels were not identified by XRD pattern, but a decrease in quartz and increase in calcite indicate their formations with small quantities to be detected.

**Ying et al. (2020)** performed XRD tests on silty soil treated with 2% lime. The results of their study indicated that compared to the untreated samples, the quantities of illite, feldspar, quartz, chlorite, and kaolinite in the lime-treated silt after 5 months were rather similar, and no significant cementitious products appeared in XRD patterns. This is due to the low clay minerals fraction, which could not provide enough reactive silica and alumina to interact with lime, limiting the consumption of OH<sup>-</sup> and Ca<sup>2+</sup> ions in the pozzolanic reaction.

Moreover, the sulfate salts such as gypsum (CaSO<sub>4</sub>,2H<sub>2</sub>O) are highly associated with the formation of expansive phases in cemented soils such as Ettringite (Aldaood et al., 2014a, 2014b; Hunter, 1988; Jha and Sivapullaiah, 2015; Rajasekaran, 2005). In a highly alkaline environment, Ca<sup>2+</sup> and Al<sup>3+</sup> ions react with SO<sub>4</sub><sup>2-</sup> in the presence to produce such an expansive phase. Its reaction equation was simplified by Hunter (1988) as follows:

$$6\text{Ca}^{2+}$$
 (from lime or cement) +  $2\text{Al}(0\text{H})_4^-$  (released from caly or cement) +  $4(0\text{H})^-$  (from lime or cement) +  $3(\text{SO}_4)^{2-}$  (dissoultion of sulphate ions) +  $26\text{H}_2\text{O}$  (water)  $\rightarrow$  Ca<sub>6</sub>Al<sub>2</sub>(SO<sub>4</sub>)<sub>2</sub>(OH)<sub>12</sub>.  $26\text{H}_2\text{O}$  (ettringite) (8)

This phase can induce distress in the soil structure of cemented soils through heaving and/or consuming part of cementitious compounds (Hunter, 1988; Puppala et al., 1996). Besides, its negative effect could increase high moisture content (A. Aldaood et al., 2014a).

Ionization of calcium-based materials in soil pore water released Ca<sup>2+</sup> ions. These ions could react with atmospheric CO<sub>2</sub>, resulting in the precipitation of calcite (CaCO<sub>3</sub>), which is known as the carbonatation process. This process is unfavorable for soil stabilization due to its Ca<sup>2+</sup> consumption, which will obstruct the formation of cementitious compounds and thus limit the strength of development during curing. In other words, with curing time, a competition between cementitious products and calcite precipitation, in which the soil strength improvement is highly associated with this competition. Notably, the carbonation process is more pronounced with lime than cement, as the former provides higher Ca<sup>2+</sup> ions. Many researchers investigated the effect of carbonation of lime-treated soils (Das et al., 2022; Kleib et al., 2024; Padmaraj et al., 2024; Vitale et al., 2021). However, according to Vitale et al. (2021), carbonation is a time-scale reaction involving two progressive mechanisms. (i) Lime carbonation in the short term corresponds to the progressive carbonation of portlandite (ii) and carbonation of secondary reaction products in the long term, which weakens the cementing bonding bridges within soil particles.

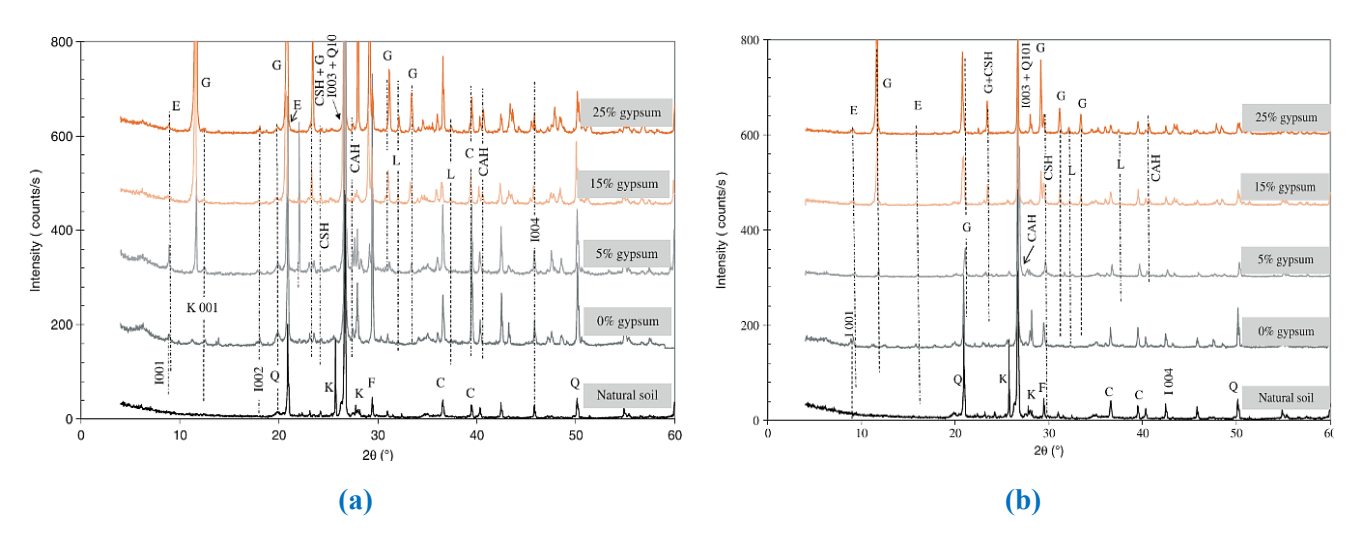


Fig 2-2. XRD patterns of the soil specimens: (a) after 28-day curing (b) and after 90-day soaking E, ettringite; L, lime; G, gypsum; Q, quartz; C, calcite; F, feldspars; K, kaolinite; I, illite.

#### 2.4.2. Fourier transform infrared spectroscopy characterization

If the products of the chemical reactions cannot be detected by XRD analysis due to their amorphas state and/ or too small size to be detected, the Fourier transform infrared spectroscopy (FTIR) and thermogravimetric (TG) tests could probably be best for these newly formed compounds (Wei et al., 2020). FTIR is a rapid, simple (low-cost), precise, and commonly available technique in universities and research laboratories (Higl et al., 2021; Shi et al., 2019). The FTIR gives qualitative and quantitative information (molecular information) about the different components of the specimen through its absorption and transmission of infrared radiation by the sample (Kaufhold et al., 2012). Besides, it provides information about the presence of physical or chemical reactions in the materials (Jozanikohan and Abarghooei, 2022).

In the analysis of untreated soil samples, several IR spectral bands were identified. The vibrations observed at 3696 cm<sup>-1</sup> and 3446 cm<sup>-1</sup> represent the presence of kaolinite and montmorillonite clay minerals (Xing et al., 2021). The band located at 1454 cm<sup>-1</sup>, attributed to O-C-O stretching vibration, indicates carbonate compounds within the soil matrix (Zhou et al., 2021). The bands noticed near 1115.0, 1031.0 and 1007.0 cm<sup>-1</sup> which can be related to Si–O stretching (Saeed and Fartosy, 2022). Further examination revealed bands at 871 cm<sup>-1</sup> and 713 cm<sup>-1</sup>, characteristic of calcite minerals (Gao et al., 2005). Additionally, the peak at 796 cm<sup>-1</sup> corresponds to Si-O symmetric stretching, indicating the presence of quartz (Mimboe et al., 2020). The observation of a peak at 695 cm<sup>-1</sup> suggests the existence of crystalline quartz minerals with high crystallinity (Chandrasekaran et al., 2015).

**Sharma et al. (2018)** conducted an experimental study on the independent roles of lime and cement in the stabilization of problematic soil. Meanwhile, XRD results indicated the formation of new peaks when lime/cement was added. The IR spectra showed a new absorption band at 1424 cm<sup>-1</sup>, corresponding to the development of the Ca-OH bond of lime/cement.

Wei et al. (2020) studied the stabilizing mechanism of stabilized saline soils (S) with four stabilizers, which are lime (L), cement (C), fly ash (FA), and SH agent (SH). Their findings indicate that the IR spectra were coherent with XRD results where there are no functional groups of L-SH-S compared to L-S, indicating that S-S did not react with lime or favored pozzolanic reaction.

#### 2.4.3. Thermogravimetric-differential thermal analysis

The Thermogravimetric-differential thermal analysis (TG-DTA) can identify quantitively (mass loss by TG) and qualitatively (peak range by DT) the soil mineralogy and cementitious products (Meng et al., 2021).

Al-Mukhtar et al. (2014) investigated the lime consumption by five soils that contain distinct clay minerals, which are illite, kaolinite, smectite, smectite-illite, and smectite-kaolinite with 10% lime content. The study suggested that the peaks between 110 and 400-500 °C correspond to the dehydration of the Ca-hydrates produced from the pozzolanic reaction. The peaks between about 400 and 550 °C characterize the dihydroxylation of kaolinite, and those between 500 and 650 °C are associated with smectite and illite (Fig 2-3). The later peak ranged around 600-650 °C and 700-750 °C, which is related to the decarbonization of calcite (from soil, with lime addition, and could be from lime carbonation). This is also confirmed by several researchers in which the dehydration of kaolinite minerals appeared around 520 °C (Cheng et al., 2010; YILMAZ, 2011) while the hydrates produced from pozzolanic reaction and cement hydration will decompose and dehydrate at temperature level around 440 °C(Hara et al., 2024; Kuliffayová et al., 2012; Tironi et al., 2014).

For the saline soils, the peaks appeared at 120 °C, 711 °C, and 1000 °C, corresponding to gypsum dehydration, calcite decomposition/decarbonization, and halite melting (Fatah et al., 2024; Hafhouf and Abbeche, 2023).

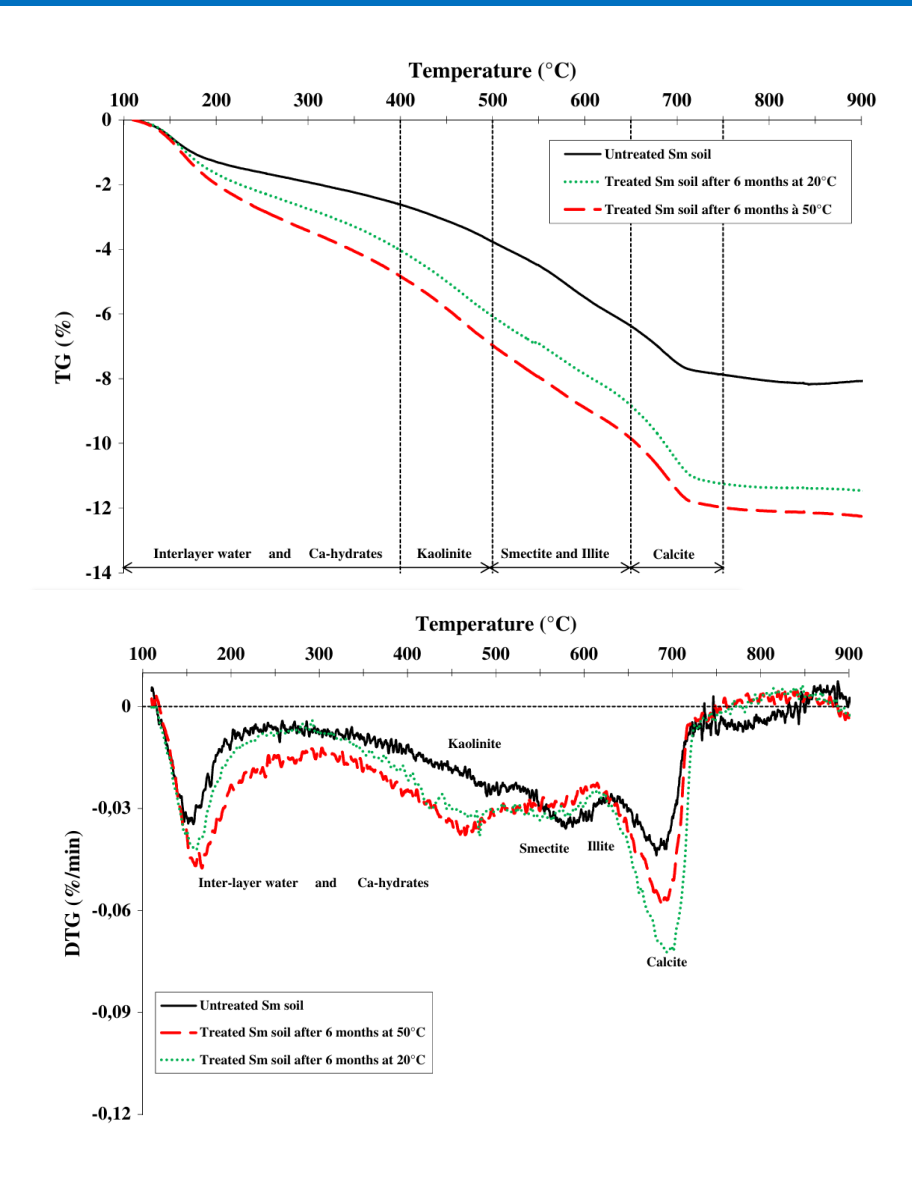


Fig 2-3. Thermogravimetric analysis of untreated and lime treated smectite (Sm) soil.

#### 2.4.4. pH & Electrical Conductivity (dS/m)

pH method is based on the concentration of the hydrogen ions (H<sup>+</sup>) and hydroxide (OH<sup>-</sup>) ions measured in water solution, which gives information about the soil's alkalinity or acidity. Those later properties highly affected the chemical reaction produced in soil pore water; thus, soil characteristics were also affected (Thomas, 1996). Besides, soil salinity is usually assessed by determining the total soluble salts through the electrical conductivity (EC) measurement of either a 1:5 distilled water: soil dilution or a saturated paste extract; however, the former is a more simple,

rapid, and precise method for soil salinity measurement (Hafhouf et al., 2022; Hardie and Doyle, 2012).

Wang et al. (2024) studied the conductivity evolution of stabilized chloride saline soil with ground granulated blast furnace slag (GS) and calcium carbide residue (CR) compared to traditional binder PC. EC of cemented soil revealed a decreasing trend with the curing period (Fig 2-4a). EC of the GS/CR binder ratio of 80/10 or 4/1 at 7 days is 4.56 dS/m, which is 21.4% less than that of the PC specimens, and its conductivity at 28 days is around 14.7% lower than at 7 days. Moreover, the soil's EC is highly related to the strength development in cemented soils due to the UCS with the curing period (Fig 2-4a and b). These results were coherent with those of Zhang et al. (2015), who found that an increase in EC has an adverse effect on structural soil stability.

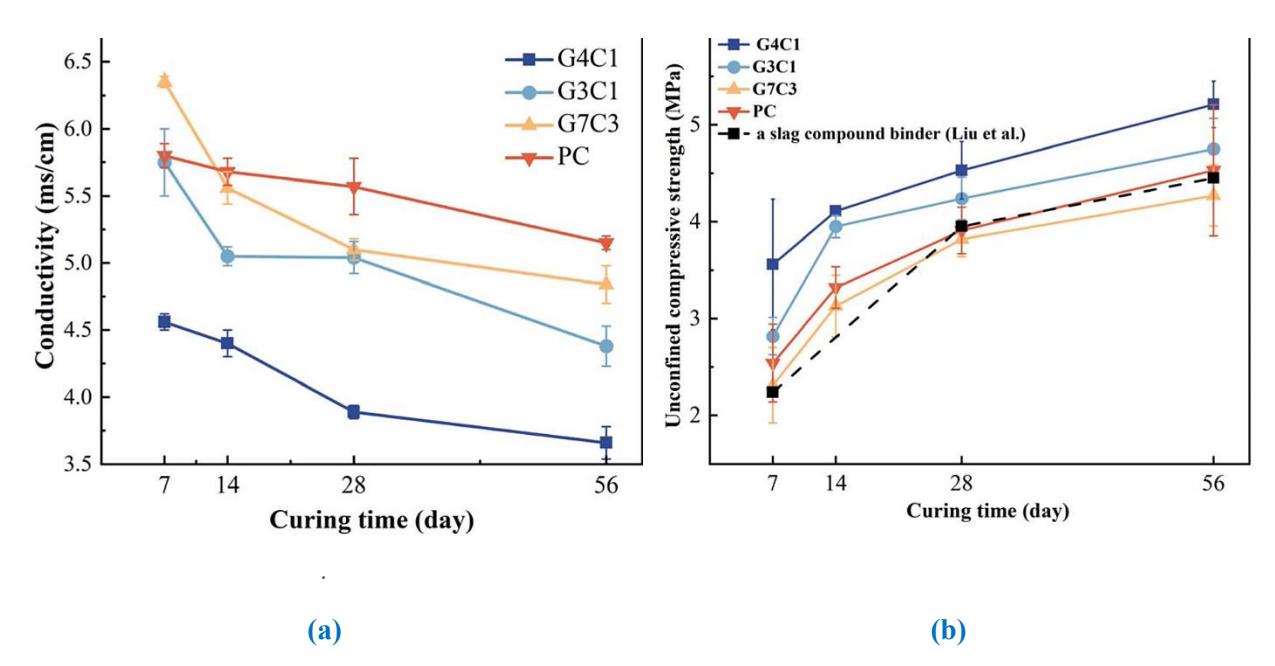


Fig 2-4. Relationship between: (a) EC of modified soil and curing period and (b) UCS of modified soil and curing period

To this end, although several studies have been conducted on the strength of treated-saline soils considering their physiochemical and mineralogical variations, less effort has been focused on literature to study such behavior for Sebkha soils. Moreover, to the author's knowledge, no research study has been devoted to the subject of carbonation effects on the micro-macro behavior of cemented Sebkha soils and even saline soils.

### 2.5. Salinity effect on the physic-chemical and geotechnical properties of treated saline (Sebkha) soils

Aldaood et al. (2021) investigated the influence of gypsum (0, 5, 15, and 25% by dry mass) and lime (0, 3, and 10% by dry mass) amounts on the UCS of a fine-grained soil considering their mineralogical and microstructural variations. Besides, the effects of curing periods and temperature were also studied. The results indicate that in addition to curing time, the percentage of lime also had an influence on the UCS of modified soil with gypsum. Indeed, the optimum lime and gypsum content beyond which the development of strength was reduced was 5%. After 28d of curing, the XRD patterns showed that the plain soil contained calcite, quartz, kaolinite, illite, and feldspars, while in the modified gypseous, new products can be observed with low to moderate intensity peaks. Which involved ettringite mineral and pozzolanic compounds (CAH and CSH). Moreover, kaolinite peaks decreased with curing time while that of illite remained almost constant, indicating that illite participated less in the pozzolanic reaction than kaolinite. From 28d to 180d of curing, no apparent variations in mineralogical properties can be observed. However, this does not indicate that no new phases were produced since the decrease in pH and EC value can be associated with producing new compounds (Al-Mukhtar et al., 2010). For the pH measurement, the effect of gypsum contents seems insignificant. The pH values decreased gradually with curing time for 3% and 5% lime addition, indicating lime consumption in pozzolanic reaction with time. In comparison, with a 10% lime addition, no noticeable decrease was observed due to the availability of unreacted lime (Fig 2-5). For the EC measurement, the same behavior was observed compared to that of pH (Fig 2-6), which indicates that both EC and pH can be good tests for evaluating the development of the pozzolanic and hydration reactions.

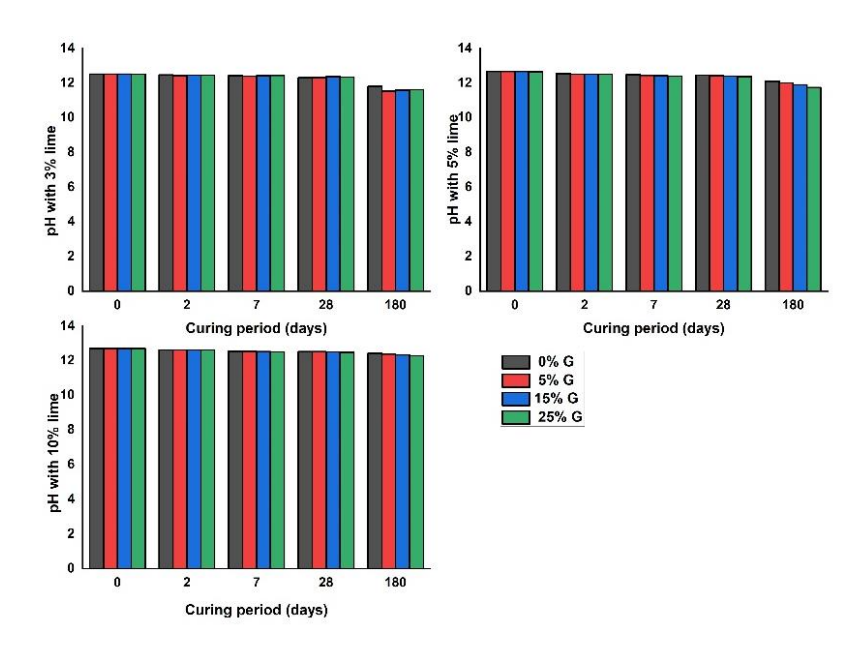


Fig 2-5. Effects of gypsum and lime contents on the pH of treated soil for different cured period (Aldaood et al., 2021).

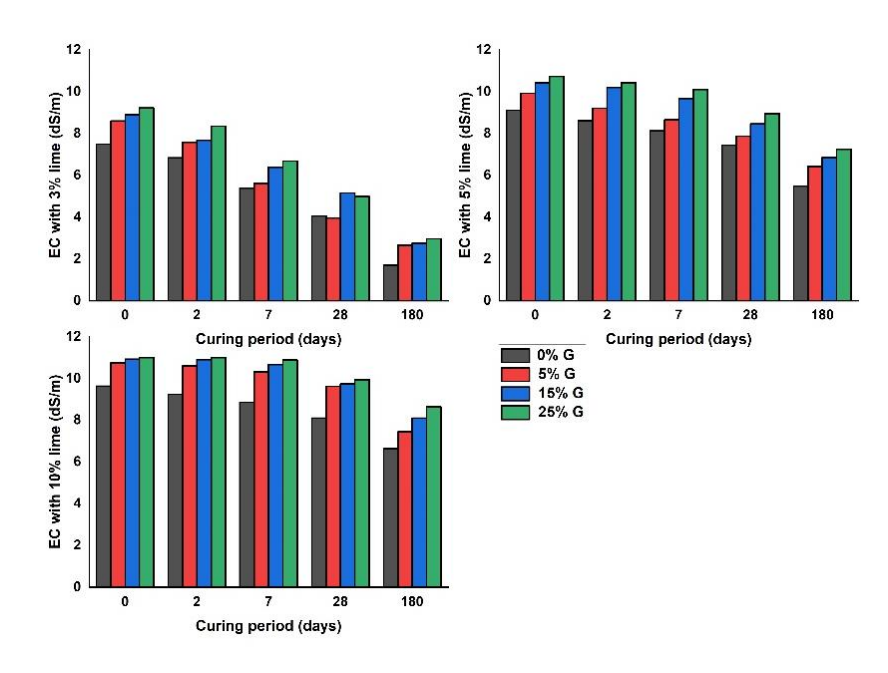


Fig 2-6. Effects of gypsum and lime contents on the EC of treated soil for different cured period (Aldaood et al., 2021).

Lv et al. (2018) investigated the effect of salt content (0.3%,0.8%,1.3%,1.8%,2.3%, and 2.8% by dry weight) on the UCS of treated sulfate saline soil with lime-fly ash, sodium silicate, and their

combination. The results showed an optimum salt content of 1.8%, after which the strength development was reduced. Moreover, the IR peaks obtained revealed no prominent hydration products; however, these peaks shift to lower wavenumbers, changing a certain functional group with less vibration energy and thus demonstrating the effect on the chemical environment (new phases mainly were formed).

**Ebailila et al. (2022)** conducted tests on the effect of gypsum (G) contents (0, 3, 6, and 9 % by dry soil) on the physicochemical and mechanical behavior of treated soil with 4 and 6% lime (L) addition considering. The high UCS value was obtained with a G/L ratio of 1.5 due to the pozzolanic reactions and ettringite minerals observed in DTG results. However, ettringite formation depends on gypsum, lime, humid conditions, and curing time.

Li et al. (2016) studied the effect of chlorine salt on the physical and mechanical properties of inshore saline soil treated with 12% lime. Their findings indicate that the UCS decreased by 50% with increasing salt content up to 8%, which revealed the adverse effect of salt content on treated soil structure. Moreover, the conductivity remained almost constant with curing period times, indicating that no new ions were produced during curing and that chlorine did not participate in the chemical reaction.

**Xing et al.** (2009) carried out tests on salt-rich soil treated with cement, including UCS and X-ray diffraction tests. Their findings indicated that the strength of the treated soil was not enhanced. This was attributed to the presence of Cl<sup>-</sup>and Mg<sup>2+</sup>, which hinder the formation of CSH and CAH, reducing the cementitious bonding between soil particles and thereby obstructing soil strength development.

Hafhouf et al. (2022) investigated the strength behavior of the Sebkha under the effect of salinity (expressed by ECe) and drying-wetting (D-W) cycles. With increasing D-W cycles, both UCS and ECe decreased. Indeed, ECe decreased during the D-W cycles, in which ECe decreased from 16.5 dS/m to 3.8 dS/m for the first and fourth D-W cycles, respectively. However, the pH slightly increased from 6.53 to 7.04 for the first and fourth D-W cycles. This is confirmed also by Xinlu et al. (2020), in which a positive connection/correlation can be found between EC and soil salinity. From the above-mentioned research studies, salinity effect of the physic-chemical and mechanical properties of untreated and treated Sebkha soil is rare. To the author's knowledge, there is only a recent study that investigated the effects of salt content on Sebkha soil using the deep soil mixing (DSM) method (Hammad et al., 2023). Therefore, it was interesting to investigate some macro

and micro behavior of untreated and treated Sebkha with a traditional binder (lime and cement), which can aid geotechnical engineers in ensuring the stability of structures when this soil type is encountered in situ.

#### 2.6. Conclusion

This chapter discussed the physic-chemical and mechanical behavior of untreated and treated saline (Sebkha) soils in which the mechanism of treated soil with calcium-based materials (i.e., lime and cement) is first presented, after which the micro-macro behavior of saline (Sebkha) soils considering the effects of salinity is followed. The following conclusions can be drawn:

- (1) Heterogeneity of Sebkha system from one region to another one and even in same location renders this kind of soil unique, and thus, its geotechnical properties, such as UCS and GSDC, should be investigated considering its chemical and mineralogical variations. Moreover, a high potential for construction problems has been associated with this unusual soil.
- (2) Due to the dissolution-crystallization of salts within soil fabric under humidity, grain size distribution curve variation is highly anticipated for two main reasons: (i) a decrease in solid portion for a specific mass unit where some crystals transform to fluid; (ii) a decrease in coarser aggregates due to solubility of bonding bridge between soil particles. To this end, studying such physical properties is crucial to understanding Sebkha behavior, especially from the strength side, as the strength state is strongly associated with the grain size distribution curve.
- (3) Carbonation is adversely affected cemented soils. However, rare studies investigated the calcite precipitation on the strength of untreated and Sebkha treated. Moreover, even in saline soils, this effect does not exist.
- (4) In situ field conditions, the salinity of Sebkha is repeatedly varied by underwater precipitation (salinity decreased) and water evaporation (salinity increased). However, in the literature, the salinity effect on Sebkha's physicochemical and mechanical behavior is rare, indicating the crucial need to investigate such behavior.

#### References

- Abduljauwad, S.N., Al-Amoudi, O.S.B., 1995. Geotechnical behaviour of saline sabkha soils. Géotechnique 45, 425–445. https://doi.org/10.1680/geot.1995.45.3.425
- Aiban, Sa., Al-Ahmadi, Hm., Asi, Im., Siddique, Zu., Al-Amoudi, O.S.B., 2006. Effect of geotextile and cement on the performance of sabkha subgrade. Building and Environment 41, 807–820.
- Akula, P., Little, D.N., 2020. Analytical tests to evaluate pozzolanic reaction in lime stabilized soils. MethodsX 7, 100928.
- Al-Amoudi, O.S.B., 2008. Testing and stabilization of saline sabkha soils: a review.
- Al-Amoudi, O.S.B., 2002. Characterization and Chemical Stabilization of Al-Qurayyah Sabkha Soil. J. Mater. Civ. Eng. 14, 478–484. https://doi.org/10.1061/(ASCE)0899-1561(2002)14:6(478)
- Al-Amoudi, O.S.B., 1994. Chemical stabilization of sabkha soils at high moisture contents. Engineering geology 36, 279–291.
- Al-Amoudi, O.S.B., Abduljauwad, S.N., El-Naggar, Z.R., 1992. Response of sabkha to laboratory tests: a case study. Engineering Geology 33, 111–125.
- Al-Amoudi, O.S.B., Asi, I.M., El-Naggar, Z.R., 1995. Stabilization of an arid, saline sabkha soil using additives. Quarterly Journal of Engineering Geology 28, 369–379.
- Al-Ayedi, E.S., 1996. Chemical stabilization of Al-Qurayyah eastern Saudi sabkha soil (Master's Thesis). King Fahd University of Petroleum and Minerals (Saudi Arabia).
- Al-Dakheeli, H., Bulut, R., Scott Garland, G., Clarke, C.R., 2021. Utilization of Blast-Furnace Slag as a Standalone Stabilizer for High Sulfate-Bearing Soils. J. Mater. Civ. Eng. 33, 04021257. https://doi.org/10.1061/(ASCE)MT.1943-5533.0003880
- Aldaood, A., Bouasker, M., Al-Mukhtar, M., 2021. Mechanical behavior of gypseous soil treated with lime. Geotechnical and Geological Engineering 39, 719–733.
- Aldaood, A., Bouasker, M., Al-Mukhtar, M., 2014a. Impact of wetting-drying cycles on the microstructure and mechanical properties of lime-stabilized gypseous soils. Engineering Geology 174, 11-21.
- Aldaood, A., Bouasker, M., Al-Mukhtar, M., 2014b. Geotechnical properties of lime-treated gypseous soils. Applied Clay Science 88, 39–48.

- Aldaood, Abdulrahman, Bouasker, M., Al-Mukhtar, M., 2014. Soil-water characteristic curve of lime treated gypseous soil. Applied Clay Science 102, 128-138.
- Al-Homidy, A.A., Dahim, M.H., Abd El Aal, A.K., 2017. Improvement of geotechnical properties of sabkha soil utilizing cement kiln dust. Journal of Rock Mechanics and Geotechnical Engineering 9, 749–760.
- Al-Mukhtar, M., Khattab, S., Alcover, J.-F., 2012. Microstructure and geotechnical properties of lime-treated expansive clayey soil. Engineering geology 139, 17–27.
- Al-Mukhtar, M., Lasledj, A., Alcover, J.F., 2014. Lime consumption of different clayey soils. Applied Clay Science 95, 133–145.
- Al-Mukhtar, M., Lasledj, A., Alcover, J.-F., 2010. Behaviour and mineralogy changes in limetreated expansive soil at 20 C. Applied clay science 50, 191–198.
- Al-Otaibi, F.A., 2006. Assessment of the possibility of stabilising Sabkha soils using oil lake residue—Reuse of waste materials. Cardiff University (United Kingdom).
- Aziz, M., Sheikh, F.N., Qureshi, M.U., Rasool, A.M., Irfan, M., 2021. Experimental Study on Endurance Performance of Lime and Cement-Treated Cohesive Soil. KSCE J Civ Eng 25, 3306–3318. https://doi.org/10.1007/s12205-021-2154-7
- Bell, F.G., 1996. Lime stabilization of clay minerals and soils. Engineering geology 42, 223-237.
- Benrebouh, I., Douadi, A., Hafhouf, I., Merdas, A., Meguellati, A., 2024a. Transformative Effects of Salinity on Sebkha Soil Properties: Unveiling Strength, Structure, and Stability through Advanced Remediation Strategies. Journal of Architectural and Engineering Research 7, 60-70.
- Benrebouh, I., Hafhouf, I., Douadi, A., Merdas, A., Marathe, S., 2025. Effect of sulfate resistance cement treatment on saline soil (Sebkha) subgrades. Indian Geotechnical Journal 1–19.
- Benrebouh, I., Hafhouf, I., Douadi, A., Merdas, A., Meguellati, A., Faria, P., 2024b. Salinity Effects on the Physicochemical and Mechanical Behavior of Untreated and Lime-Treated Saline Soils. Minerals 14, 1217.
- Bhattacharja, S., Bhatty, J., 2003. Comparative performance of portland cement and lime stabilization of moderate to high plasticity clay soils. Portl. Cem. Assoc 2066, 60-67.
- Bhuvaneshwari, S., Robinson, R.G., Gandhi, S.R., 2014. Behaviour of lime treated cured expansive soil composites. Indian Geotechnical Journal 44, 278–293.

- Cabane, N., 2004. Sols traités à la chaux et aux liants hydrauliques: Contribution à l'identification et à l'analyse des éléments perturbateurs de la stabilisation (PhD Thesis). Université Jean Monnet-Saint-Etienne.
- Chandrasekaran, A., Ravisankar, R., Rajalakshmi, A., Eswaran, P., Vijayagopal, P., Venkatraman, B., 2015. Assessment of natural radioactivity and function of minerals in soils of Yelagiri hills, Tamilnadu, India by Gamma Ray spectroscopic and Fourier Transform Infrared (FTIR) techniques with statistical approach. Spectrochimica Acta Part A: Molecular and Biomolecular Spectroscopy 136, 1734–1744.
- Cheng, H., Yang, J., Liu, Q., He, J., Frost, R.L., 2010. Thermogravimetric analysis-mass spectrometry (TG-MS) of selected Chinese kaolinites. Thermochimica Acta 507, 106– 114.
- Cho, G.-C., Dodds, J., Santamarina, J.C., 2007. Closure to "Particle Shape Effects on Packing Density, Stiffness, and Strength: Natural and Crushed Sands" by Gye-Chun Cho, Jake Dodds, and J. Carlos Santamarina. J. Geotech. Geoenviron. Eng. 133, 1474–1474. https://doi.org/10.1061/(ASCE)1090-0241(2007)133:11(1474)
- Ciancio, D., Beckett, C.T.S., Carraro, J.A.H., 2014. Optimum lime content identification for lime-stabilised rammed earth. Construction and Building Materials 53, 59–65.
- Committee, A.C.I., 1990. State-of-the-art report on soil cement. ACI Materials Journal 87, 8-12.
- Consoli, N.C., Bittar Marin, E.J., Quiñónez Samaniego, R.A., Scheuermann Filho, H.C., Miranda, T., Cristelo, N., 2019. Effect of Mellowing and Coal Fly Ash Addition on Behavior of Sulfate-Rich Dispersive Clay after Lime Stabilization. J. Mater. Civ. Eng. 31, 04019071. https://doi.org/10.1061/(ASCE)MT.1943-5533.0002699
- Consoli, N.C., Da Silva Lopes, L., Foppa, D., Heineck, K.S., 2009. Key parameters dictating strength of lime/cement-treated soils. Proceedings of the Institution of Civil Engineers -Geotechnical Engineering 162, 111–118. https://doi.org/10.1680/geng.2009.162.2.111
- Das, G., Razakamanantsoa, A., Saussaye, L., Losma, F., Deneele, D., 2022. Carbonation investigation on atmospherically exposed lime-treated silty soil. Case Studies in Construction Materials 17, e01222.
- Eades, J.L., Grim, R.E., 1966. A quick test to determine lime requirements for lime stabilization. Highway research record.

- Ebailila, M., Kinuthia, J., Oti, J., 2022. Role of gypsum content on the long-term performance of lime-stabilised soil. Materials 15, 5099.
- Emarah, D.A., Seleem, S.A., 2018. Swelling soils treatment using lime and sea water for roads construction. Alexandria engineering journal 57, 2357–2365.
- Fatah, A., Al-Yaseri, A., Theravalappil, R., Radwan, O.A., Amao, A., Al-Qasim, A.S., 2024. Geochemical reactions and pore structure analysis of anhydrite/gypsum/halite bearing reservoirs relevant to subsurface hydrogen storage in salt caverns. Fuel 371, 131857. https://doi.org/10.1016/j.fuel.2024.131857
- Fattahpour, V., Baudet, B.A., Moosavi, M., Mehranpour, M., Ashkezari, A., 2014. Effect of grain characteristics and cement content on the unconfined compressive strength of artificial sandstones. International Journal of Rock Mechanics and Mining Sciences 72, 109–116.
- Firoozi, Ali Akbar, Guney Olgun, C., Firoozi, Ali Asghar, Baghini, M.S., 2017. Fundamentals of soil stabilization. Geo-Engineering 8, 26. https://doi.org/10.1186/s40703-017-0064-9
- Gao, B.-Y., Chu, Y.-B., Yue, Q.-Y., Wang, B.-J., Wang, S.-G., 2005. Characterization and coagulation of a polyaluminum chloride (PAC) coagulant with high A113 content. Journal of environmental management 76, 143–147.
- Hafhouf, I., Abbeche, K., 2023. Impact of drying-wetting cycles on shear properties, suction, and collapse of sebkha soils. Heliyon 9.
- Hafhouf, I., Bahloul, O., Abbeche, K., 2022. Effects of drying-wetting cycles on the salinity and the mechanical behavior of sebkha soils. A case study from Ain M'Lila, Algeria. Catena 212, 106099.
- Hammad, M.A., Mohamedzein, Y., Al-Aghbari, M., 2023. Improving the Properties of Saline Soil Using a Deep Soil Mixing Technique. CivilEng 4, 1052–1070.
- Hammad, M.A., Mohamedzein, Y.E.-A., Al-Aghbari, M., 2024. Effect of Salt Content on Sabkha Soil Using Deep Soil Mixing Technique: Physical and Numerical Modelling.
- Hara, H., Ikeda, K., Yoshimoto, N., 2024. Strength reduction mechanism of cement-treated soil under seawater environment. Soils and Foundations 64, 101425.
- Hardie, M., Doyle, R., 2012. Measuring Soil Salinity, in: Shabala, S., Cuin, T.A. (Eds.), Plant Salt Tolerance, Methods in Molecular Biology. Humana Press, Totowa, NJ, pp. 415–425. https://doi.org/10.1007/978-1-61779-986-0\_28

- Hatefi, M.H., Arabani, M., Payan, M., Ranjbar, P.Z., 2024. The influence of volcanic ash (VA) on the mechanical properties and freeze-thaw durability of lime kiln dust (LKD)-stabilized kaolin clayey soil. Results in Engineering 24, 103077.
- Hebbache, K., Boutlikht, M., Douadi, A., Belebchouche, C., Benrebouh, I., Hammouche, R., Moretti, L., Chajec, A., Czarnecki, S., 2024. Integrated Techno-Environmental Analysis of Finely Ground Silica Sand in Sustainable Mortar Production. Buildings 14, 3295.
- Higl, J., Hinder, D., Rathgeber, C., Ramming, B., Lindén, M., 2021. Detailed in situ ATR-FTIR spectroscopy study of the early stages of CSH formation during hydration of monoclinic C3S. Cement and Concrete Research 142, 106367.
- Hilt, G.H., Davidson, D.T., 1960. Lime fixation in clayey soils. Highway Research Board Bulletin.
- Hunter, D., 1988. Lime-Induced Heave in Sulfate-Bearing Clay Soils. J. Geotech. Engrg. 114, 150–167. https://doi.org/10.1061/(ASCE)0733-9410(1988)114:2(150)
- Hussain, W.A.S., Awn, S.H.A., 2015. Effect of some chemical additives on the behavior of sabkha soil. Journal of Engineering and Sustainable Development 19, 1–17.
- Jha, A.K., Sivapullaiah, P.V., 2015. Mechanism of improvement in the strength and volume change behavior of lime stabilized soil. Engineering Geology 198, 53-64.
- Jozanikohan, G., Abarghooei, M.N., 2022. The Fourier transform infrared spectroscopy (FTIR) analysis for the clay mineralogy studies in a clastic reservoir. J Petrol Explor Prod Technol 12, 2093–2106. https://doi.org/10.1007/s13202-021-01449-y
- Kaufhold, S., Hein, M., Dohrmann, R., Ufer, K., 2012. Quantification of the mineralogical composition of clays using FTIR spectroscopy. Vibrational Spectroscopy 59, 29–39.
- Kleib, J., Lesueur, D., Maherzi, W., Benzerzour, M., 2024. Carbonation of a lime treated soil subjected to different curing conditions. Transportation Geotechnics 44, 101174.
- Kuliffayová, M., Krajči, L., Janotka, I., Šmatko, V., 2012. Thermal behaviour and characterization of cement composites with burnt kaolin sand. Journal of thermal analysis and calorimetry 108, 425–432.
- Li, H., Yang, M., 2024. Study on unconfined compressive strength and deformation characteristics of chlorine saline soil. Scientific Reports 14, 1478.

- Li, J., Lin, H., Liu, J., Fang, J., 2023. Macro-micro characteristics of geopolymer-stabilized saline soil in seasonal frozen soil region. Case Studies in Construction Materials 19, e02496.
- Li, M., Chai, S., Du, H., Wang, C., 2016. Effect of chlorine salt on the physical and mechanical properties of inshore saline soil treated with lime. Soils and Foundations 56, 327–335.
- Li, W., Yi, Y., Puppala, A.J., 2022. Effects of curing environment and period on performance of lime-GGBS-treated gypseous soil. Transportation Geotechnics 37, 100848.
- Li, Y., 2013. Effects of particle shape and size distribution on the shear strength behavior of composite soils. Bulletin of Engineering Geology and the Environment 72, 371–381.
- Liu, L., Li, Z., Liu, X., Li, Y., 2018. Effect of salt content on freezing temperature and unconfined compression strength of lime-treated subgrade clay. Applied Clay Science 158, 65-71.
- Liu, M.D., Indraratna, B., Horpibulsuk, S., Suebsuk, J., 2012. Variations in strength of limetreated soft clays. Proceedings of the Institution of Civil Engineers - Ground Improvement 165, 217–223. https://doi.org/10.1680/grim.11.00025
- Liu, Y., Wang, Q., Liu, S., ShangGuan, Y., Fu, H., Ma, B., Chen, H., Yuan, X., 2019.
  Experimental investigation of the geotechnical properties and microstructure of lime-stabilized saline soils under freeze-thaw cycling. Cold Regions Science and Technology 161, 32–42.
- Lv, Q., Jiang, L., Ma, B., Zhao, B., Huo, Z., 2018. A study on the effect of the salt content on the solidification of sulfate saline soil solidified with an alkali-activated geopolymer. Construction and Building Materials 176, 68-74.
- Marks, B.D., Haliburton, T.A., 1972. Acceleration of Lime-Clay Reactions with Salt. J. Soil Mech. and Found. Div. 98, 327–339. https://doi.org/10.1061/JSFEAQ.0001742
- Meng, H., Shu, S., Gao, Y., Yan, B., He, J., 2021. Multiple-phase enzyme-induced carbonate precipitation (EICP) method for soil improvement. Engineering Geology 294, 106374.
- Mimboe, A.G., Abo, M.T., Djobo, J.N.Y., Tome, S., Kaze, R.C., Deutou, J.G.N., 2020. Lateritic soil based-compressed earth bricks stabilized with phosphate binder. Journal of Building Engineering 31, 101465.
- Mitchell, J.K., Soga, K., 2005. Fundamentals of soil behavior. John Wiley & Sons New York.

- Modmoltin, C., Voottipruex, P., 2009. Influence of salts on strength of cement-treated clays.
  Proceedings of the Institution of Civil Engineers Ground Improvement 162, 15–26.
  https://doi.org/10.1680/grim.2009.162.1.15
- Mohamedzein, Y.E.-A., Al-Rawas, A.A., 2011. Cement-stabilization of sabkha soils from Al-Auzayba, Sultanate of Oman. Geotechnical and Geological Engineering 29, 999–1008.
- Mubaraki, M., 2019. Improving road construction on sabkha soil by using lime stabilization and groundwater table monitoring. Journal of Testing and Evaluation 47, 1935–1948.
- Nan, J., Liu, J., Chang, D., Li, X., 2022. Mechanical characteristics and microstructure study of saline soil stabilized by quicklime after curing and freeze-thaw cycle. Cold Regions Science and Technology 201, 103625.
- Nelson, J., Miller, D.J., 1997. Expansive soils: problems and practice in foundation and pavement engineering. John Wiley & Sons.
- Padmaraj, D., Cherian, C., Arnepalli, D.N., 2024. Multi-scale analysis of carbon mineralization in lime-treated soils considering soil mineralogy. Journal of Rock Mechanics and Geotechnical Engineering.
- Pai, R.R., Patel, S., 2019. Effect of GGBS and Lime on the Strength Characteristics of Black Cotton Soil, in: Thyagaraj, T. (Ed.), Ground Improvement Techniques and Geosynthetics, Lecture Notes in Civil Engineering. Springer Singapore, Singapore, pp. 319–328. https://doi.org/10.1007/978-981-13-0559-7\_36
- Pongsivasathit, S., Horpibulsuk, S., Piyaphipat, S., 2019. Assessment of mechanical properties of cement stabilized soils. Case Studies in Construction Materials 11, e00301.
- Prakasha, K.S., Chandrasekaran, V.S., 2005. Behavior of Marine Sand-Clay Mixtures under Static and Cyclic Triaxial Shear. J. Geotech. Geoenviron. Eng. 131, 213–222. https://doi.org/10.1061/(ASCE)1090-0241(2005)131:2(213)
- Puppala, A.J., Mohammad, L.N., Allen, A., 1996. Engineering Behavior of Lime-Treated Louisiana Subgrade Soil. Transportation Research Record 1546, 24–31. https://doi.org/10.1177/0361198196154600103
- Rajasekaran, G., 2005. Sulphate attack and ettringite formation in the lime and cement stabilized marine clays. Ocean engineering 32, 1133–1159.
- Saeed, K.A., Fartosy, S.H., 2022. Using Infrared Spectroscopy to Examine the Influences of Stabilizers on the Molecular Structure of Stabilized Contaminated Clay Soils. in:

- Karkush, M.O., Choudhury, D. (Eds.), Geotechnical Engineering and Sustainable Construction. Springer Singapore, Singapore, pp. 781–791. https://doi.org/10.1007/978-981-16-6277-5\_63
- Santos, T., Gomes, M.I., Silva, A.S., Ferraz, E., Faria, P., 2020. Comparison of mineralogical, mechanical and hygroscopic characteristic of earthen, gypsum and cement-based plasters. Construction and Building Materials 254, 119222.
- Sariosseiri, F., Muhunthan, B., 2009. Effect of cement treatment on geotechnical properties of some Washington State soils. Engineering geology 104, 119–125.
- Shabel, I.M., 2006. Stabilization of Jizan sabkha soil using cement and cement kiln dust. Civil Engineering Department, College of Engineering, King Saud University.
- Sharma, L.K., Sirdesai, N.N., Sharma, K.M., Singh, T.N., 2018. Experimental study to examine the independent roles of lime and cement on the stabilization of a mountain soil: A comparative study. Applied Clay Science 152, 183–195.
- Shi, T., Gao, Y., Corr, D.J., Shah, S.P., 2019. FTIR study on early-age hydration of carbon nanotubes-modified cement-based materials. Advances in Cement Research 31, 353–361.
- Shooshpasha, I., Shirvani, R.A., 2015. Effect of cement stabilization on geotechnical properties of sandy soils. Geomech Eng 8, 17–31.
- Talero, R., Trusilewicz, L., Delgado, A., Pedrajas, C., Lannegrand, R., Rahhal, V., Mejía, R., Delvasto, S., Ramírez, F.A., 2011. Comparative and semi-quantitative XRD analysis of Friedel's salt originating from pozzolan and Portland cement. Construction and building materials 25, 2370–2380.
- Tang, A.M., Vu, M.N., Cui, Y.-J., 2011. Effects of the maximum soil aggregates size and cyclic wetting-drying on the stiffness of a lime-treated clayey soil. Géotechnique 61, 421-429. https://doi.org/10.1680/geot.SIP11.005
- Thomas, G.W., 1996. Soil pH and soil acidity. Methods of soil analysis: part 3 chemical methods 5, 475–490.
- Tironi, A., Trezza, M.A., Scian, A.N., Irassar, E.F., 2014. Thermal analysis to assess pozzolanic activity of calcined kaolinitic clays. Journal of Thermal Analysis and Calorimetry 117, 547–556.

- Tran, T.D., Cui, Y.-J., Tang, A.M., Audiguier, M., Cojean, R., 2014. Effects of lime treatment on the microstructure and hydraulic conductivity of Héricourt clay. Journal of Rock Mechanics and Geotechnical Engineering 6, 399–404.
- Verbrugge, J.-C., De Bel, R., Correia, A.G., Duvigneaud, P.-H., Herrier, G., 2011. Strength and Micro Observations on a Lime Treated Silty Soil, in: Road Materials and New Innovations in Pavement Engineering. Presented at the GeoHunan International Conference 2011, American Society of Civil Engineers, Hunan, China, pp. 89–96. https://doi.org/10.1061/47634(413)12
- Vitale, E., Deneele, D., Russo, G., 2021. Effects of carbonation on chemo-mechanical behaviour of lime-treated soils. Bull Eng Geol Environ 80, 2687–2700. https://doi.org/10.1007/s10064-020-02042-z
- Wang, Y., Duc, M., Cui, Y.-J., Tang, A.M., Benahmed, N., Sun, W.J., Ye, W.M., 2017. Aggregate size effect on the development of cementitious compounds in a lime-treated soil during curing. Applied Clay Science 136, 58–66.
- Wang, Z., Zhu, J., Ma, T., 2024. Review on monitoring of pavement subgrade settlement: Influencing factor, measurement and advancement. Measurement 115225.
- Wei, L., Chai, S., Guo, Q., Wang, P., Li, F., 2020. Mechanical properties and stabilizing mechanism of stabilized saline soils with four stabilizers. Bull Eng Geol Environ 79, 5341–5354. https://doi.org/10.1007/s10064-020-01885-w
- Xing, H., Yang, X., Xu, C., Ye, G., 2009. Strength characteristics and mechanisms of salt-rich soil-cement. Engineering Geology 103, 33-38.
- Xing, Z., Du, C., Shen, Y., Ma, F., Zhou, J., 2021. A method combining FTIR-ATR and Raman spectroscopy to determine soil organic matter: Improvement of prediction accuracy using competitive adaptive reweighted sampling (CARS). Computers and Electronics in Agriculture 191, 106549.
- Xinlu, L., Jie, P., Chunhui, F., 2020. Inversion model for soil conductivity in cotton field in South Xinjiang based on EM38-MK2 data. Acta Pedologica Sinica 57, 646–655.
- YILMAZ, G., 2011. The effects of temperature on the characteristics of kaolinite and bentonite. Scientific research and essays 6.
- Ying, Z., 2021. Hydro-mechanical behavior of lime-treated/untreated soils under the effects of salinity and wetting-drying cycles (PhD Thesis). École des Ponts ParisTech.

- Ying, Z., Cui, Y.-J., Benahmed, N., Duc, M., 2022a. Changes in microstructure and water retention property of a lime-treated saline soil during curing. Acta Geotech. 17, 319–326. https://doi.org/10.1007/s11440-021-01218-5
- Ying, Z., Cui, Y.-J., Duc, M., Benahmed, N., 2022b. Effect of salt solution on the optimum lime contents of bentonite and silt. Acta Geotech. 17, 3731–3745. https://doi.org/10.1007/s11440-022-01488-7
- Zhang, D., Liu, S., Fan, L., Deng, Y., 2012. Effect of Salt Concentrations on the Electrical Resistivity of Cement-Treated Soils, in: GeoCongress 2012. Presented at the GeoCongress 2012, American Society of Civil Engineers, Oakland, California, United States, pp. 1016–1025. https://doi.org/10.1061/9780784412121.105
- Zhang, T., Wang, T., Liu, K.S., Wang, L., Wang, K., Zhou, Y., 2015. Effects of different amendments for the reclamation of coastal saline soil on soil nutrient dynamics and electrical conductivity responses. Agricultural water management 159, 115–122.
- Zhou, S., Li, J., Rong, L., Xiao, J., Liu, Y., Duan, Y., Chu, L., Li, Q., Yang, L., 2021.
  Immobilization of uranium soils with alkali-activated coal gangue-based geopolymer. J
  Radioanal Nucl Chem 329, 1155–1166. https://doi.org/10.1007/s10967-021-07812-x
- Zi, Y., Cui, Y., Benahmed, N., Duc, M., 2020. Changes in mineralogy and microstructure of a lime-treated silty soil during curing time, in: E3S Web of Conferences. EDP Sciences, p. 03044.

#### **CHAPTER 3.**

# SALINITY EFFECTS ON THE PHYSICOCHEMICAL AND MECHANICAL BEHAVIOR OF UNTREATED AND LIME-TREATED SALINE SOILS (SEBKHA SOILS)

#### 3.1. Introduction

In semi-arid and arid climates, soil salinity is considered one of the main problems for engineering practice, inducing soil degradation and structure instability and thus limiting sustainable development. In dry conditions, those salts are considered natural cementing bonds between soil particles giving strength to the soil. However, with seasonal water action within saline soil (Sebkha soil), some solid parts (i.e., salt crystals) turned into a liquid phase after dissolving, resulting in simultaneous/double movement of water and soluble salts within the soil fabric. This effect results in serious strength failure that depends on the decreasing bonding cementing bridge and the decreasing solid portion. Therefore, investigating salinity effects on the strength of soils considering their physicochemical behaviour is crucial. While untreated Sabkha soils often exhibit poor engineering properties, lime treatment has emerged as a potential solution for improving their performance. Lime is a common stabilization technique which proves its effectiveness for problematic soils. Therefore, this chapter examines the relationship between salinity levels and the mechanical behaviour of untreated and lime-treated Ain M'lila Sebkha soils, focusing on changes in their physicochemical properties with curing periods. Unconfined compressive strength, granulometry and carbonation tests were first conducted. After that, X-ray diffraction, X-ray fluorescence, and thermogravimetricdifferential thermal analysis were used to monitor chemical reaction development and their potential interaction with soluble salts.

Sebkha soils are saline soils containing salts that are hygroscopic, soluble in and transported by water. These soils develop in regions where evaporation rates exceed rainfall. The salinity of the Sebkha is mainly influenced by natural conditions such as drying-wetting cycles. When the Sebkha comes into contact with water, soluble salts dissolve and are moved downward by gravity, resulting in lower salinity. However, the effects of evaporation on the groundwater cause salts to move upward, increasing soil salinity. According to Liu et al. (2019), soil salinity variation is a critical factor that requires special attention in the construction of civil engineering projects. It induced a significant degradation in these projects, such as differential settlement (Alshenawy et al., 2021), collapses (Moayed et al., 2012; Youssef and Maerz, 2013; Zhao et al., 2017), and strength losses (Al-Homidy et al., 2017; Moayed et al., 2012).

Several researchers have studied the effect of salinity on the physicochemical and mechanical properties of soils (Nu et al., 2020; Shen et al., 2024; Spagnoli et al., 2017; Tang et al., 2021; Ying et al., 2022). Their findings indicated that the degree of salinity's influence varied significantly based on soil type, salt type, and salt content. According to a study by Xiao-hua et al. (2020), coarse-grained soil's physical and mechanical characteristics correlated with particle structure and salt concentration. Velde and Meunier (2008) demonstrated that increasing the salinity of irrigation water leaded to the breakdown of soil aggregates due to swelling and dispersion of clay platelets, resulting in a loose soil structure. Mohammed and Abdullah (2016) found that increasing water salinity significantly decreases the clay fraction in fine soils, with the reduction varying by soil type. Saline soils consistently have a lower clay fraction than non-saline soils. The consolidating effect of salts, namely from sea water, rich in sodium chloride (NaCl), can be also observed on simple earthen constructions built were NaCl is produced naturally by the seaside for human consumption (Rodrigues et al., 2011). However, and although the use and research of earth, extracted from the soil, is increasing due to environmental issues (Faria et al., 2024), the saline soils are frequently rejected also from this use. Therefore, it is important to find ways to improve the mechanical performance of earthen building products produced with this type of soils, as well as their durability (Gallipoli et al., 2017).

The salinity of the Sebkha soil decreased from 16.3 dS.m<sup>-1</sup> to 3.8 dS.m<sup>-1</sup> due to leaching of ions from soluble salts such as halite and gypsum (Hafhouf et al., 2022). Ying et al. (2021) confirmed that the salinity had a significant effect on the water retention capacity. A recent study conducted by Li and Yang (2024) showed that an increase in chloride content leaded to the formation of more particle agglomerates in the soil. However, an excess of salt content changed the soil structure and reduced its resistance. Shen et al. (2024) demonstrated that increased NaHCO<sub>3</sub> content led to higher liquidity and plasticity limits but reduced mechanical properties. This adverse impact was also supported by Nu et al. (2020) who found that higher salinity in soft soil resulted in lower shear strength and increased liquid limit. Zhang et al. (2020) also showed that higher salinity decreased resistance.

Based on the results of the aforementioned studies, several techniques have been implemented in recent years to improve the physicochemical and mechanical characteristics of saline soils. These include the leaching technique to reduce salt content, the use of geotextiles as insulation layers, and the incorporation of mineral binders, such as air lime (Aiban et al., 2006; Liu et al., 2019; Yu et al., 2018). However, the latter technique is widely favored in road construction

for its reliability, low costs, and exceptional strength (Dhar and Hussain, 2021; Di Sante et al., 2020; Negi et al., 2013). Determining the optimum lime content (OLC) is crucial for construction projects. The Eades and Grim pH method (Eades and Grim, 1966) defines OLC as the lime amount yielding the highest solution pH. However, this method is affected by ions from lime and soil, and research on the influence of soluble soil ions on pH values is still limited. In this respect, Emarah and Seleem (2018) found that adding hydrated lime to soil treated with Red Sea water raises the suspension's pH linearly, stabilizing at 3-4% lime content. Beyond this point, the pH continues to increase with additional lime content. On the other hand, a strong correlation between OLC and salinity was observed in a study conducted by Ying et al. (2022). The OLC levels were 1.5%, 3%, and 4% by dry weight for the deionized waterquick lime, synthetic seawater-quick lime, and mixed salt solution-quick lime suspensions. Recently, several researchers (Li et al., 2012; Liu et al., 2019; Moayed et al., 2012) have been investigating the use of lime to treat saline soils. According to Moayed et al. (2012), saline soils can be used as a sub-based for flexible pavements because adding 2% hydrated lime leads to an almost two-fold increase in UCS after 7 d compared to untreated soil. Pei and Shouxi (2011) investigated the potential use of saline soil from the Gulf of Bohai as a material for filling roads. They concluded that the soil's UCS improved significantly after adding lime, making it suitable for road construction. Previous research conducted by Jiang et al. (2024) and Wei et al. (2024) also noted an increase in soil strength when Portland cement and hydrated lime were added. However, several researchers show that the negative effect of salts remains after adding a hydraulic or aerial binder (Aldaood et al., 2014; Koslanant, 2006; Li et al., 2016; Xing et al., 2009; Zhang et al., 2014). Koslanant (2006) concluded that the increase in soil strength after increasing salinity is attributed to the coagulation of organic matter in these soils by salts, which encourages clay particles to react with the hydraulic binder. Zhang et al. (2014) showed that after 28 days of curing, the soil's UCS treated with 10% cement decreased by 33% from 0.27 MPa to 0.18 MPa when the salt content increased from 2.5% to 5%. Soluble salt ions negatively impacted the cementing bonding between the soil particles. Li et al. (2016) found that adding 8% chloride salt (Cl<sup>-</sup>) to a lime-treated chloride soil decreased UCS by 50% after 28 days. While Cl<sup>-</sup> ions do not participate in hydration, they are adsorbed onto soil pores and surfaces. Xing et al. (2009) conducted tests on salt-rich soil treated with a cement including UCS and X-ray diffraction tests. Their findings indicated that the strength of the treated soil was not enhanced. This was attributed to the presence of Cl<sup>-</sup> and Mg<sup>2+</sup>, which hinder the formation of CSH and CAH, thereby preventing soil strength improvement. Research conducted by Cuisinier et al. (2011) and Carteret et al. (2014) indicated that Cl<sup>-</sup> negatively impacted the resistance of treated soils in the short and long term. Furthermore,  $SO_4^{2-}$  ions negatively impact the mechanical properties of treated soil by reacting with  $Al^{3+}$  and  $Ca^{2+}$  ions. This reaction produces ettringite, an expansive phase that disrupts the soil structure and decreases its resistance (**Khadka et al., 2020; Xing et al., 2009; Zhang et al., 2014**). In addition, a study carried out by **Rica et al. (2016)** on the disruptive effects of salts on treated silty soil deduced that the presence of combinations of salts with  $SO_4^{2-}$  ions aggravated the latter's deleterious effects on the treated soil.

The studies mentioned above indicate that the nature of the soil, salt, and salt content could negatively affect the physicochemical and mechanical behavior of saline soils without or with treatment by binder addition. It is essential to note that most of these studies have generally investigated the effect of a single type of salt. In contrast, in natural field conditions, interactions between several types of salt are more likely to occur. Moreover, studies conducted by **Nie et al. (2024)** and **Zhang et al. (2013)** indicated that the structure of soil containing at least 10% clay was significantly influenced by the chemical environment of the pore solution. However, with high evaporation in summer, a significant quantity of salts is generally produced in the Sebkha system.

Algeria has 254 Sebkha zones and has revealed substantial economic growth in recent years (Ouadah-Bedidi and Vallin, 2013). The high plains have a semi-arid climate and contain approximately 20 Sebkha areas (Koull et al., 2016). One of these areas is the Sebkha of Ain M'lila (Ez Zemoul). This Sebkha experiences winter rainfall, reducing soil salinity, with salinity also decreasing horizontally from the edges toward the center. However, increased civil engineering projects, such as roads and railways, have strained these virgin areas. Notably, the intersection of the National Road RN03 with the Sebkha has caused issues like cracks and subsidence. To prevent similar problems in future projects, the present study is conducted aiming to examine the impact of salinity (natural types of salt and different levels found in the soil) on the physical, chemical, and mechanical properties of untreated and binder-treated Sebkha soil in Ain M'lila. This study involves physical tests using granulometric analysis, mechanical tests including UCS, chemical tests via calcimeter and XRF, and mineralogical tests including XRD and TGA

#### 3.2. Materials and Methods

#### 3.2.1. Materials

#### **3.2.1.1. Study area**

The study site (Fig 3-1), known as Lake Mezouri or Sebkha Ez Zemoul, is located 13.5 km south of Ain-M'lila town and 10.5 km east of the town of Souk Naaman in the province of Oum el Bouaghi in northeast Algeria. The Sebkha covers an area of around 61 km<sup>2</sup> and is located at 35°53' N, 06°30' E, altitude of 784 m above sea level (Amarouayache et al., 2010), and it was classified as one of the Mediterranean Ramsar sites in 2004.

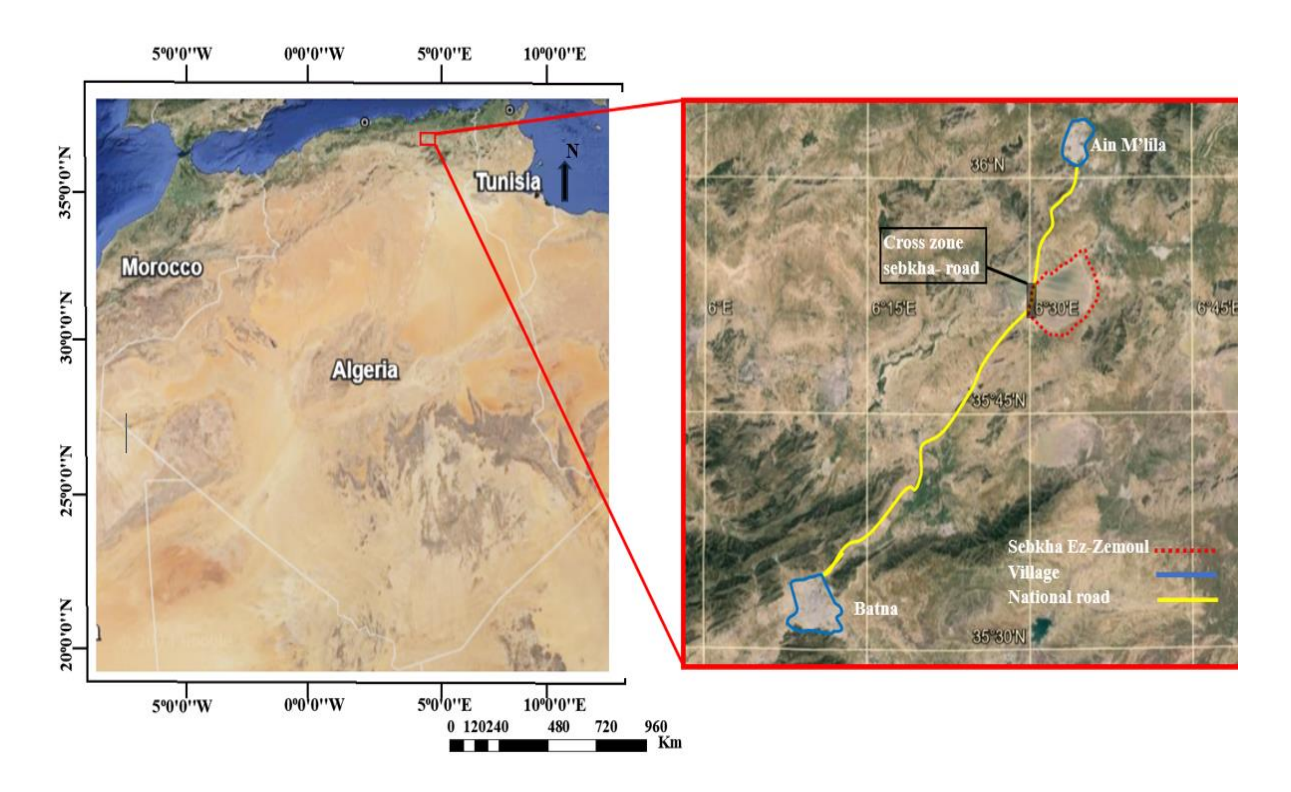


Fig 3-1. Ain M'lila Sebkha soil location.

Meteorological data from the Constantine region (approximately 40 km a way) shows an annual rainfall of 700 mm, with 77% occurring between December and April. The evaporation rate is approximately 1013 mm (Amarouayache et al., 2010), nearly 1.5 times the rainfall, leading to a distinctive white layer on the Sebkha's surface (Fig 2-2a). The zoom of the open survey state (Fig 2-2b) indicates that the Sebkha profile revealed that it contains sand, silt and clay (Fig 2-2c). However, this study is limited to the dry areas along the RN03 due to the high salinity levels compared to inside the Sebkha. In addition, the runoff from the sewerage systems of the town of Souk Naaman renders access to these wet areas of the Sebkha soil difficult. In summer, the surface of the Sebkha develops a white crust with high solubility, indicating the presence of

halite minerals. In contrast, deeper in the sedimentary profile, gypsum crystals with low solubility were found (Fig 2-2d). To this end, the summer season and the edge of the Sebkha (all along the RN03) were chosen for collecting samples, following the procedure described by Aiban et al. (2006) (i.e., excluding pieces of salt crystals).

#### 3.2.1.2. Soil and lime characteristics

Some geotechnical characteristics of the Sebkha soil are presented in **Table 3-1**. The maximum dry density is  $\gamma_{dopn} = 1.841 \text{g/cm3}$ , corresponding to the optimum water content of  $w_{opt} = 11.8\%$ , obtained according to standard **NF P94-093**. The particle size distribution, determined by dry sieving and sedimentation methods, revealed that the silt content (66%) was the highest, followed by sand (26%) and clay (10%). In addition, the plastic limit (Pl) and index (PI) were 16.51% and 16.49%, respectively. According to the USCS soil classification system, the soil is classified as sandy silt clay (CL). However, textural classification suggests it should be classified as silt loam (USDA).

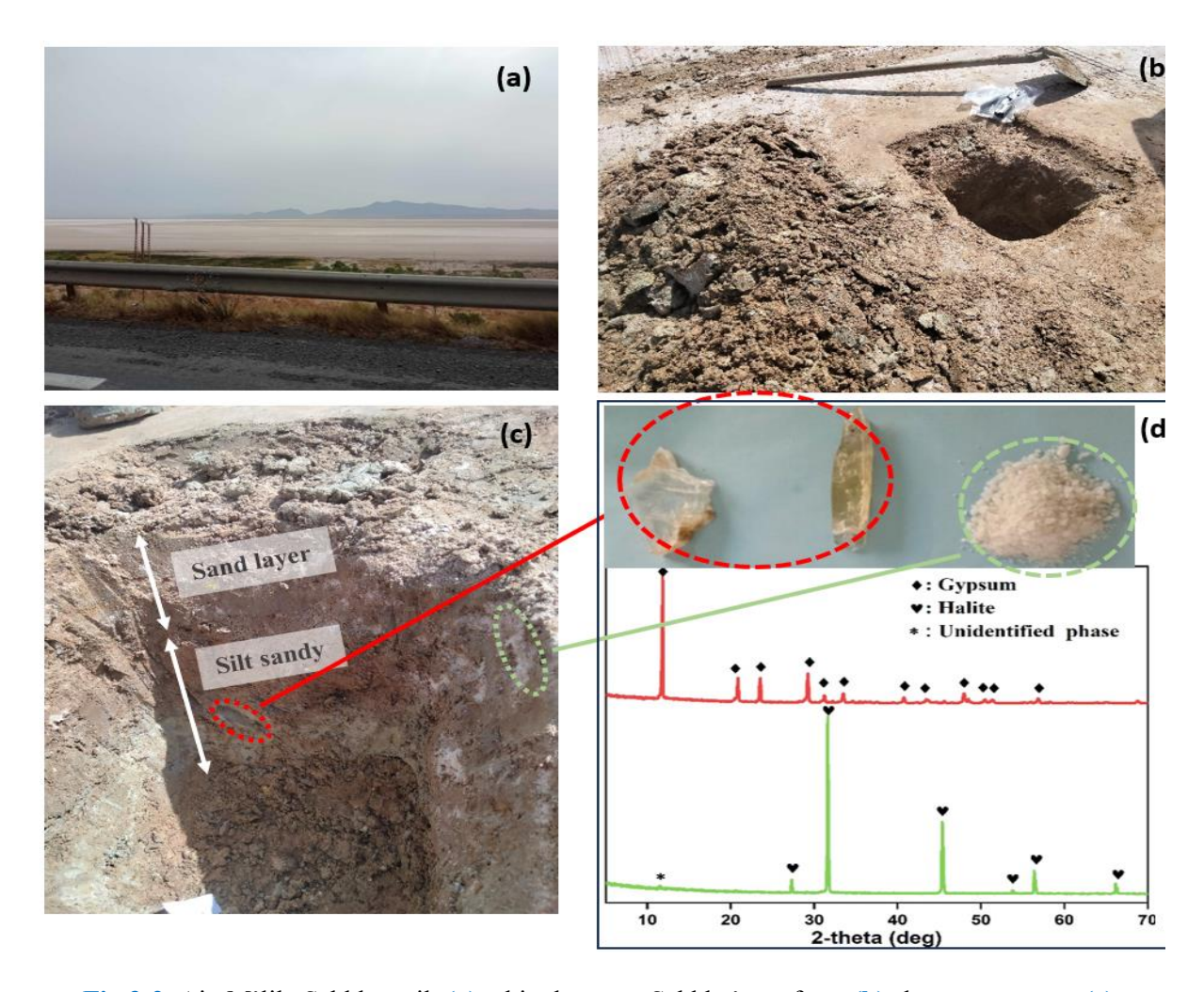


Fig 3-2. Ain M'lila Sebkha soil: (a) white layer on Sebkha's surface; (b) sky survey state; (c) Sebkha profile; (d) mineralogy of soluble salts.

Table 3-1. Geotechnical characteristics of Sebkha soil.

Soil's parameters (unit)	Value	Standards				
Case: Intact soil						
UCS (kPa)	33	(NF P94-077, 1997)				
Natural water content $w_{nat}$ (%)	18.19	(NF P94-050, 1995)				
Maximum dry density $\gamma_{dopn}$	1.841	(NF P94-093, 1999)				
Optimum moisture content $w_{opt}(\%)$	11.8					
≤2 mm fraction (%)	100	(NF P94-056, 1996)				
≤80 µm fraction (%)	76	(Nr 194-030, 1990)				
≤2 µm fraction (%)	10	(NF P94-057, 1992)				
Plastic limit PL (%)	16.51	(2000)				
Plastic index PI (%)	16.49	(Standard, 2000)				
USCS classification	CL	(ASTM D-2487, 2017)				
CaCO <sub>3</sub> content (%)	31.3	(NF P94-048, 1996)				

The saturated soil paste extract method was used to measure the soil's salinity and primary soluble salt content (Table 3-2). A salinity value of 23.2 dS.m<sup>-1</sup> was determined, indicating that the soil is highly saline according to the US Salinity Laboratory Staff (Laboratory (US), 1954). In addition, the soil is classified as a neutral chloride-sulfate saline soil based on the high content of chloride (6874 mg/l) and sulfate (5605 mg/l) species present as soluble salts (Loyer, 1991). Moreover, the results of the X-ray fluorescence analysis, shown in the histogram of Figure 3a, indicate that the main chemical composition of the soil is silica (SiO<sub>2</sub>), followed by calcium oxide (CaO), alumina (Al<sub>2</sub>O<sub>3</sub>) and magnesium oxide (MgO) while sodium (Na<sub>2</sub>O), sulfate (SO<sub>3</sub>), ferrite (Fe<sub>2</sub>O<sub>3</sub>), chloride (Cl), and potassium oxide (K<sub>2</sub>O) all exist in small quantities. In addition, X-ray diffraction analysis (Fig 3-3b) reveals that the soil contains quartz, calcite, halite, gypsum, and kaolinite. The mineralogical results, verified against the ICDD Powder Diffraction File database, align with the chemical findings. These results indicate the presence of quartz (PDF Card No. 01-078-1254) and kaolinite (PDF Card No. 01-072-2300) in the silica and alumina, calcite (PDF Card No. 00-017-0763) and gypsum (PDF Card No. 00-006-0046) in the calcium oxide, and halite (PDF Card No. 01-088-2300) in the chloride.

**Table 3-2.** The chemical compositions obtained based on the saturated soil past extract: salinity, salt con-centration, pH and soluble salt content.

ECe (dS.m <sup>-1</sup> )	Salt concentration (g.l <sup>-1</sup> )	pH Soluble salt content (mg. l-1)							
23.2	17.64	6.81	$Ca^{2+}$	$Mg^{2+}$	Na+	K+	$SO_3$	Cl-	HCO <sub>3</sub> -
23.2		0.01	466.1	172.3	4452	56	5605	6874	12

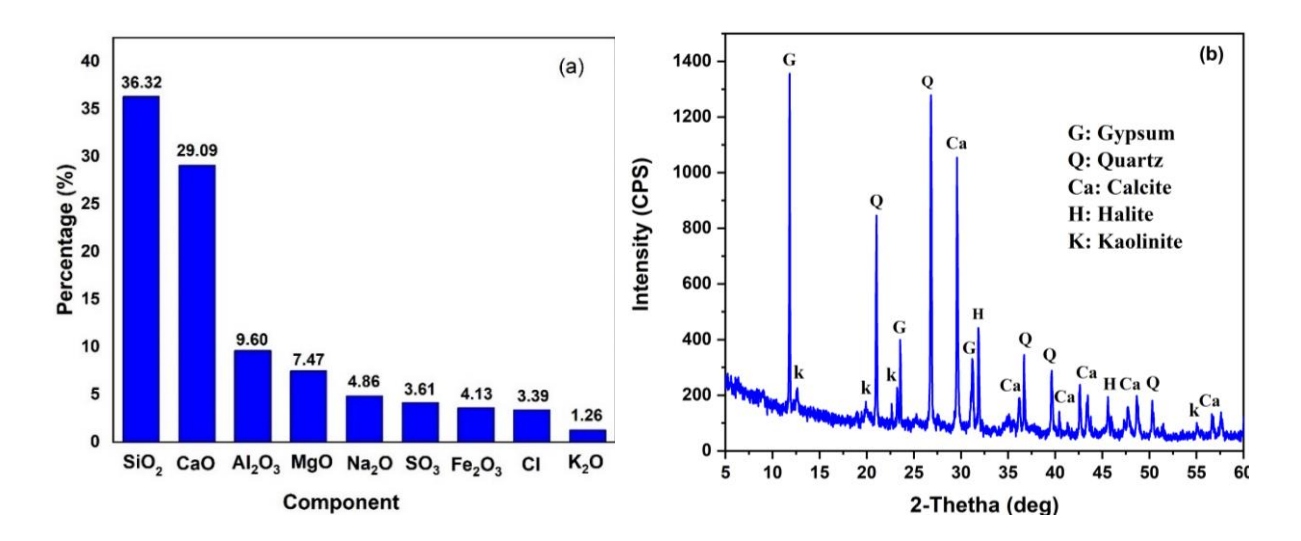


Fig 3-3. Chemical composition by XRF (a) and mineralogical composition by XRD (b) of Sebkha soil ECe3.

## Chapter 3. Salinity effects on the physicochemical and mechanical behavior of untreated and lime-treated saline soils (Sebkha soils)

This study utilized quicklime (CaO > 83.3%) (see **Table 3-3**) as a dry white powder sourced from Saida province in western Algeria. This powder has been stored in plastic bags to prevent contact with moisture, hydration and carbonation.

**Table 3-3.** Chemical composition of lime.

Physical state	Specified density	> 90 µm fraction (%)	Chemical elements (%)						
Dry white powder	2	<90	CaO >83.3	SiO <sub>2</sub> <2.5	Fe <sub>2</sub> O <sub>3</sub> <2.0	Al <sub>2</sub> O <sub>3</sub> <1.5	MgO <0.5	SO <sub>3</sub> <0.5	Na <sub>2</sub> O 0.4-0.5

#### 3.2.2. Methods

#### 3.2.2.1. Soil sampling and preparation

On 4 October 2021, three open pit survey holes were excavated along RN03 using a handle shovel at depths ranging from 0~1m. The soil was collected and oven-dried at 50°C due to its sensitivity to heat. The samples were then lightly crushed with a plastic hammer to break the natural cementing bonds between the soil particles. However, some salt crystals and soil aggregates were still visible (Fig 3-4a), so this process was repeated until all the material had passed through a 2 mm opening sieve. The dry-sieved samples were divided into three parts. The unwashed part consisted of highly saline soil (ECe3=23.2 dS.m<sup>-1</sup>). In contrast, the other parts were washed separately with demineralized water (D-W) to create two groups of samples with different salinities: moderately saline soil (ECe2=8.3 dS.m<sup>-1</sup>) and slightly saline soil (ECe1=2.32 dS.m<sup>-1</sup>). The washing process is illustrated in Figure 4b where the Sebkha is washed with D-W using a cylindrical steel bar. After washing, the mixture is left to stand for 24 hours before removing the clear water using a plastic tube based on the gravimetric method. The oven-dried Sebkha soils with three different salinities were then crushed and sieved.

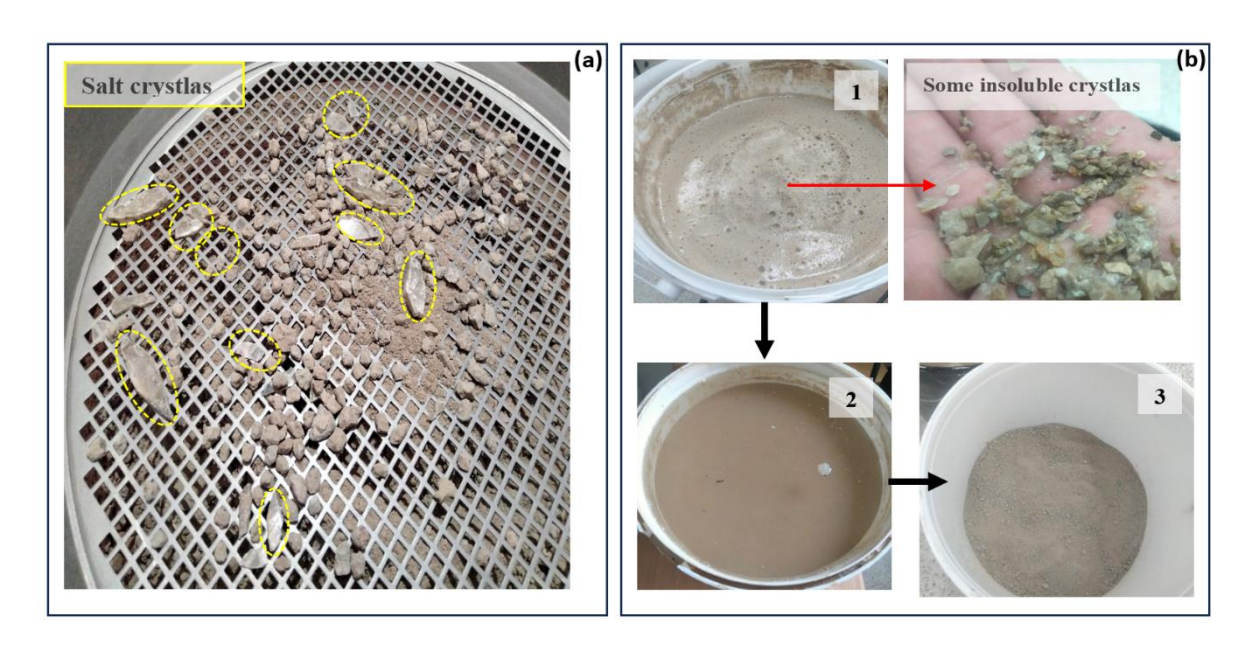


Fig 3-4. Samples preparation: (a) soil crystals and aggregates; (b) washing process.

The salinity levels of each soil were tested to determine their OLC. pH tests, following the pH method (Eades and Grim, 1966) were conducted initially to minimize the required tests for the continuing experimental program for the treated samples with the addition of 1%, 2%, 3%, 4% and 5% (in mass) of lime. The results of these tests are shown in Fig 4-5.

Before adding lime, the pH of natural soil ECe3 was lower (6.81) compared to ECe1 and ECe2 (8.05 and 8.2, respectively) due to increased salinity. According to a study by **Thomas (2018)**, in a saline soil solution, if the negative charge of the ions exceeds the positive charge, the pH decreases because of the release of more H<sup>+</sup> than OH<sup>-</sup>. As shown in Table 3-2, in the present study, for natural soil ECe3, the total charge of anions (negative charge) is greater than that of cations (positive charge) (8299 mg/l vs. 2920.7 mg/l). It is also important to note that the decrease in salinity for ECe1 and ECe2 soils after the washing operations reduces the total negative charge due to the leaching of halite and some gypsum. This reduction explains the increase in pH with the decrease in salinity of the Ain M'lila Sebkha soil. The pH levels increased when lime was added to the different soil types. The increase was more pronounced for the ECe1 soil than the ECe2 and ECe3 soils, as the lime content varied from 1% to 5%. After adding 1% of lime, the pH values for the ECe1 and ECe2 soils rapidly rose to 12.42 and 12.35, respectively.

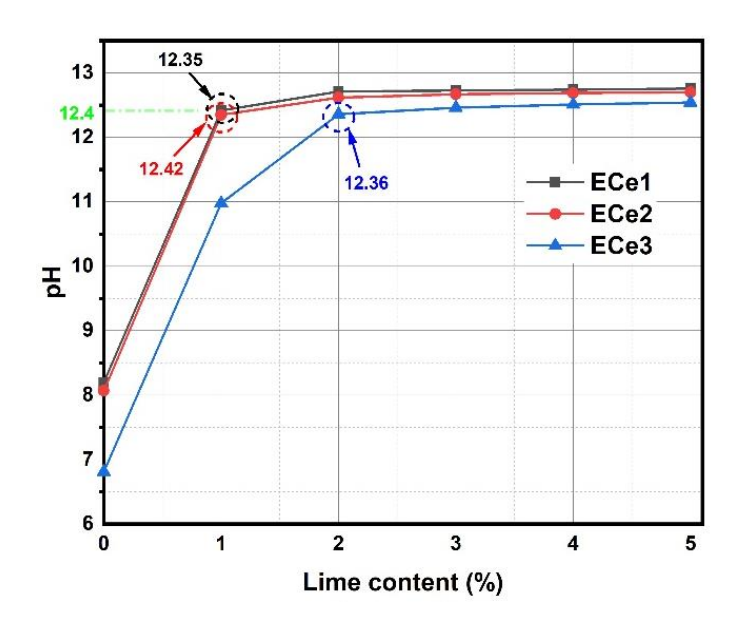


Fig 3-5. Lime and salinity impact on the pH of solution.

These values then slightly increased to 12.76 and 12.70, respectively, after adding 5% of lime. However, for soil ECe3, the pH value increased considerably up to 2% lime content, and then only slightly from 12.46 to 12.56 as the lime content varied between 3% and 5%. According to several studies (Al-Mukhtar et al., 2010; Di Sante et al., 2014; Eades and Grim, 1966; Negawo et al., 2019), the OLC is the minimum amount needed to achieve the highest pH in a soil-lime-water mixture. Based on previous research and the present study findings, the OLC for ECe1 and ECe2 soils is 1%, while for ECe3 soil, it is 2%. Hence, higher salinity levels require a higher OLC. The pH values for this ECe3 soil were expected to be lower than for ECe2 and ECe1 soils due to the consumption of OH- released by Mg<sup>2+</sup> and Ca<sup>2+</sup> ions in the saline solution inducing the precipitation of Mg(OH)<sub>2</sub> and CaCO<sub>3</sub>, causing greater lime consumption (Ying et al., 2022). To ensure that the three saline soils contain sufficient quantities of Ca<sup>2+</sup> for a pozzolanic reaction during curing and to create a favorable alkaline environment for this reaction, higher dosages of lime (1.5% for the ECe1 and ECe2 soils and 3% for the ECe3 soil) were selected and supplementary specimens were prepared for the UCS tests.

The following steps were carried out for each group of samples: the soil, lime, and water were thoroughly mixed for approximately three minutes to obtain a homogeneous mixture using an automated mixer. Each sample consisted of three layers, each being compacted at a constant speed of 1.27 mm/min using the CBR machine until they reached 95% of the dry density

obtained in the standard Proctor tests (e.g.1.749 g/cm<sup>3</sup> for the untreated samples). Before preserving each sample in a climatic chamber (relative humidity =  $90 \pm 2\%$  and T =  $20 \pm 2$ °C), it was wrapped in plastic film and paraffin after checking the mass tolerance by weighing to two decimal places (0.01 g).

#### 3.2.2.2. Chemical, mineralogical and geotechnical tests

The carbonate (CaCO<sub>3</sub>) content in a soil sample was determined using the volumetric method specified in standard **NF P94-048**. This method involved shaking 10 ml of 37% diluted hydrochloric acid (HCl) with 1 g of soil sample sieved to 0.2 mm. As a result, the soil dissolved and released CO<sub>2</sub>, causing a decrease in the water level in a graduated tube. It is important to note that the dissolution of 4 mg of CaCO<sub>3</sub> corresponds to the release of 1 cm<sup>3</sup> of CO<sub>2</sub>, based on the chemical Equation (1) for the reaction:

$$CaCO_3 + 2HCl \rightarrow CaCl_2 + H_2O + CO_2 \tag{1}$$

The Dietrich-Frühling calcimeter (Fig 3-6) was used for this process.

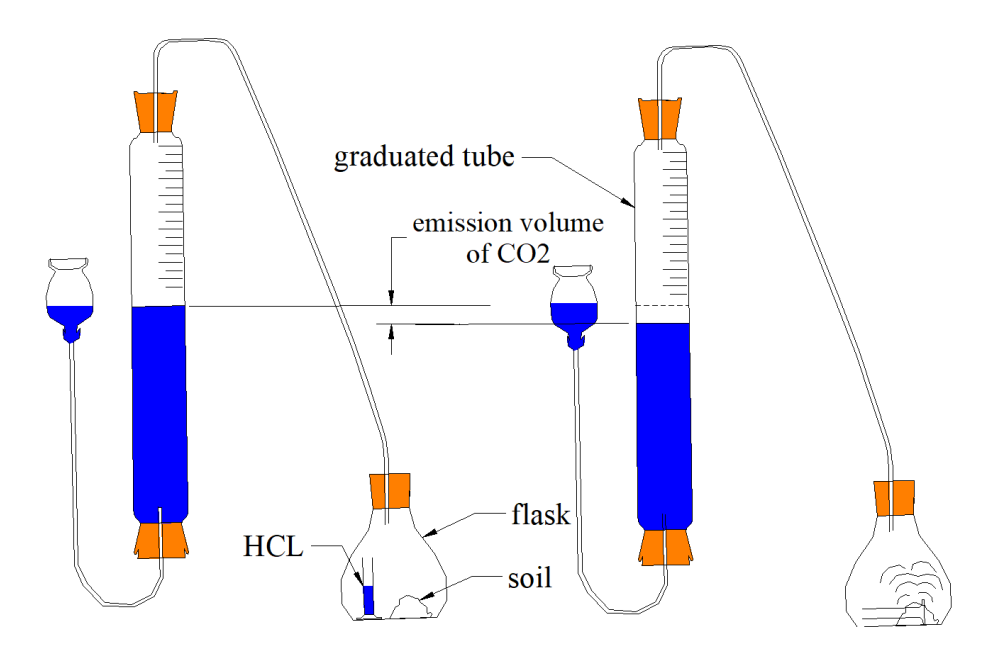


Fig 3-6. Dietrich-Frühling calcimeter.

The mineralogical composition of this soil was determined by X-ray diffraction (XRD) after pulverizing soil samples. This analysis used a Siemens D500 powder diffractometer and a Bruker AXS model equipped with a nickel anti-cathode ( $K\alpha = 1.5406$  Å) connected to a microcomputer for data collection and processing. The X-ray tube settings were 20 mA and 30 kV.

The elemental chemical composition of the Sebkha soil was analyzed by X-ray fluorescence spectrometry (XRF) using a Rigaku ZSX Prisus IV instrument. XRF is a semi-quantitative analytical technique used to determine the concentration of chemical elements in powdered soil samples. In addition, soil pH was measured based on soil extract 1/2.5. However, Electrical conductivity (EC) was measured using an Inolab-Cond conductivity meter (WTW 1CA301) to assess soil salinity based on the diluted soil extract method (1/5). This method provides the salinity of the soluble salts in the pore water, quantified in dS.m<sup>-1</sup>. The cations and anions of various soluble salts were determined using the volumetric measurement methods detailed by Pansu and Gautheyrou (2006).

A model SDT Q600 equipment (TA Instrument) was used for thermogravimetric analysis (TGA). This instrument is connected to a computer system for data acquisition and processing. Each platinum crucible contained 35 mg of ground soil. The samples were heated at 10°C/min from 20 to 950°C while exposed to a flow of 99.99% pure argon at 50 ml/min.

The geotechnical properties of this soil, including particle size analysis and Atterberg limits, were determined following the standards NF P94-056, NF P94-057 and ASTM D4318-00. Standard Proctor compaction tests were conducted per NF P94-093.

#### 3.2.2.3. Unconfined Compressive Strength test

The Unconfined Compressive Strength (UCS) test was performed using a Zwick testing machine following the **NF P94-077** standard. Specimens from the humid chamber were unsealed from the plastic film and quickly placed (to inhibit moisture evaporation) on the lower platen, and the movable upper platen made contact with it. A 1 mm/min displacement speed was used, which equals approximately 1.66% of the specimen's height per minute. Data was collected using a computer connected to the system, and the maximum force and corresponding failure strain were recorded for each axial force-strain curve. The UCS strength is determined by the ratio of the maximum axial force (F) to the average cross-sectional area of the sample (A) (Eq. (2)):

$$UCS = \frac{F}{A} \quad \text{and } A = \frac{A_0}{(1 - \varepsilon_l)}$$
 (2)

 $A_0$  represents the initial mean cross-sectional area, and  $\epsilon_l$  represents the axial deformation caused by the applied force. The result is the average of three triplicate specimens.

#### 3.3. Results and Discussion

#### 3.3.1. Effect of salinity on carbonation content of untreated Sebkha soil

**Fig 3-7** illustrates the impact of salinity on the calcium carbonate (CaCO<sub>3</sub>) content of untreated samples at various salinity levels. The results demonstrate that soil salinity significantly affects the CaCO<sub>3</sub> content, with higher soil salinity leading to lower measured CaCO<sub>3</sub> content. In the ECe3 soil, the CaCO<sub>3</sub> content is 41.58%, while in the ECe2 and ECe1 soils, it is 43.05% and 43.51%, respectively. The mineralogical characterization of the collected Sebkha soil (ECe3) showed that halite and gypsum are the predominant minerals in the saline phase. The chemical composition of this soil revealed a CaO content of 29.7%

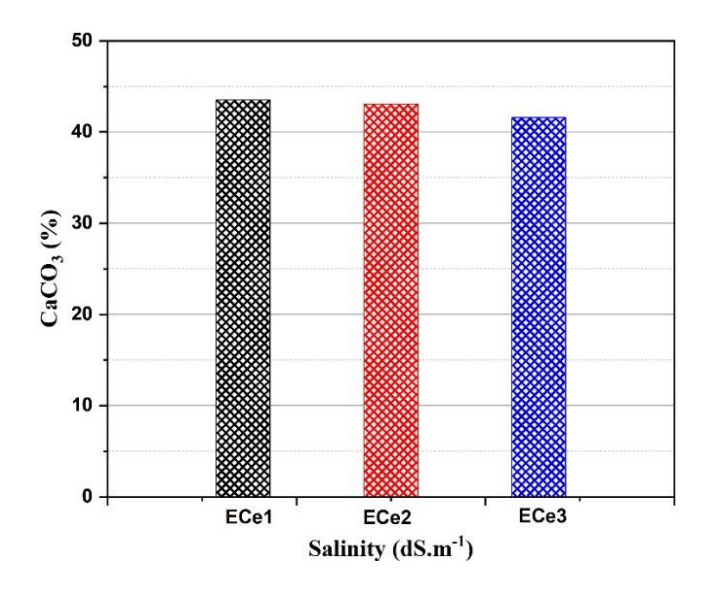


Fig 3-7. CaCO<sub>3</sub> content of ECe1, ECe2, and ECe3 soil by calcimeter.

According to Klein and Hurlbut (1985), gypsum (CaSO<sub>4</sub>,2H<sub>2</sub>O) contains 32.6% calcium oxide (CaO), 46.5% sulfur trioxide (SO<sub>3</sub>), and 20.9% combined water (H<sub>2</sub>O). Since the ECe3 soil contains a large amount of gypsum, and gypsum contains almost 1/3 CaO of its total mass, more calcium cations will be captured by the sulfate anions. Thus, a greater decrease in the salinity of the ECe3 soil will result in a higher dissolution of gypsum, thereby providing a greater availability of Ca<sup>2+</sup> within the system. These Ca<sup>2+</sup> ions may then react with the dissolved CO<sub>2</sub> present in the interstitial water, inducing the precipitation of CaCO<sub>3</sub>. Consequently, the ECe1 soil, which has a greater availability of Ca<sup>2+</sup> ions (i.e. a lower salinity), is characterised by a high CaCO<sub>3</sub> content. The XRF results also confirms that the amount of sulfate continues

to decrease after washing, leading to higher precipitation of CaO<sub>3</sub> content in the ECe1 soil compared to the ECe3 soil, as illustrated in equation (3):

$$Ca^{2+} + CO_3^{2-} \rightarrow CaCO_3 \downarrow \tag{3}$$

The decrease in salinity to ECe1 in Ain M'lila Sebkha soil leads to an increase in the precipitation of CaCO<sub>3</sub> due to the decrease in sulfate.

#### 3.3.2. Effect of salinity on the granulometry and mineralogy of the untreated Sebkha soil

In order to study the effect of salinity on the particle size, chemical composition, and mineralogy of the Sebkha soil, as mentioned before, a washing operation was conducted. The particle size curves obtained for each salinity level are illustrated in Fig 3-8a.

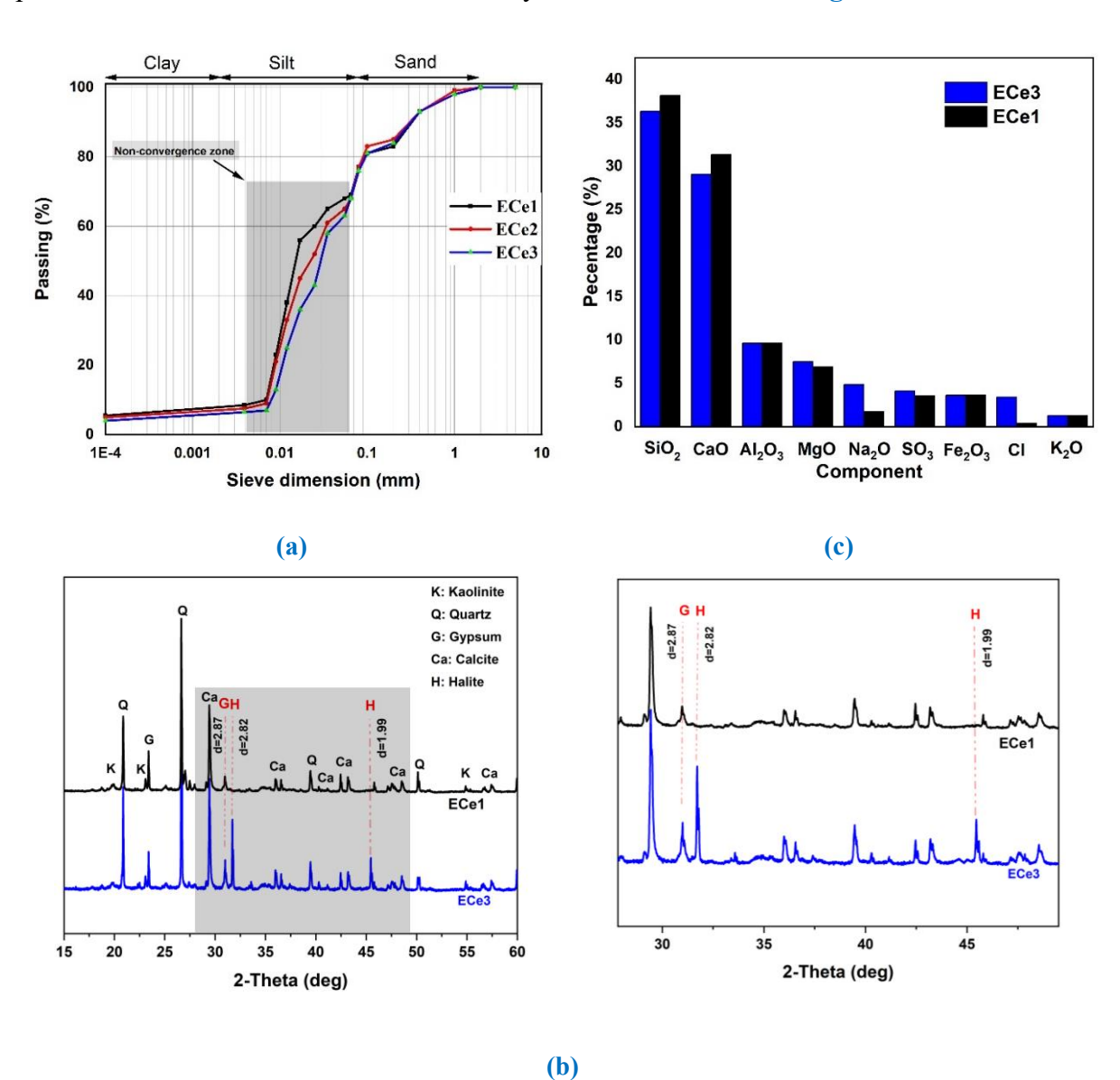


Fig 3-8. Grain distribution curves of ECe1, ECe2, and ECe3 soils (a), mineralogic composition of ECe1 and ECe3 soils by XRD (b), chemical composition of ECe1 and ECe3 soils by XRF (c).

The latter shows the effect of salinity level on the shape of these curves. It was observed that salinity affects the silty fraction much more than the other fraction of the soil. The granulometric curves show a non-convergent trend in the range of silt grain sizes. This trend was more pronounced between the ECe1 and ECe3 soils. In ECe1 and ECe3 soils, 75% of the grains passed through the 80 µm sieve opening. Additionally, 56% and 38% of the grains in ECe1 and ECe3 soils had a diameter of less than 20 µm, showing a difference of 18%. This difference suggests the influence of saline mineral phases in binding and agglomerating soil particles, thereby impacting the particle size distribution. These saline mineral phases increase the binding bridges and induce the cementation of particles with smaller specific surface areas, resulting in larger agglomerates and reduced finer particles. Leaching dissolves the weak cementitious bond between agglomerates, particularly the solubility of halite and some gypsum, resulting in more fine particles in ECe1 soil than in ECe3 soil. On the other hand, Li and Yang (2024) found that an increase in chlorine salt content was associated with a significantly higher number of agglomerates in the soil. However, in the present study the effect of salt is not observable in clay-sized particles, due to their low content (i.e., 10%).

**Fig 3-8b** presents the results of X-ray diffraction (XRD) analysis of soil powders from two soil types, ECe1 and ECe3. The XRD diffractogram of the ECe1 soil revealed the disappearance of two peaks after the leaching process compared with the collected Sebkha soil (i.e., ECe3). These two peaks correspond to the halite mineral phases at (2Θ) =31.7° (d=2.82°) and (2Θ) =45.4° (d=1.99°), respectively. In addition, ECe1 soil showed a decrease in the size of the gypsum (CaSO<sub>4</sub>,2H<sub>2</sub>O) peak at (2Θ) =31.1° (d=2.87°), which explains the decrease in the amount of this saline mineral phase. In addition, XRF elemental chemical analysis showed a significant decrease in the quantity of chloride (Cl) and sulfate (SO<sub>3</sub>) after washing (**Fig 3-8c**). However, this effect was more pronounced for chloride than sulfate, consistent with the XRD results. These results confirm that leaching soluble salts led to a decrease in salinity from ECe=23.2 dS.m<sup>-1</sup> to ECe=2.32 dS.m<sup>-1</sup>, accompanied by the disappearance of halite and a decrease in gypsum. These results confirm those of **Hafhouf et al.** (2022) carried out on the soil of the Ain M'lila Sebkha. It could, therefore, be deduced from these results that the variation in the granulometry of the soil as a function of the salinity level for the silty fraction is due to the

variation in the quantity of saline mineral phases such as halite and gypsum, which play the role of a natural binder ensuring the bond between the soil grains.

#### 3.3.3. Effect of salinity on untreated Sebkha soil UCS

Fig 3-9a shows the stress-strain curves obtained during UCS tests on compacted soil samples at different salinity levels (ECe1, ECe2, and ECe3).

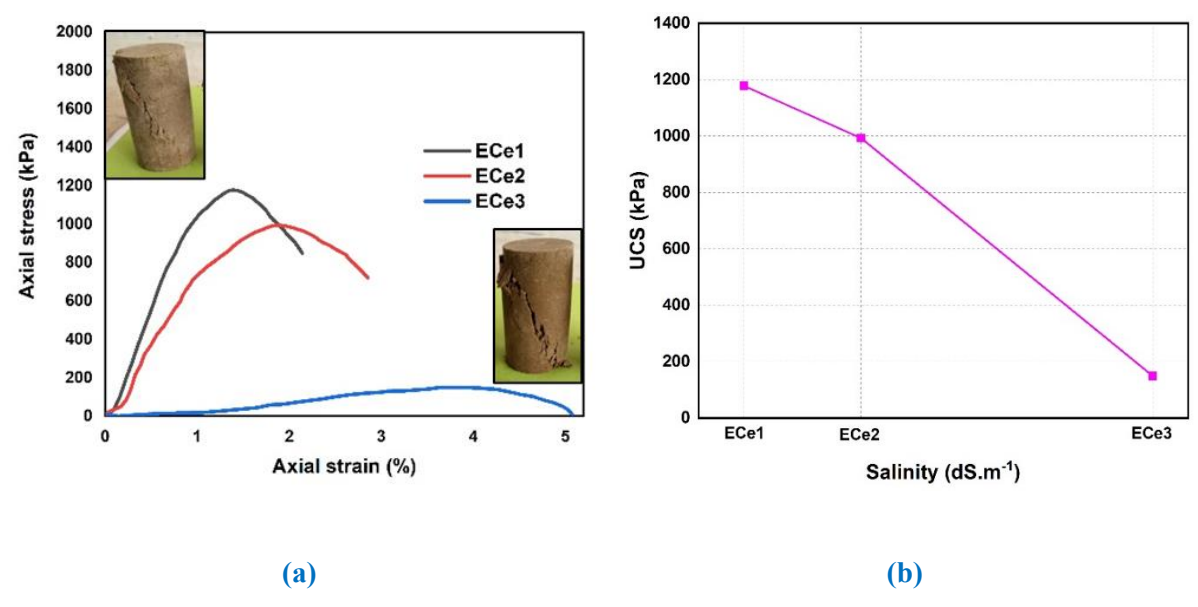


Fig 3-9. Stress-strain curves of ECe1, ECe2, and ECe3 soils (a), UCS at different salinity levels (b).

These curves show that all the samples exhibit a softening-deformation behavior. The ductile behavior is more pronounced with increasing salinity. For instance, the ECe3 soil does not exhibit a prominent peak, and the strength decreases gradually after failure. Conversely, the stress-strain curve shows a clear peak for the ECe1 soil, with the strength decreasing rapidly. It is crucial to note that the maximum deformation associated with the maximum stress at failure is higher when the latter is low. For example, for ECe3 soil, the maximum deformation corresponding to rupture and its strength are respectively  $\varepsilon = 3.79\%$  and a UCS = 149.8 kPa, whereas for ECe1 soil, the latter values become  $\varepsilon = 1.4\%$  and UCS = 1178.9 kPa. The rate of increase in resistance is 57.06 kPa per unit decrease in salinity when varied from ECe3 to ECe2, whereas it is 29.77 kPa when varied from ECe2 to ECe1 (Fig 3-9b). However, these curves show that the slope of the segment before fracture increases with decreasing salinity, which explains the increase in soil rigidity with decreasing salinity. This observation is illustrated by the rupture mode of the soil specimens (Fig 3-8a). The soil with lower salinity level, ECe1, has

a single large, apparent oblique crack. However, for the soil with higher salinity level, ECe3, the main oblique crack is preceded by small cracks before rupture, which explains the low rigidity of the latter compared with that of ECe1.

It is important to note that, with a specific water content, as the salinity of the soil pore water increases (i.e., higher salt solution concentration), it induces a significant precipitation of crystallized salts. These salts are considered natural cementitious compounds in the soil, which enhances the bonding of soil grains and aggregates, resulting in improved strength (Li et al., 2016; Zhang et al., 2020). However, in the present study, it was found that increasing salinity decreased the strength of the soil tested on a continuous trend. Mineralogical analysis of the Ain M'lila Sebkha soil revealed that it is mainly composed of the mineral phases halite (NaCl) and gypsum (CaSO<sub>4</sub>,2H<sub>2</sub>O), which are the main cementitious agents in this Sebkha soil. After washing the ECe3 soil with D-W, the ECe1 soil was obtained. This latter showed the disappearance of NaCl and a decrease in CaSO<sub>4</sub>,2H<sub>2</sub>O. A recent study by Li and Yang (2024) examined the influence of water and salt content on soil strength characteristics. The researchers determined that the critical point where a change in strength occurs is when the water content reaches 12%. Beyond this point, increased salt content leads to decreased soil resistance. Moreover, research by Dai et al. (2017) showed that the moderate dissolution rate of CaSO<sub>4</sub>,2H<sub>2</sub>O (0.2%) increases in the presence of other salts, such as NaCl. In the present study, the increase in the dissolution rate of CaSO<sub>4</sub>,2H<sub>2</sub>O in the presence of highly soluble NaCl salt and a relatively high water content of wopt=11.8% resulted in an overall increase in the total dissolution rate of soluble salt crystals for compacted samples with ECe3 salinity level. In the dry state, part of the solid particles in the soil could be replaced by soluble salt crystals. When these salt crystals dissolve at a higher rate, some salt crystals are transferred to the fluids in the soil, causing a portion of solid particles to disappear. Hence, friction between the soil particles is reduced. This results in the dispersion of the soil structure and, ultimately, weakens the soil's resistance. Finally, a reduction in the salinity of Ain M'lila Sebkha soil is associated with a reduction in the weak cementitious bonds of minerals such as halite and gypsum, inducing a significant increase in the strength of this soil at its woot.

These results can be linked to observations in the field. Hot, arid climates with low rainfall and high evaporation rates characterize the lands of the Sebkha. When these solute solutions evaporate, they leave behind a crust of white, highly soluble salt, such as halite. This crust forms a hard surface supporting a vehicle (Akili and Ahmed, 1983; Glennie, 2010; Moayed et al., 2012). However, the saline crust's high dissolution, due to its high content of soluble salts such

as halite and direct contact with surface rainwater, causes the highly soluble ions to be washed laterally and downward. This process weakens the soil support surface, making it easier for vehicle wheels to get stuck (Fig 3-10).



Fig 3-10. Damage caused on Sebkha surface by track's wheels.

In practice, to use this soil as a base for embankments and to make it easy to access and compact the embankments effectively, it is crucial to reduce the salinity of this soil. The resistance of ECe3 soil is significantly reduced at its  $w_{opt}$ . It should be noted that this effect is more likely to increase in natural conditions because the  $w_{ntr}$  is generally higher than the water (11.8% vs. 18.19%). Therefore, steps should be taken to protect against water exposure or improve this type of soil by binder treatment before starting construction projects.

#### 3.3.4. Effect of salinity and curing time on carbonation content of Sebkha soil

**Fig 3-11** shows the impact of salinity and curing time on samples' calcium carbonate (CaCO<sub>3</sub>) content at different salinity levels after lime treatment. The ECe3 soil showed a greater rate of increase in CaCO<sub>3</sub> than the ECe2 and ECe1 soils. After treatment, the CaCO<sub>3</sub> increased from 41.58% to 47.63% for ECe3, whereas it increased from 43.05% to 47.23% and from 43.51% to 47.33% for ECe2 and ECe1, respectively. This result confirms the hypothesis mentioned previously that the higher OLC of soil ECe3 is due to the higher precipitation of CaCO<sub>3</sub> after adding lime compared to the other soils (i.e., ECe1 and ECe2). Therefore, the higher salt content in the Ain M'lila Sebkha soil induces more significant precipitation of CaCO<sub>3</sub> after treatment, requiring more lime to ensure the pozzolanic reaction.

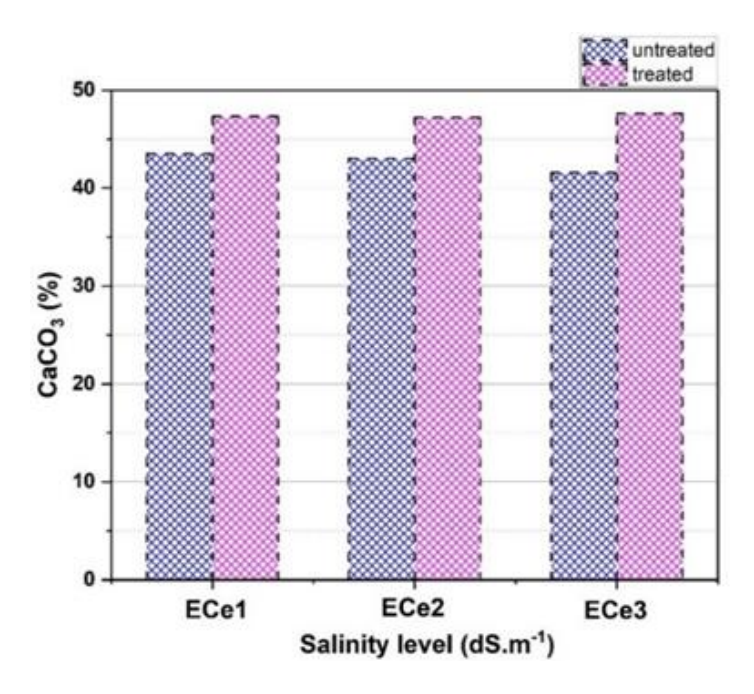


Fig 3-11. CaCO3 content of untreated and ECe1, ECe2, and ECe3-treated soil by calcimeter.

#### 3.3.5. Effect of salinity and curing time on Sebkha soil UCS

Fig 3-12 illustrates the effect of curing times (0 d, 3 d, 7 d, 14 d and 28 d) on the stress-strain curves of three saline soil samples treated with lime. These results show that the slope of the stress-strain curves before failure decreased with increasing curing time up to 3 d, after which the slope increased to 28 d of curing. This behavior is distinguished because this slope becomes more remarkable after 28 curing days than for the untreated soils. However, this behavior is only observed for the ECe1 and ECe2 soils. Notably, the slope increase, which indicates the stiffness of the soil, is higher for the ECe1 soil than the ECe2 soil. However, for the ECe3 soil, the stiffness increased rapidly after 3 d of curing and remained almost constant for up to 28 d. Based on these findings, the addition of lime had a significant impact on the stiffness of the soil during the different curing periods for the ECe1 and ECe2 soils but had a negligible effect on

the ECe3 highly saline soil. Regarding the maximum deformations that correspond to failure, it was found that for the ECe3 soil, the maximum deformation that corresponds to failure is influenced only by the curing time from 0 to 3 d because  $\varepsilon$  =3.79% at 0 d, decreasing to  $\varepsilon$  =1.28% after 3 d of curing. After this period the latter remains almost constant with increasing curing time ( $\varepsilon$ =1.23% vs.  $\varepsilon$ =1.28%). However, for the ECe1 and ECe2 soils, this deformation decreases with increasing curing time. For example, for the ECe1 soil, the value of  $\varepsilon$ =1.40% at 0 d decreases to  $\varepsilon$ =1.15% after 28 d of curing.

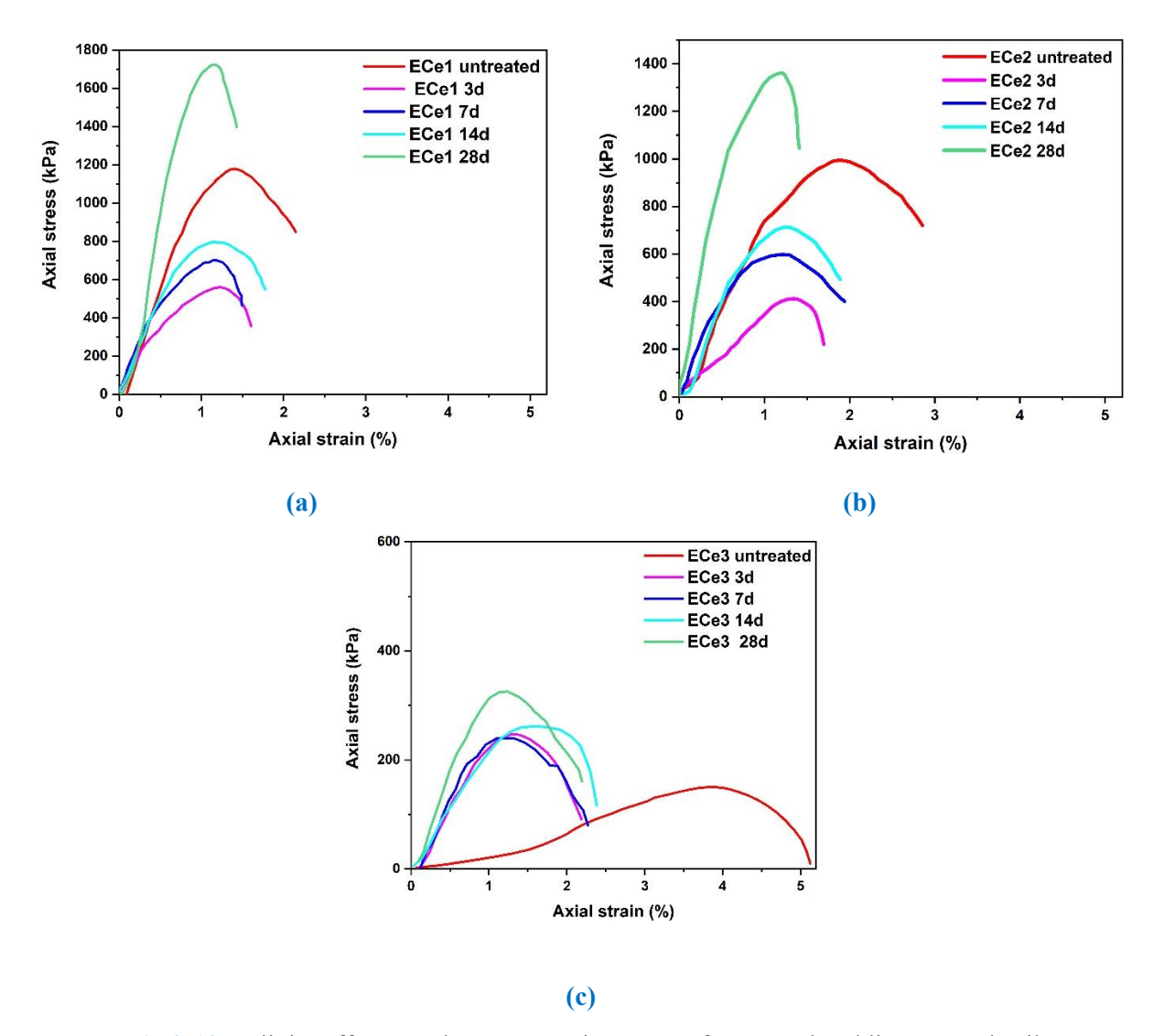


Fig 3-12. Salinity effects on the stress-strain curves of untreated and lime treated soils at different curing periods (0 d, 3 d, 7 d, 14 d, and 28 d): (a) ECe1 soil, (b) ECe2 soil and (c) ECe3 soil.

From these observations, it can be deduced that adding lime reduces these maximum deformations, i.e., increases the brittleness of the treated soil. Regarding maximum failure

strength, the ECe3 soil strength increases from 146 kPa in the untreated state to 239 kPa, 255 kPa, and 325 kPa at 3 d, 14 d, and 28 d of curing, respectively. This represents an increase of 63.7% from 0 d to 3 d, 6.7% from 3 d to 14 d and 27.5% from 14 d to 28 d, for a total increase of 36% from 3 d to 28 d of curing. However, the maximum strength for the ECe1 and ECe2 soils decreases by 52.5% and 49.8% from 0 d to 3 d of curing, respectively. After that, and for the ECe1 soil, it increases by 42.4% and 116.5% from 3 d to 14 d and from 14 d to 28 d while it increases by 40.5% and 94.6% for the same periods for the ECe2 soil. Hence, a short curing period of 3 d is considered a critical point for the strength of Sebkha soil treated with different salinities. In the ECe1 and ECe2 soils, the strength decreases and then increases until it reaches a value higher than the initial untreated value after 28 d of curing (1178.9 kPa vs. 1723.48 kPa and 1000 kPa vs. 1362.22 kPa).

On the other hand, the strength increases significantly below this point, then increases with a low value for the ECe3 soil. This can be justified by a cation exchange (CE) occurring rapidly after adding lime to the soil-water mixture. However, a study by **Mohd Yunus et al. (2017)** showed that the dissolution rate of salts in water is faster than that of lime and provided sufficient cations for CE. Therefore, CE in this Sebkha soil is strongly related to the cations present in the pore water. These cations can be increased by increasing the amount of binder and the existence of soluble salts. However, in the present study, the intensity of CE in the ECe3 soil is expected to be higher than in the other soils (ECe1 and ECe2) because the ECe3 soil has higher OLC (3% vs. 1.5%) and has higher salt content (i.e., halite and gypsum). As a result, the strength of this soil increases significantly from 0 d to 3 d of curing.

Furthermore, mineralogical analysis of ECe1 soil shows a disappearance of halite and a decrease in gypsum. The quantity of gypsum remaining after adding lime and water disrupted the strength of this soil during the curing period. In fact, after mixing the soil with lime and water, primary ettringite appears rapidly due to the dissolution of gypsum (Rajasekaran, 2005). Ettringite is an expansive phase that destroys the structure of the ECe1 soil. However, this effect is more pronounced in soil ECe2, which contains an intermediate salt content, with higher quantity of gypsum than soil ECe1. Therefore, it seems the harmful effect of gypsum in the short term is also linked to their quantity.

Xing et al. (2009) found that the presence of Mg<sup>2+,</sup> Cl<sup>-</sup>, and SO<sub>4</sub><sup>2-</sup>ions in a salt-rich soil with cement inhibits the formation of cementitious compounds. The present study findings are supported by the lack of strength improvement in ECe3-treated soil, which is attributed to the harmful effects of chloride and sulfate salts in the soil. The increase in strength also confirms

this, as salinity is reduced in ECe1 and ECe2 soil. Hence, in the present study, the high concentration of vulnerable ions in the pore water between ECe3 soil particles with low clay fraction enhances their capacity to coat finer particles and limits their exposure to lime hydration. As a result, coating the finer particles, these ions prevent them from being exposed to lime hydration, disrupting the formation of hydration products and interfering with strength development.

Finally, it can be deduced that the low clay fraction and the high salinity are two factors that affect the resistance of the originally collected soil ECe3. The high salinity results in the high ions content present in the interstitial water that envelops the fine particles, slowing the pozzolanic reaction on the one hand. Since the latter is also directly related to the clay fraction, their existence in small quantities does not allow a normal pozzolanic reaction between the lime and the mineral phases, disturbing the strength of the ECe3 soil.

#### 3.3.6. Effect of salinity on the mineralogy of cured soils

After 28 days of curing, powders of the untreated and lime treated soils were analyzed by X-ray diffraction for the two types of soil, ECe 1 and ECe 3 (Fig 3-13a and b) and variations in the diffractograms are observed. The lime-treated ECe3 soil shows that the mineralogical composition does not change after 28 days of curing. In addition, the mineral salt phases remain essentially constant during the curing process, indicating that these minerals do not participate in the hydration reaction.

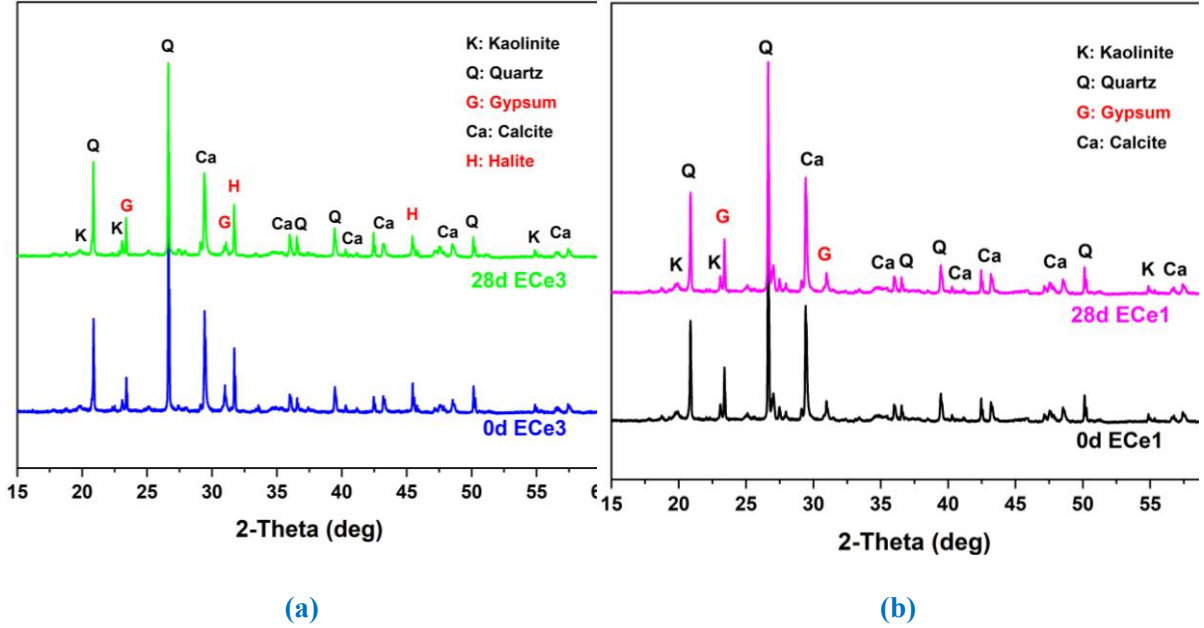


Fig 3-13. Mineralogy composition by XRD of untreated and treated soil samples: (a) ECe3 soil and (b) ECe1 soil.

On the other hand, no new peak corresponding to cementitious products (CAH and CSH) are observed for the ECe1 soil. However, the latter's strength increases with the curing time. As the XRD results show no significant change in the mineralogical composition of lime-treated samples at different salinity levels, thermal analyses (TGA) (Fig 3-14a) were also carried out. The results obtained show that the untreated ECe3 and ECe1 soil powders have a mass loss of 2.92% and 2.29% between 100°C and 200°C, respectively, indicating dehydration of the water molecules constituting the gypsum (Fig 3-14b). Also, a mass loss of 16.95% and 17.78% between 650°C and 750°C for ECe3 and ECe1 soil is observed, indicating decomposition/decarbonization of the calcite (Fig 3-14c). In addition, a mass loss between 800°C and 1100°C is noted with values of 8.89% and 0.98% for ECe3 and ECe1 soil, respectively, corresponding to the melting phase of halite (Fig 3-14d). These results are consistent with previous results, which indicate the disappearance of halite, diminution of gypsum, and increase of calcite for ECe1 soil compared to ECe3 soil.

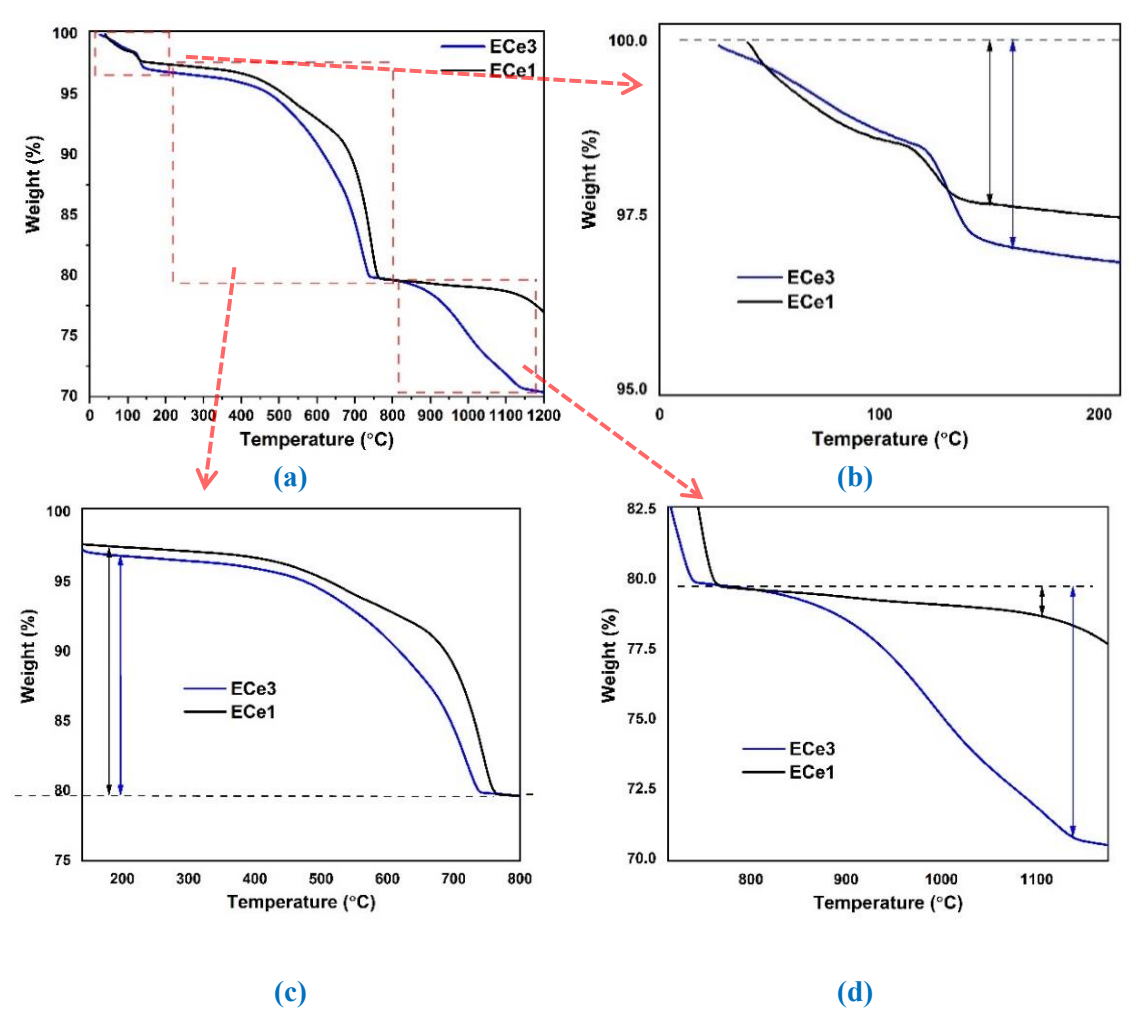


Fig 3-14. Loss of mass by TGA of untreated ECe3 and ECe1 soils (a), dehydration of gypsum (b), decomposition of calcite (c) and melting of halite (d).

However, the ECe1 and ECe3 treated samples show the formation of a new mineral phase, portlandite, represented by a loss of mass illustrated between 400°C and 500°C (Fig 3-15a and b). The loss of this phase is 1.5% and 1.2% for the ECe1 and ECe3 soils, respectively (Fig 3-15c). It should be noted that the OLC in the ECe3 soil is higher than that in the ECe1 soil (3% vs. 1.5%), although the results obtained for the content of portlandite developed are inversed, indicating that the saline phases have a detrimental effect on the lime hydration process. However, portlandite is in the amorphous state because the XRD tests do not detect this phase, or because of the detection limit of the physicochemical equipment (i.e., the quantity to be measured with only 1.5% and 3% lime treatment). Nevertheless, this amorphous phase is considered a cementitious compound that increases the bridges and strengthens the adhesion between soil particles, thus improving the mechanical behavior of ECe1 soil `

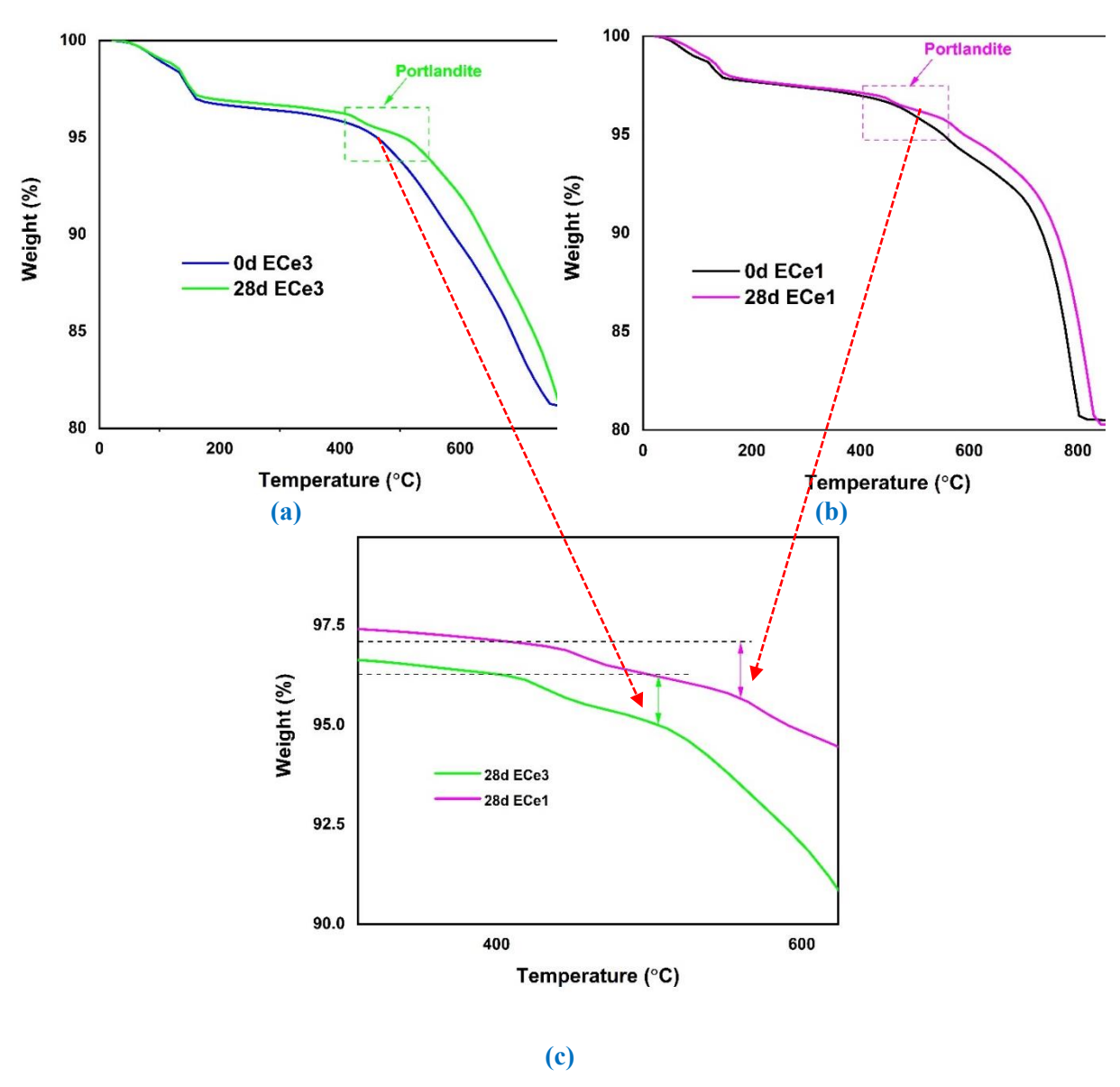


Fig 3-15. Loss of mass by TGA of untreated and treated ECe3 (a) and ECe1 (b) soils and dehydration of portlandite (c).

#### 3.4. Conclusions

This study examines the impact of salinity on the physicochemical and mechanical properties of untreated and air lime-treated Sebkha soils from Ain M'lila. To this end, an experimental program, comprising physicochemical and mechanical tests, was carried out on a soil tested originally (ECe3) and after washing to provide samples with medium (ECe2) and lower (ECe1) salinity. The results of this program show a significant effect of salinity on the tested soil resistance. The conclusions of this work can be cited as follows:

- (1) A higher soil salinity requires greater incorporation of lime to achieve acceptable performance. This incorporation reaches 1.5% for the ECe1 soil and 3% for the ECe3 soil. This difference is due to the consumption of OH<sup>-</sup> and Ca<sup>2+</sup> ions, present in the saline interstitial solution, by Mg<sup>2+</sup> and HCO<sup>3-</sup> ions, leading to the precipitation of Mg (OH)<sub>2</sub> and CaCO<sub>3</sub>.
- (2) Salinity significantly impacts the shape of the particle size curve, particularly on the silty fraction. The reduction in salinity is linked to a decrease in gypsum content and the total disappearance of halite, which minimizes the cementation of aggregates. Consequently, more fine particles are observed in the ECe1 soil, with 18% increase in fine particles less than 20  $\mu$ m in diameter.
- (3) For untreated soil, salinity affects CaCO<sub>3</sub> precipitation. The latter decreases with increasing salinity. The ECe3 soil contains a large amount of gypsum (CaSO<sub>4</sub>,2H<sub>2</sub>O) and, as it contains almost 1/3 CaO of its total mass, more calcium cations (Ca<sup>2+</sup>) are captured by the sulfate anions (SO<sub>4</sub><sup>2-</sup>), resulting in a decrease in CaCO<sub>3</sub> compared with the ECe2 and ECe1 soils. However, for the treated soil, the precipitation of CaCO<sub>3</sub> is higher in the ECe3 soil compared to the ECe2 and ECe1 soils. This is probably due to the reaction of HCO<sup>3-</sup>, Ca<sup>2+</sup>, and OH<sup>-</sup> ions between them, leading to the precipitation of CaCO<sub>3</sub>.
- (4) Unconfined compressive strength (UCS) for untreated soil increases when salinity decreases. In fact, in the presence of halite and relatively high w<sub>opt</sub> of 11.8%, gypsum dissolution is accelerated, thus reducing the number of solid particles and leading to a significant decrease in the UCS of the ECe3 soil. However, in the case of lime treated soil, and since a highly saline environment characterizes the ECe3 soil, the SO<sub>4</sub><sup>2-</sup> and Cl<sup>-</sup> ions present in the pore water have probably covered the low clay fraction, thus disturbing the mechanical strength of the ECe3 soil.

# Chapter 3. Salinity effects on the physicochemical and mechanical behavior of untreated and lime-treated saline soils (Sebkha soils)

(5) For treated saline soils, the participation of gypsum and halite is not observed in the formation of cementitious compounds in the ECe3 soil, as shown by the results of the XRD analyses, and no new peaks corresponding to cementitious compounds are detected for both ECe1 and ECe3 soils. However, thermogravimetric analysis (TGA) shows the presence of portlandite. This latter phase is higher in the ECe1 soil than in the ECe3 soil, despite the latter containing a higher lime content than the ECe1 soil. This indicates the negative effect of soluble salts on the strength of the ECe3 soil (natural Sebkha soil from Ain M'lila) after lime treatment. In conclusion, improving the resistance of highly saline soils, similar to the Ain M'lila Sebkha soil, with the addition of lime may be insufficient. However, identifying the season when the Sebkha has lower salinity can be beneficial from a technical, economic, and environmental point of view. Lime treating saline soils when they have lower salinity (whenever it is possible) increases its resistance and reduces the optimal quantity of lime to use. However, if the soil contains a low clay fraction, which plays a vital role in the hydration and formation of cementitious compounds, it may be helpful to enrich the soil with pozzolanic fractions such as silica-rich dune sand. Further studies on the optimization of performance of saline soils can also be helpful to increase the use of these soils as building materials for earthen construction, as

saline earth is currently rejected and not used for building.

#### References

- Aiban, Sa., Al-Ahmadi, Hm., Asi, Im., Siddique, Zu., Al-Amoudi, O.S.B., 2006. Effect of geotextile and cement on the performance of sabkha subgrade. Building and Environment 41, 807–820.
- Akili, W., Ahmed, N., 1983. The sabkhas of eastern Saudi Arabia: geotechnical considerations, in: Proceedings, First Saudi Engineering Conference. pp. 300-322.
- Aldaood, A., Bouasker, M., Al-Mukhtar, M., 2014. Impact of freeze-thaw cycles on mechanical behaviour of lime stabilized gypseous soils. Cold Regions Science and Technology 99, 38-45.
- Al-Homidy, A.A., Dahim, M.H., Abd El Aal, A.K., 2017. Improvement of geotechnical properties of sabkha soil utilizing cement kiln dust. Journal of Rock Mechanics and Geotechnical Engineering 9, 749-760.
- Al-Mukhtar, M., Lasledj, A., Alcover, J.-F., 2010. Behaviour and mineralogy changes in limetreated expansive soil at 20 C. Applied clay science 50, 191–198.
- Alshenawy, A.O., Hamid, W.M., Alnuaim, A.M., 2021. A review on the characteristics of sabkha soils in the Arabian Gulf Region. Arab J Geosci 14, 2018. https://doi.org/10.1007/s12517-021-08275-w
- Amarouayache, M., Derbal, F., Kara, M.H., 2010. Caractéristiques écologiques et biologiques d'Artemia salina (Crustacé, Anostracé) de la Sebkha Ez-Zemoul, Algérie nord-est. Revue d'Écologie (La Terre et La Vie) 65, 129–138.
- Carteret, R.D., Buzzi, O., Fityus, S., Liu, X., 2014. Effect of Naturally Occurring Salts on Tensile and Shear Strength of Sealed Granular Road Pavements. J. Mater. Civ. Eng. 26, 04014010. https://doi.org/10.1061/(ASCE)MT.1943-5533.0000938
- Cuisinier, O., Le Borgne, T., Deneele, D., Masrouri, F., 2011. Quantification of the effects of nitrates, phosphates and chlorides on soil stabilization with lime and cement. Engineering Geology 117, 229–235.
- Dai, Z., Kan, A.T., Shi, W., Zhang, N., Zhang, F., Yan, F., Bhandari, N., Zhang, Z., Liu, Y., Ruan, G., Tomson, M.B., 2017. Solubility Measurements and Predictions of Gypsum, Anhydrite, and Calcite Over Wide Ranges of Temperature, Pressure, and Ionic Strength with Mixed Electrolytes. Rock Mech Rock Eng 50, 327–339. https://doi.org/10.1007/s00603-016-1123-9
- Dhar, S., Hussain, M., 2021. The strength and microstructural behavior of lime stabilized subgrade soil in road construction. International Journal of Geotechnical Engineering 15, 471–483. https://doi.org/10.1080/19386362.2019.1598623
- Di Sante, M., Di Buò, B., Fratalocchi, E., L\u00e4nsivaara, T., 2020. Lime treatment of a soft sensitive clay: A sustainable reuse option. Geosciences 10, 182.
- Di Sante, M., Fratalocchi, E., Mazzieri, F., Pasqualini, E., 2014. Time of reactions in a lime treated clayey soil and influence of curing conditions on its microstructure and behaviour. Applied Clay Science 99, 100–109.
- Eades, J.L., Grim, R.E., 1966. A quick test to determine lime requirements for lime stabilization. Highway research record.
- Emarah, D.A., Seleem, S.A., 2018. Swelling soils treatment using lime and sea water for roads construction. Alexandria engineering journal 57, 2357–2365.
- Faria, P., Beckett, C.T.S., Fabbri, A., Keita, E., Morel, J.-C., Perlot, C., Perrot, A., 2024. RILEM Contribution to Earthen Building, in: Beckett, C., Bras, A., Fabbri, A., Keita,

- E., Perlot, C., Perrot, A. (Eds.), Second RILEM International Conference on Earthen Construction, RILEM Bookseries. Springer Nature Switzerland, Cham, pp. 194–205. https://doi.org/10.1007/978-3-031-62690-6\_20
- Gallipoli, D., Bruno, A.W., Perlot, C., Mendes, J., 2017. A geotechnical perspective of raw earth building. Acta Geotech. 12, 463–478. https://doi.org/10.1007/s11440-016-0521-1
- Glennie, K.W., 2010. Desert sedimentary environments. Elsevier.
- Hafhouf, I., Bahloul, O., Abbeche, K., 2022. Effects of drying-wetting cycles on the salinity and the mechanical behavior of sebkha soils. A case study from Ain M'Lila, Algeria. Catena 212, 106099.
- Jiang, Y., Dai, H., Fisonga, M., Li, C., Hong, Z., Xia, C., Deng, Y., 2024. Feasibility and mechanism of high alumina cement-modified chlorine saline soil as subgrade material. Construction and Building Materials 429, 136411.
- Khadka, S.D., Jayawickrama, P.W., Senadheera, S., Segvic, B., 2020. Stabilization of highly expansive soils containing sulfate using metakaolin and fly ash based geopolymer modified with lime and gypsum. Transportation Geotechnics 23, 100327.
- Klein, C., Hurlbut, C.S., 1985. Jr. Manual of mineralogy.
- Koslanant, S., 2006. Influence of storage conditions on geotechnical properties of Ariake clay and on its chemical stabilization. PhD diss, Dissertation, Saga University, Japan.
- Koull, N., Chehma, A., GUEZZOUN, N., HAMOUDA, N., BELLAHCENE, O., 2016. Qualité des eaux des zones humides du bas Sahara algérien.
- Laboratory (US), R.S., 1954. Diagnosis and improvement of saline and alkali soils. US Department of Agriculture.
- Li, H., Yang, M., 2024. Study on unconfined compressive strength and deformation characteristics of chlorine saline soil. Scientific Reports 14, 1478.
- Li, M., Chai, S., Du, H., Wang, C., 2016. Effect of chlorine salt on the physical and mechanical properties of inshore saline soil treated with lime. Soils and Foundations 56, 327–335.
- Li, M., Chai, S.X., Zhang, H.Y., Du, H.P., Wei, L., 2012. Feasibility of saline soil reinforced with treated wheat straw and lime. Soils and foundations 52, 228-238.
- Liu, Y., Wang, Q., Liu, S., ShangGuan, Y., Fu, H., Ma, B., Chen, H., Yuan, X., 2019. Experimental investigation of the geotechnical properties and microstructure of lime-stabilized saline soils under freeze-thaw cycling. Cold Regions Science and Technology 161, 32–42.
- Loyer, J.-Y., 1991. Classification des sols salés: les sols Salic. Cahier ORSTOM, série Pédologie 51–61.
- Moayed, R.Z., Izadi, E., Heidari, S., 2012. Stabilization of saline silty sand using lime and micro silica. J. Cent. South Univ. 19, 3006–3011. https://doi.org/10.1007/s11771-012-1370-1
- Mohammed, M.S., Abdullah, E.J., 2016. Heavy metals pollution assessment of the soil in the northern site of east Baghdad oil field, Iraq. Iraqi Journal of Science 57, 175-183.
- Mohd Yunus, N.Z., Wanatowski, D., Marto, A., Jusoh, S.N., 2017. Strength improvement of lime-treated clay with sodium chloride. Geotechnical Research 4, 192–202. https://doi.org/10.1680/jgere.17.00001

- Negawo, W.J., Di Emidio, G., Bezuijen, A., Verastegui Flores, R.D., François, B., 2019. Lime-stabilisation of high plasticity swelling clay from Ethiopia. European Journal of Environmental and Civil Engineering 23, 504–514. https://doi.org/10.1080/19648189.2017.1304272
- Negi, A.S., Faizan, M., Siddharth, D.P., Singh, R., 2013. Soil stabilization using lime. International journal of innovative research in science, engineering and technology 2, 448-453.
- NF P94-048, 1996. Determination of the carbonate content Calcimeter method. AFNOR., n.d.
- NF P94-050, 1995. Determination of moisture content. Oven drying method. AFNOR., n.d.
- NF P94-056, 1996. Granulometric analysis Dry sieving method after washing. AFNOR., n.d.
- NF P94-057, 1992. Granulometric analysis Hydrometer methodle., n.d.
- NF P94-077, 1997. Uniaxial compressive test. AFNOR., n.d.
- NF P94-093, 1999. Determination of the compaction characteristics of a soil Standards Proctor test - Modified Proctor test. AFNOR, n.d.
- Nie, Y., Ni, W., Lü, X., Tuo, W., 2024. Exploring the mechanical behavior and microstructure of compacted loess subjected to dry-wet cycles and chemical contamination. Journal of Rock Mechanics and Geotechnical Engineering.
- Nu, N.T., Duong, N.T., Son, B.T., Thinh, P.H., 2020. Investigation of salt, alum content in soft soils and their effects on soil properties: Case study in coastal areas of Vietnam. The Iraqi Geological Journal 19–34.
- Ouadah-Bedidi, Z., Vallin, J., 2013. Fertility and population policy in Algeria: Discrepancies between planning and outcomes. PoPulation and develoPment review 38, 179–196.
- Pansu, M., Gautheyrou, J., 2006. Handbook of Soil Analysis. Springer Berlin Heidelberg, Berlin, Heidelberg. https://doi.org/10.1007/978-3-540-31211-6
- Pei, W., Shouxi, C., 2011. LABORATORY AND IN-SITU TESTS ON SOLIDIFIED SALINE SOILS FOR HIGHWAY FILLINGS. gcdzxb 19, 440–446.
- Rajasekaran, G., 2005. Sulphate attack and ettringite formation in the lime and cement stabilized marine clays. Ocean engineering 32, 1133-1159.
- Rica, H.C., Saussaye, L., Boutouil, M., Leleyter, L., Baraud, F., 2016. Stabilization of a silty soil: Effects of disruptive salts. Engineering Geology 208, 191–197. https://doi.org/10.1016/j.enggeo.2016.04.032
- Rodrigues, C.M., Bio, A., Amat, F., Vieira, N., 2011. Artisanal salt production in Aveiro/Portugal - an ecofriendly process. Saline Syst 7, 3. https://doi.org/10.1186/1746-1448-7-3
- Shen, J., Wang, Q., Chen, Y., Zhang, X., Han, Y., Liu, Y., 2024. Experimental investigation into the salinity effect on the physicomechanical properties of carbonate saline soil. Journal of Rock Mechanics and Geotechnical Engineering 16, 1883–1895.
- Soil, A.C.D.-18 on, Rock, 2017. Standard practice for classification of soils for engineering purposes (unified soil classification system) 1. ASTM international.
- Spagnoli, G., Sridharan, A., Oreste, P., Di Matteo, L., 2017. A probabilistic approach for the assessment of the influence of the dielectric constant of pore fluids on the liquid limit of smectite and kaolinite. Applied Clay Science 145, 37–43.

- Standard, A., 2000. Standard test methods for liquid limit, plastic limit, and plasticity index of soils. ASTM International, West Conshohocken, PA.
- Tang, S., She, D., Wang, H., 2021. Effect of salinity on soil structure and soil hydraulic characteristics. Can. J. Soil. Sci. 101, 62-73. https://doi.org/10.1139/cjss-2020-0018
- Thomas, G.W., 2018. Soil pH and Soil Acidity, in: Sparks, D.L., Page, A.L., Helmke, P.A., Loeppert, R.H., Soltanpour, P.N., Tabatabai, M.A., Johnston, C.T., Sumner, M.E. (Eds.), SSSA Book Series. Soil Science Society of America, American Society of Agronomy, Madison, WI, USA, pp. 475–490. https://doi.org/10.2136/sssabookser5.3.c16
- USDA, 1987. Soil Mechanics Level I. Module 3–USDA Textural Soil Classification. Study Guide, n.d.
- Velde, B.B., Meunier, A., 2008. The origin of clay minerals in soils and weathered rocks. Springer Science & Business Media.
- Wei, L., Chai, S., Wang, P., 2024. Mechanical properties of stabilized saline soil as road embankment filling material. Geomechanics and Engineering 37, 499-510.
- Xiao-hua Y., Sha-sha Z., Wei L.I.U., Ze-long Y.U., 2020. Research progress on engineering properties of coarse-grained saline soil. jtysgcxb 20, 22-40. https://doi.org/10.19818/j.cnki.1671-1637.2020.05.002
- Xing, H., Yang, X., Xu, C., Ye, G., 2009. Strength characteristics and mechanisms of salt-rich soil-cement. Engineering Geology 103, 33-38.
- Ying, Z., Cui, Y.-J., Benahmed, N., Duc, M., 2021. Investigating the salinity effect on water retention property and microstructure changes along water retention curves for limetreated soil. Construction and Building Materials 303, 124564.
- Ying, Z., Cui, Y.-J., Duc, M., Benahmed, N., 2022. Effect of salt solution on the optimum lime contents of bentonite and silt. Acta Geotech. 17, 3731–3745. https://doi.org/10.1007/s11440-022-01488-7
- Youssef, A.M., Maerz, N.H., 2013. Overview of some geological hazards in the Saudi Arabia. Environ Earth Sci 70, 3115–3130. https://doi.org/10.1007/s12665-013-2373-4
- Yu, X., Dan, H.-C., Xin, P., 2018. Method for Improving Leaching Efficiency of Coastal Subsurface Drainage Systems. J. Irrig. Drain Eng. 144, 04018019. https://doi.org/10.1061/(ASCE)IR.1943-4774.0001330
- Zhang, D., Cao, Z., Fan, L., Liu, S., Liu, W., 2014. Evaluation of the influence of salt concentration on cement stabilized clay by electrical resistivity measurement method. Engineering Geology 170, 80–88.
- Zhang, F., Wang, G., Kamai, T., Chen, W., Zhang, D., Yang, J., 2013. Undrained shear behavior of loess saturated with different concentrations of sodium chloride solution. Engineering Geology 155, 69-79.
- Zhang, S., Yang, X., Xie, S., Yin, P., 2020. Experimental study on improving the engineering properties of coarse grain sulphate saline soils with inorganic materials. Cold Regions Science and Technology 170, 102909.
- Zhao, X., Shen, A., Guo, Y., Li, P., Lv, Z., 2017. Pavement mechanic response of sulfate saline soil subgrade section based on fluid-structure interaction model. International Journal of Pavement Research and Technology 10, 497-506.

### **CHAPTER 4.**

# EFFECT OF SULFATE-RESISTANCE-CEMENT TREATMENT ON SALINE SOIL (SEBKHA SOIL) SUBGRADES

#### 4.1. Introduction

In road construction, the presence of weak subgrades is a common challenge that can adversely affect construction site development and lead to substantial financial losses. In arid and semi-arid regions, saline soils (Sebkha soils) frequently occur as road subgrades and present significant challenges for pavement design due to their soluble salt content, which substantially impacts road performance and stability. Researchers have typically employed three methods to address this issue: soil replacement, increasing layer thickness, and incorporating binders, with the latter being the most preferred approach. This chapter investigates the potential stabilization of Sebkha soil from the Ain M'lila region in Algeria using sulfate-resistance-cement (SRC). The first part of the study focuses on strength development assessment through unconfined compressive strength (UCS) tests, complemented by physicochemical techniques including X-ray diffraction (XRD), thermogravimetric analysis (TGA), Fourier transform infrared spectroscopy (FTIR), pH, and electrical conductivity (EC) measurements to better understand and observed the complex reactions within the cement-soil-salts mixture. The second part presents a comparative analysis of untreated and treated Sebkha subgrades using a local Algerian flexible pavement design framework, providing insights into practical applications.

Saline soils, known in Arabic as Sebkha soils, are unique and problematic in construction engineering, particularly pavement design, due to their high salt content and shallow groundwater table. Pavement engineers often encounter the challenge of designing and constructing a solid road foundation on top of very soft soils such as Sebkha soils (Benmebarek et al., 2015). Recently, in Algeria, various problems were faced with pavement and road structure in such saline Sebkha soils. A study focusing on the national road RN03 has found various types of road damage on pavement surface between the regions of Batna and Ain M'lila, especially near Sebkha (Hafhouf et al., 2022; Hafhouf and Abbeche, 2023). A construction project of a road embankment crosses a section of about 11 km on the Sebkha of Chott El Hodna, Algeria, posed significant challenges during the investigation of the subsurface soil and the construction of the first embankment layers (Benmebarek et al., 2015). Furthermore, the foundation layer of the Es-Senia Oran airport near the extensive Sebkha of Oran in western Algeria has been affected by natural cavities formed by

water containing carbon dioxide, posing a long-term risk of collapse (Chikhaoui et al., 2015). Sebkha soil is a fine-grained soil consisting of clay, silt, and sand cemented together by various salts (e.g., halite, gypsum, and calcite). The repetitive salt dissolution crystallization process, as a consequence of high climatic conditions fluctuations (humidity and temperature) in this region, distresses the soil structure and manifests in various forms, such as salt expansion, collapse, differential settlement, etc. (Moayed et al., 2012; Zhang et al., 2020). The soluble sulfate in the solid phase causes collapsibility deformation when the subgrade is immersed, leading to a dramatic drop in stability and strength (Zhao et al., 2017). Sulfate saline soil in highway engineering causes subgrade swell, payement cracks, and slope loss. Additionally, salt heave in the soil subgrade led to two levels of elevation changes: first, it elevated the asphalt pavement above the surrounding ground level; second, the concrete apron became 4-5 cm higher than the asphalt pavement surface (Zhang and Dong, 2003). Salt heave and frost heave caused varying degrees of damage to the subgrade and pavement of southern Xinjiang roads, resulting in significant economic losses (Yang et al., 2020). If coarse-grained soil with a soluble salt content higher than 2% is directly used as embankment fill material, it can lead to salt expansion and collapsibility, causing excessive uneven deformation of the subgrade and posing a threat to the operation of high-speed railways (Zhang et al., 2020). Therefore, saline soils are disallowed as subgrade and embankment materials in pavement structures. The construction of pavement structures is quite expensive, and their performance is directly affected by the strength and durability of the underlying foundation soil (Caliendo, 2012; Pereira and Pais, 2017). When construction projects encounter unsuitable soil conditions, costs can rise significantly because appropriate fill materials for both the subgrade and embankment need to be brought in from distant locations. However, using local and raw materials at construction sites can save a substantial amount of money. Hence, it is crucial to address the poor engineering properties of this soil to use it effectively in pavement construction (Zhang et al., 2020). Several researchers have employed various soil enhancement techniques such as deep soil mixing (Fattah et al., 2012), vibro-compactor and replacement (Hammad et al., 2023), and chemical treatment (Moayed et al., 2012). Among these techniques, chemical treatment has proven its efficiency through its resulting high strength, easy application, and cost-effectiveness (Moayed et al., 2012; Pei and Shouxi, 2011). Cement stabilization, for example, is a widely used chemical treatment for soil, dating back to 1948. When cement is mixed with soil and water, it tends to increase the pH of the soil-pore water, creating an alkaline environment. This environment promotes fast hydration reactions, leading to the formation of portlandite (Ca(OH)<sub>2</sub>) and nanostructured cementitious compounds like calcium silicate hydrate (CSH), calcium aluminate hydrate (CAH), and calcium alumina-silicate hydrate (CASH) through pozzolanic reactions. These hydration products improve the density of soil by filling pore spaces and strengthening the soil by bonding soil particles together.

Numerous studies indicate that adding binders can significantly enhance strength, thereby reducing soil distress associated with salt. The unconfined compressive strength (UCS) of the embankment fill material, saline (sodium sulfate) coarse-grain soil, increased with a higher binder content. Specifically, the addition of 11% slaked lime or 15% slaked lime-volcanic ash caused the UCS to exceed 0.35 MPa. This improvement is attributed to the enhancement of particle contact, resulting from the change in chemical composition from sodium sulfate to calcium sulfate and calcium carbonate, both of which are insoluble or slightly soluble in water (Zhang et al., 2020). Pei and Shouxi (2011) studied the potential of using saline soil as embankment filling materials for road pavement after adding calcium-based material. Their study denoted that after binder addition, the soil improved significantly and was satisfy the requirements of highway specification. Hammad et al. (2023) explored the potential of using ordinary Portland cement (OPC) and marble powder (MP) to enhance the strength of Sebkha soil. A combination of 70% of OPC and 30% of MP showed the highest UCS with a value of 5.26 MPa. Shuja et al. (2022) examined the strength of the Sebkha of Oman using OPC and cement clean dust (CKD). Their findings indicate that 10% of OPC Sebkha soil was included in the sub-base construction of rigid pavements. Moreover, the usage of 20% of CKD in stabilizing Sebkha soil may promote economical benefits as it reduces the required amount of OPC by 5%. Hossain and Mol (2011) showed that the addition of 5% of CKD to clayey soil increased its UCS to 2.3 MPa after 28 days of curing. Consequently, the improved clayey soils becomes suitable for road subgrade applications. The viability of adopting medium-chlorine-content saline soil as embankment construction after being stabilized by four agents, namely lime, fly ash, SH agent (composed of modified polyvinyl alcohol (PVA) and water), and cement, was inspected by Wei et al. (2020). The UCS of the soil in the study increased by a factor of seven (300 kPa vs. 2400 kPa) after 28 days of curing using a combination of 6% cement and 4% lime, indicating that the soil is suitable for use as embankment filling. Furthermore, the Fourier Transform Infrared Spectroscopy (FTIR) and thermal gravimetric analysis (TGA) are expected to be the most effective methods for detecting reaction products, as they are undetectable

by the XRD method due to their amorphous state. In a study by Lv et al. (2018), the stabilization of fine sulfate saline soil was investigated using lime, fly ash, and sodium silicate. The introduction of 9% of lime and 18% of fly ash in the saline soil, comprising a 2.8% salt content, resulted in a 23-fold increase in the UCS of treated soil compared to the plain soil after 30 days of curing. Moreover, no substantial difference in the XRD patterns was observed, due to the abundant production of non-crystalline phase material. However, the stabilization process significantly impacts the chemical environment by reducing the sulfate concentration in the soil and, consequently, limiting salt expansion. Collapsibility was significantly reduced after a 5% cement addition, and shear strength increased fivefold (Bahmyari et al., 2021). Jefferson et al. (2005) suggested that adding 4 to 7% of cement provides an excellent UCS for preconstruction treatment on collapsible soils. Razeghi et al. (2022) analyzed the UCS, XRD, and FTIR of alkali-activated cement-stabilized chloride sandy soil. With a 1% of NaCl content, the UCS developed by 244%. This increase is due to the formation of CSH and CASH gels, which reduced the samples porosity and increased their strength. Jiang et al. (2024) used high alumina calcium (HAC), ordinary Portland cement (OPC), slaked lime (SL), and fly ash (FA) to modify the coastal chlorine saline soil as roadbed backfilling materials. Based on XRD analysis, a combination of HAC-SL binder supplied more aluminum and calcium phases, which are beneficial to the formation of calcium aluminate chloride hydrate (3CaO·Al<sub>2</sub>O<sub>3</sub>·CaCl<sub>2</sub>·10 H<sub>2</sub>O), known as Friedel's salt and hydration products. In addition, 6% HAC-SL incorporation (3% of HAC and 3% of SL) achieved an optimal chlorine fixation (approximately 20.5%). Cheng et al. (2017) demonstrated that the NaCl in saline soil reacts with the stabilizer to form Friedel's salt. This precipitation reduces voids in the soil matrix, significantly increasing the strength of stabilized soil.

Apart from this, other researchers agree that the effect of salinity remains after treatment. **Xing et al.** (2009) highlighted the effect of OPC and Mg<sup>2+</sup>, Cl<sup>-</sup>, and SO<sub>4</sub><sup>2-</sup> content on the UCS of salt-rich soft soils. Their results confirmed that an increase in the cement ratio enhances the strength of treated soil. At the same time, Mg<sup>2+</sup>, Cl<sup>-</sup>, and SO<sub>4</sub><sup>2-</sup> influences the resistance by hindering the formation of CSH and CAH cementitious compounds. The results of **Calvello et al.** (2005) and **Carteret et al.** (2014) validate that Cl<sup>-</sup> ions negatively affect the short- and long-term resistance of the treated soil. **Kalipcilar et al.** (2018) underlined the influence of varying sodium and magnesium sulfate concentrations on the strength of cement-stabilized kaolin clay. Their results demonstrated that increased cement amount and curing time enhances strength. Conversely,

magnesium sulfate compromises the hydration bonding between soil and cement by consuming Ca(OH)<sub>2</sub> and producing brucite (Mg(OH)<sub>2</sub>), that causes a subsequent decrease in the pH value of the solution. Kalipcilar et al. (2016) illustrated that sulfate ions are the primary cause of strength loss. Thus, the utilization of sulfate-resistant cement (SRC) is recommended as a means of limiting such strength loss. Zhang et al. (2014a) found that the strength of saline soil with 10% salt content decreased by 33% compared to soil with 2.5% salt content after including 10% of OPC and curing for 28 days. This decrease is triggered by the reaction of chloride (Cl) with C3A, which reduces the formation of CAH. CAH is a primary hydration product, so its strength decreases significantly. Horpibulsuk et al. (2012) investigated the salinity and substitution of OPC by waste ashes effect on the strength of soft saline clay. Their results indicated that when salt content increased from 0.075% to 3% after 28-day curing period, the UCS reduced by 28.16% (from 2784 kPa to 2000 kPa). Tumwiine et al. (2024) emphasized the influence of pore fluid on the strength of a stabilized marl sample with 7.5% of OPC, cured for 28 days. The UCS decreased by 46.9, 30.7, and 49.1% for 25, 50, and 100% Sebkha brine (highly concentrated salt water within Sebkha profile) concentrations, respectively. This decrease can be linked to the significant impact of the pore fluid environment on the chemical composition, resulting in significant alterations to the primary minerals (silicates and calcium) involved in the cementitious reaction.

The existing literature reveals an apparent lack of research on the effect of SRC on the mechanical behavior of highly saline soils (i.e., EC>16 dS.m<sup>-1</sup>) (Laboratory (US), 1954), mainly inland chloride-sulfate soils (Loyer, 1991). Particularly, the high salinity level and the presence of bi-salt types in the soil profile reflect the actual field conditions observed in the Ain M'lila Sebkha. Indeed, the Sebkha is situated in the eastern region of Algeria, a key trading hub. Given that roads represent the primary commercial infrastructure in Algeria, the national road RN03, which traverses this Sebkha, has recently exhibited considerable deterioration (Hafhouf et al., 2022; Hafhouf and Abbeche, 2023). Moreover, the government has recently initiated a project to link the RN100 to the Batna-Chelghoum Laid highway via a 45 km, 2x2 lane road. This highway intersects the RN03 near the Sebkha of Ain M'lila. Consequently, earthen construction near these problematic soils could induce unexpected deformation of the infrastructure in the short and long term, impeding economic and infrastructure development in semi-arid zones. Therefore, the primary objective of this study was to investigate the potential of using an SRC stabilizer to enhance the strength of Sebkha soil for its application as subgrade material in flexible pavement

construction. After sampling and preparing the soil, UCS tests were conducted to assess the soil's strength. Subsequently, XRD, FTIR, TGA, pH and EC measurement tests were performed to connect microstructural observations with macroscopic behavior and to understand the impact of salt phases, such as halite and gypsum, on hydration reactions. Finally, a flexible pavement structure was designed for both untreated and SRC-treated Sebkha soil, assessing the effect of the SRC stabilizer on total pavement thickness and construction costs.

#### 4.2. Materials and methods

#### 4.2.1. Materials

The soil under examination was sourced from the Sebkha of Ain M'lila, located in the Oum El Bouaghi province in northern Algeria, covering an area of 61 km² (Fig 4-1). Sebkha soil typically forms in arid and semi-arid climates where evaporation rates exceed precipitation. This climatic condition leads to the evaporation of concentrated solutions from the soil surface, resulting in saline crust formation—a process known as upward salinization (Heurteaux and Servant, 1979). During winter, these soluble salts are carried by water to deeper soil layers. A survey conducted in October 2021 (Figs 4-2a) revealed a heterogeneous Sebkha profile. The upper part of the profile contained halite (NaCl) crystals, while deeper layers exhibited pieces of gypsum (CaSO<sub>4</sub>·2H<sub>2</sub>O). These findings align with Rouchy and Blanc-Valleron's (2006) research, which indicates that gypsum precipitates first after 80% water evaporation, followed by halite precipitation after 90% evaporation. Mineralogical analysis (see Figs 4-2b) further confirmed these results.

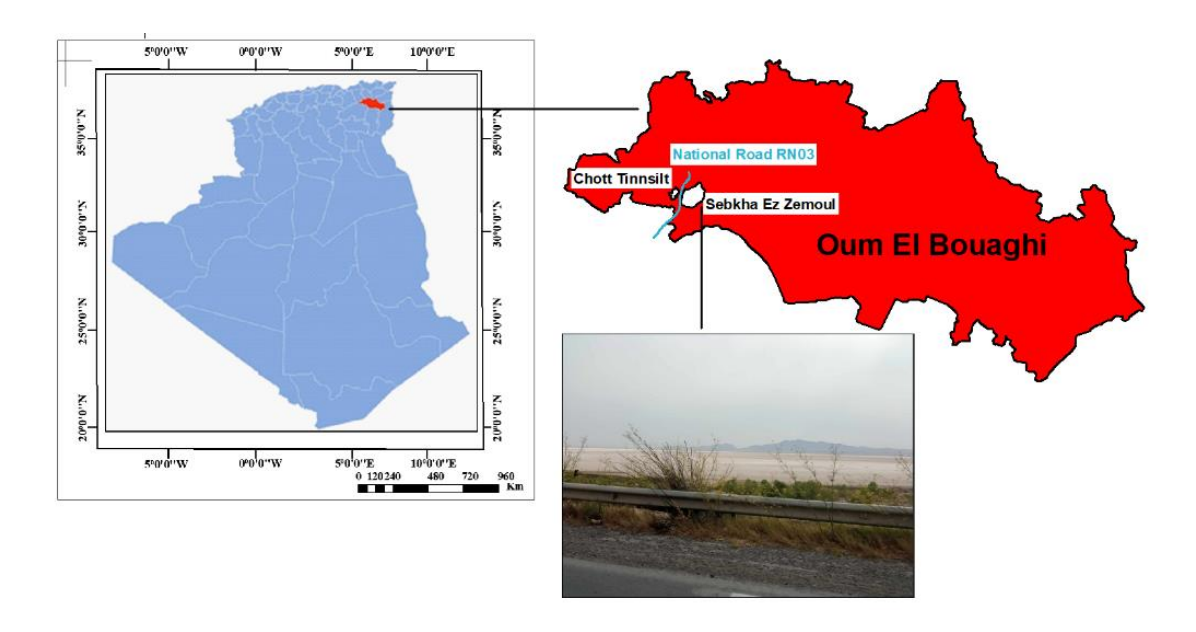


Fig 4-1. Sebkha soil study area location.

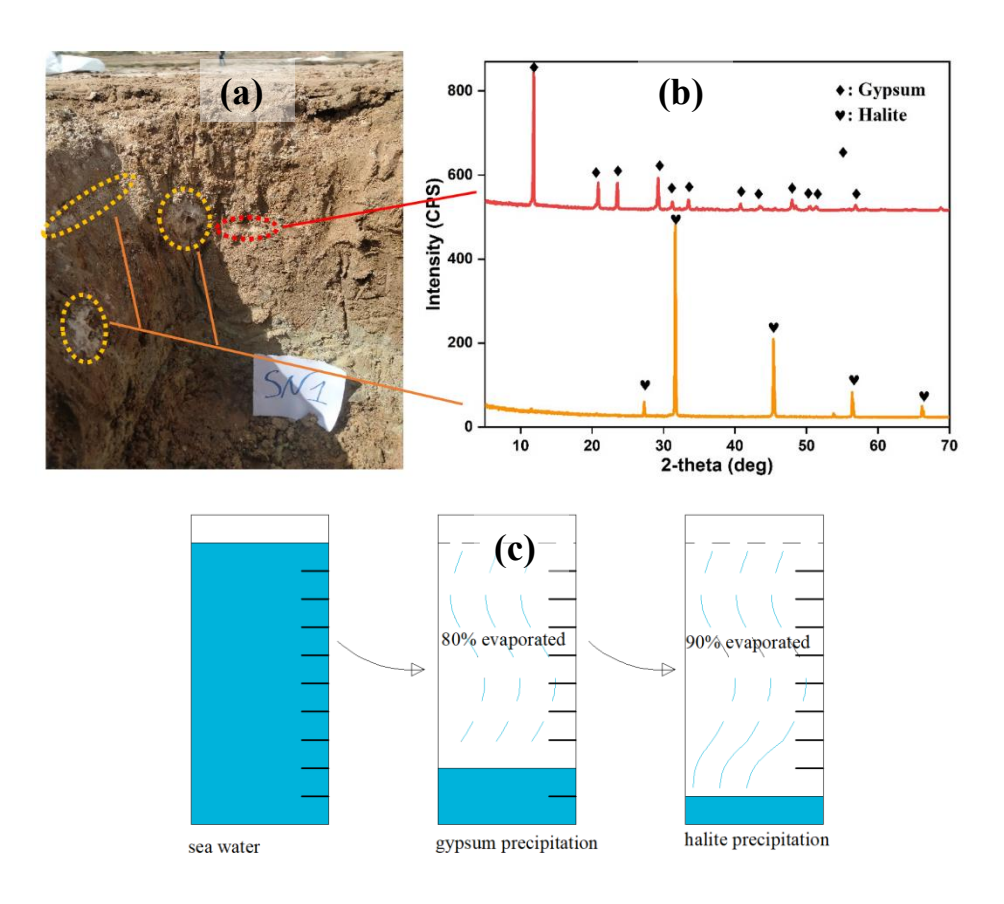


Fig 4-2. Sebkha profile (a), mineralogical phases of salt crystals within the sebkha profile (b), and theoretical diagram of salt precipitation during seawater evaporation (c).

According to the US salinity laboratory staff (Laboratory (US), 1954) and based on the measured electrical conductivity of 23.2 dS.m<sup>-1</sup> (Table 4-1.), which is greater than 16 dS.m<sup>-1</sup>, this soil is classified as high saline. The major soluble salt ions are Cl<sup>-</sup>(6874 mg.L<sup>-1</sup>) and SO<sub>4</sub><sup>2-</sup> (5605 mg.L<sup>-1</sup>), which arrange this soil in terms of salt type a chloride-sulfate soil (Loyer, 1991).

Table 4-1. The chemical compositions obtained based on the saturated soil paste extract

ECe (dS/m)	Salt	pH Solubl	H Soluble salt content (mg/L)					
	concentration							
	(g/L)							
23.2	17.64	6.81 Ca <sup>2+</sup>	$Mg^{2+}$	Na <sup>+</sup>	K <sup>+</sup>	SO <sub>3</sub> -	Cl-	HCO <sub>3</sub> -
		466.1	172.3	4452	56	5605	6874	12

The geotechnical properties of this soil are listed in Table 4-2. The soil has a liquid limit (LL) of 33% and a plasticity index (PI) of 16.49%. According to the Unified Soil Classification System (USCS), the soil is classified as (CL). The thermogravimetric analysis (TGA) and its derivative of the analyzed soil (Fig 4-3) indicated that the primary mineralogical components are quartz, calcite, gypsum, halite, and traces of kaolinite. This finding corresponds with those of Hafhouf et al. (2022) conducted on the same Ain M'lila Sebkha soil. The TGA shows mass loss peaks at 120°C, 1000°C. 711°C, and corresponding to gypsum dehydration, calcite decarbonisation/decomposition, and halite melting, respectively (Fatah et al., 2024; Hafhouf and Abbeche, 2023). These results confirm that the main mineralogical saline phases within the soil are CaSO<sub>4</sub>·2H<sub>2</sub>O (gypsum) and NaCl (halite). These findings are consistent with Hafhouf and Abbeche's (2023) differential thermal analysis (DTA) results on the same Sebkha soil. For temperatures ranging from 0 to 200°C, they observed two endothermic peaks at 90°C and 145°C, associated with water evaporation and gypsum dehydration, respectively, accompanied by a 3.2% mass loss.

Table 4-2. Geotechnical characteristics of sebkha soil.

Soil's parameters (unit)	Value	Methods
Natural water content $w_{\rm ntr}$ (%)	18.19	

Chapter 4. Effect of sulfate-resistance-cement treatment on saline soil (Sebkha soil) subgrades

Maximum dry density γ <sub>dopn</sub>	1.841	NF P94-093, 2014
Optimum moisture content $w_{\text{opn}}$ (%)	11.8	
≤2 mm fraction (%)	100	NF P94-056, 1996
≤80 µm fraction (%)	76	
≤2 µm fraction (%)	10	NF P94-057, 1992
Plastic limit PL (%)	16.51	ASTM D4318-00, 2000
Liquid limit LL (%)	33	
Plastic index PI (%)	16.49	
USCS classification	CL	ASTMD2487-00, 2000
CaCO <sub>3</sub> content (%)	31.3	NF P94-048, 1996

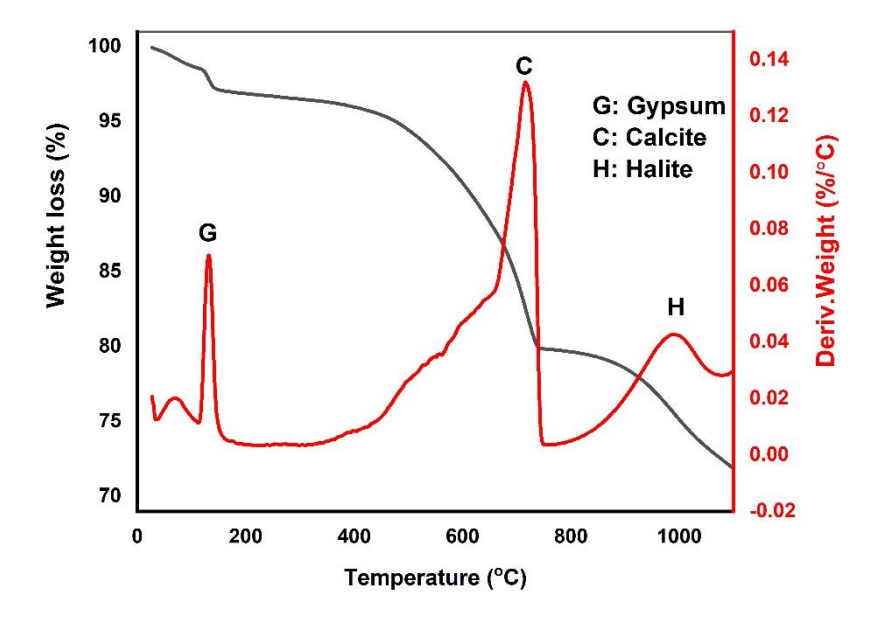


Fig 4-3. TGA curve of pure sebkha soil.

The cement used in this study is a grey powder, type CEM I 42.5 N SR3 (C<sub>3</sub>A < 3%), supplied by the GICA group industry in Setif, Algeria. Its chemical composition, as provided by the supplier, is presented in Table 3. It should be noted that due to the high sulfate levels in the soil, it is important to prevent the formation of harmful ettringite crystals. This can be achieved by using sulfate-resisting cement (SRC), which contains less than 3% of the compound C<sub>3</sub>A that typically reacts with sulfates. Although the soil also has high chloride levels, SRC is not inherently superior to regular Portland Cement (OPC) in resisting chloride damage. However, SRC offers protection against chlorides differently: it contains more silicate materials that form special gel structures (CSH gels) during the hardening process. These gels occupy more space in

the concrete, resulting in a denser structure that makes it more difficult for chlorides to migrate. Thus, it provides a more effective physical barrier against them.

Table 4-3. The chemical compositions and mineralogical phases of CEM I 42.5N SR3.

Parameters	Value	Parameters	Value
Chemical compounds		Mineralogical	
		phases	
CaO (%)	58.02	C <sub>3</sub> S (%)	59.54
SiO <sub>2</sub> (%)	21.17	C <sub>2</sub> S (%)	23.37
Fe <sub>2</sub> O <sub>3</sub> (%)	4.46	C <sub>4</sub> AF (%)	13.54
Al <sub>2</sub> O <sub>3</sub> (%)	3.90	C <sub>3</sub> A (%)	2.81
MgO (%)	3.13		
SO <sub>3</sub> (%)	2.24		
K <sub>2</sub> O (%)	0.46		
Na <sub>2</sub> O (%)	0.10		

### **4.2.2.** Methods

### 4.2.2.1. Samples preparation

In order to stabilize the Sebkha soil, SRC dosages of 2%, 5%, and 8% by dry weight of soil were selected based on recommendations by (Shuja et al., 2022; Tumwiine et al., 2024). Following the French standard NF P94-093 (AFNOR, 2014) for soil compaction tests, all soil samples (with and without cement addition), were moistened by different water content, then put in place layer by layer into a Proctor mold with a total of three dynamically compacted layers. Each layer was subjected to 25 strokes using a normalize hammer with a drop mass of 2,490 kg and a drop height of approximately 305 mm. The upper surface of the mold was scraped using a metal ruler, and the compacted samples were weighed. The density of each sample was calculated based on the mold volume and sample mass. Subsequently, the maximum dry density ( $\gamma_{dmax}$ ) and its optimum moisture ( $w_{opt}$ ) content were obtained, as shown in Table 04. The soil and SRC binder were mixed manually until a uniform mixture was achieved. Sample preparation followed a standardized protocol for each group. Soil, lime, and water were combined using an automated mixer at medium speed for three minutes to ensure thorough blending. The mixtures were then sealed in plastic bags

and left to mellow for 1 hour for untreated soils and 24 hours for cement-treated soils (Aldaood et al., 2014). Sample formation involved a three-layer structure, with each layer individually compacted using a CBR machine, operating at a consistent speed of 1.27 mm/min (Estabragh et al., 2014; Hafhouf et al., 2022). Compaction continued until the sample reached 95% of the  $\gamma_{dmax}$  previously determined by standard Proctor tests. For reference, untreated samples typically achieved a density of approximately 1.749 g/cm<sup>3</sup>. Before long-term storage, each sample was precisely weighed with a tolerance of  $\pm 0.5$  g. The samples were then carefully wrapped in plastic film and coated with paraffin to maintain their integrity. Finally, the prepared samples were placed in a climate-controlled chamber with a relative humidity of over 95% and a temperature of 20  $\pm$  2°C, following standard curing conditions (Nan et al., 2022; Zhang et al., 2014a). The curing periods were set at 3, 7, 14, and 28 days. The sample preparation process is illustrated in Fig 4-4.

 Table 4-4. Compaction characteristics of SRC treated sebkha soil.

% SRC	0	2	5	8
Properties				
Maximum dry density $(\gamma_{dmax})$ $(g/cm^3)$	1.841	1.854	1.862	1.877
Optimum moisture content $(w_{opt})$ (%)	11.8	11.5	11.6	11.4

## 4.2.2.2. Unconfined Compressive Strength test

Unconfined compression tests were conducted according to standard NF P94-077 (AFNOR,1997). The plastic film was removed, and the specimens were promptly placed in an axial loading press to prevent moisture evaporation, applying a constant displacement of 1 mm/min.



Fig 4-4. The Glimpses of Soil Sample Preparation.

# 4.2.2.3. Chemical and mineralogical tests

A Siemens D500 powder diffractometer (Bruker AXS model) with a nickel anticathode ( $\lambda K\alpha = 1.5406 \text{ Å}$ ) was used. The system is controlled by a microcomputer, automated goniometer rotation, data acquisition, and processing. Operating conditions were set at 30 kV and 20 mA. XRD analysis identified the main mineral phases in powdered saline soil specimens.

TGA was conducted using an SDT Q600 (TA Instrument) connected to a computer for data acquisition and processing. Ground soil samples (35 mg) were placed in platinum crucibles and heated from 20 to 950°C at a rate of 10 °C/min under a 50 ml/min flow of 99.99% pure argon, an inert gas that ensures a clean, non-reactive environment for the analysis.

Soil pH was measured in a 1:2.5 soil-water extract. To prepare the suspensions, 50 ml of distilled water was added to 20 g of oven-dried soil. The containers were manually shaken four times at 30-minute intervals for 1 minute each, following **Rhoades'** (1982) method. The resulting suspensions

were filtered using Whatman #42 filter paper to obtain the extracts. Soil pH was then measured using a Jenway 3510 pH meter. Electrical conductivity (EC) of saturated paste extracts was determined with an Inolab-Cond meter (WTW 1CA301), expressing salinity in dS.m<sup>-1</sup> at 25°C. Soluble cations and anions were quantified using volumetric methods (Pansu and Gautheyrou, 2006).

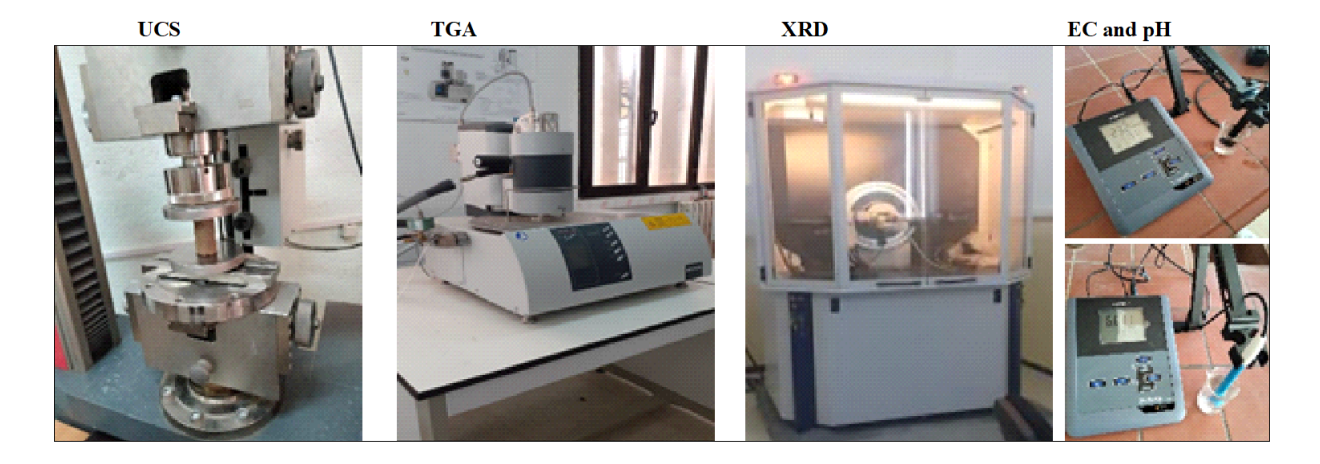


Fig 4-5. Glimpses of Strength and Microstructure Experimentations.

### 4.3. Results and discussion

### 4.3.1. UCS

## 4.3.1.1. Effect of curing time and SRC addition on stress-strain curves

Figs 4-6a, b, and c illustrate the stress-strain curves from UCS tests on Sebkha soil with different SRC dosages over various curing periods. The UCS of the untreated sample is denoted as UCS<sub>ut</sub>. The slope of the linear portion before failure indicates stiffness, while the peak of the stress-strain curve represents the material's UCS (Hafhouf et al., 2022). For each dosage, stiffness increased with curing time. However, the maximum increase was observed at 7 days for the 2% dosage and at 14 days for the 5% and 8% dosages. The long curing period and high SRC content significantly increase the stiffness of stabilized soil. The maximum stiffness is attained after 14 days of curing with 8% SRC content. Increased cement content results in the production of more hydration compounds, including CSH gels. As the hydration process advances over time, these hydration compounds gradually fill the pore spaces and interact to form a solid network, resulting in a denser

structure and higher stiffness (Dingwen et al., 2013). The failure peak was not pronounced for untreated soil, with strength decreasing gradually reaching a relatively low value. The peak corresponded to a UCS of 150.37 kPa at 4.78% strain. In contrast, SRC-treated soil exhibited brittle behavior, characterized by a sharp decrease in strength after failure with an apparent peak. This behavior became more pronounced with increasing curing time and SRC quantity. After 7 days of curing, the maximum strength of the samples increased by 320%, 596%, and 849% with the incorporation of 2%, 5%, and 8% SRC, respectively, compared to the untreated samples. After 14 days of curing, the strength increases were 318%, 740%, and 1056% for the same SRC percentages. This pattern of strength improvement closely corresponds to the stiffness, indicating that as the SRC content and curing time increase, both strength and stiffness also rise. Higher cement content leads to increased precipitation of CSH gels, which fill pores, coat soil particles, and bind them together. Consequently, higher cement content and longer curing time result in greater strength of the stabilized soil. However, after 28 days of curing, strength decreased by 27.14%, 7.78%, and 3.41% compared to the 14 days for 2%, 5%, and 8% SRC, respectively. These findings align with Xing et al. (2009), demonstrating that high soluble salt content inhibits C-S-H formation. Cl<sup>-</sup> and SO<sub>4</sub><sup>2-</sup> ions in the interstitial water could consume Ca(OH)<sub>2</sub> and/or react with cementitious products like CSH gels, forming hydrates with weak cementing properties, thus impeding soil-cement strength development. Specifically, chloride (Cl<sup>-</sup>) impacts soil-cement strength in the short, intermediate, and long terms, while sulfate (SO<sub>4</sub><sup>2-</sup>) primarily affects its longterm strength. Lucile et al. (Rica et al., 2016) studied the influence of sulfate and chloride ions, introduced as CaSO<sub>4</sub>·2H<sub>2</sub>O and NaCl, on the physical and mechanical properties of treated soil was investigated. Their results indicated that while individual addition of chloride or sulfate ions caused structural instability (low strength) at 7 and 10g of SO<sub>4</sub><sup>2</sup>-.kg<sup>-1</sup>, their combined presence resulted in structural instability at 3g of SO<sub>4</sub><sup>2</sup>-.kg<sup>-1</sup>. Saussaye et al. (2020) investigated how soil salts (anions and cations) influence the physical and mechanical properties of stabilized soil. Their findings revealed that chloride ions caused less strength disruption when combined with sodium compared to potassium, while sulfate ions showed the opposite effect. Furthermore, the simultaneous presence of sodium and potassium salts with either sulfate or chloride anions resulted in significant strength reduction (up to 75%). These results show that adding up to 8% SRC was sufficient to increase soil strength with minimal strength loss after 28 days of curing. In other

words, the negative effect of saline phases (i.e., gypsum and halite) could be significantly reduced after incorporating 8% SRC into the soil.

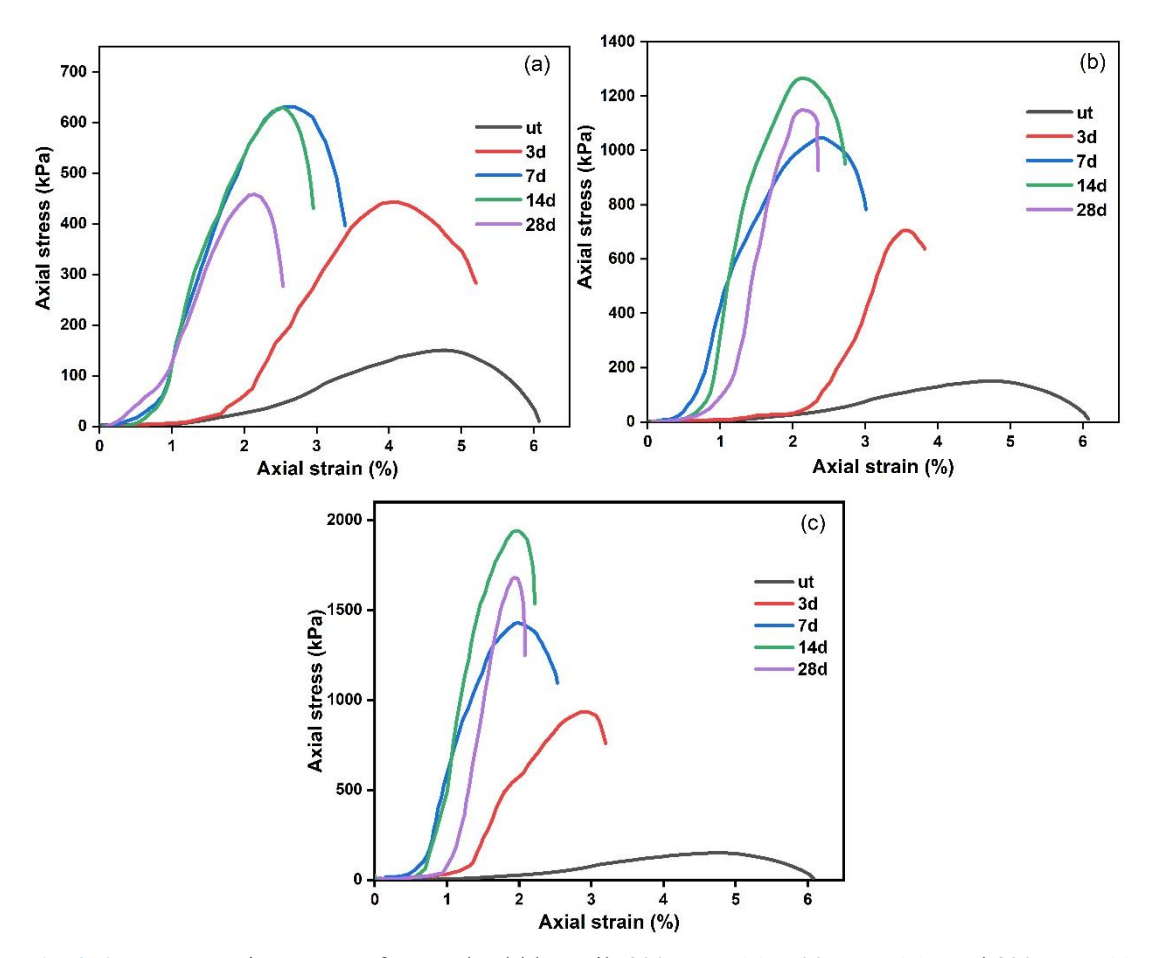
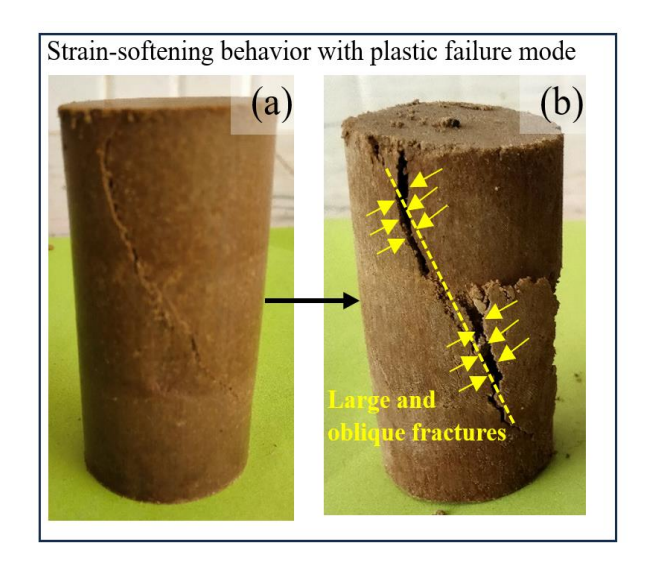


Fig 4-6. Stress-strain curves of treated sebkha soil: 2% SRC (a), 5% SRC (b), and 8% SRC (c)

**Fig 4-7** compares the typical failure modes observed on the surfaces of untreated Sebkha soil and samples treated with 8% SRC to better understand soil behavior in the presence of SRC. All specimens, without exception, exhibit strain-softening behavior. After reaching peak stress, material strength decreases with increasing strain. For untreated soil, strain-softening behavior is evident in the stress-strain curve during initial compression, corresponding to minor crack formation. As applied stress increases, these surface cracks propagate until the specimen reaches peak strength (**Fig 4-7a**). Beyond this point, stress gradually decreases with increasing strain, exhibiting plastic deformation characterized by continuous crack expansion, ultimately resulting

in large, oblique fractures (Fig 4-7b). This observation aligns with Chen et al. (2024) and Hafhouf et al. (2022), who reported similar strain-softening behavior in plain saline soils. Notably, the hygroscopic nature of salt crystals within the sample facilitates their transformation from solid (crystalline) to liquid (solution) phase at the optimum water content (wopt) (Al-Amoudi et al., 1995a). This phase change reduces structural density, contributing to the observed plastic behavior. Conversely, Li et al. (2023) and Nan et al. (2022) reported a strain-hardening behavior in compacted saline soils with high clay content (>40% of dry soil by weight). Their insights revealed a predominantly vertical crack propagation pattern and a linear stress-strain relationship postfailure. This phenomenon is associated with the salt crystals within the soil matrix acting as loadbearing structures, enables the material to withstand higher loads under low permeability conditions, characterizing high clay-content soils. This strain-hardening behavior, in contrast to the more common strain-softening observed in soils, emphasizes the significant influence of soil composition on the mechanical behavior of saline soils. However, despite this apparent hardening behavior, the inherent instability of salt crystal structures, which can readily transition between solid and liquid phases, prevents the direct use of natural saline soil as a subgrade or foundation material in engineering applications. With cement incorporation, the softening of the stress-strain relation occurs prior to peak strength, accompanied by moderate cracks (Fig 4-7c). However, the treated samples exhibit a distinct mode of plastic failure after peak strength to untreated ones, characterized by double cone cracks and peeling off/detachment of the surface in a particular area, indicating more brittle behavior (Fig 4-7d). At this point, stress rapidly decreases as strain increases, resulting in strength failure. This behavior parallels that observed in cement-treated soft soils, where cementitious materials' improved compaction density and pore-filling promote structural integrity, leading to more brittle behavior (Chen et al., 2024).



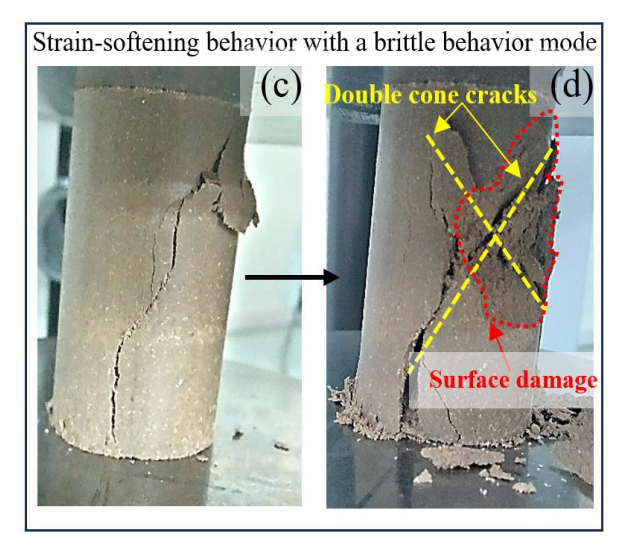


Fig 4-7. Failure patterns of sebkha soil: untreated soil before (a) and after peak strength (b), and 8% SRC-treated soil before (c) and after peak strength (d)

Fig 4-8 shows the UCS of soil samples treated with different amounts of cement (2%, 5%, and 8%) over various curing periods (3, 7, 14, and 28 days). The repeatability of UCS tests was assessed by performing three replicate tests for each level of SRC content and curing period. The coefficient of variation (CV) for the UCS results ranged from 1.95% to 7.23%, which is well within the acceptable limit of 10% (Uzielli et al., 2007). The highest variability, with a CV of 7.23%, was observed in samples containing 8% SRC after 14 days of curing. In contrast, the lowest variation, with a CV of 1.95%, was found in samples with a 2% SRC dosage after 7 days of curing. This relatively low variability indicates good reproducibility of the strength results and confirms the reliability of the testing procedures used in this study. The UCS of untreated samples (UCSut) acts as the control. The results indicate a significant increase in soil strength with higher cement content and extended curing periods. For 2% of SRC addition, the UCS increased by 2.94, 4.20, 4.18, and 3.05 times the control value after 3, 7, 14, and 28 days of curing, respectively. With 5% of SRC addition, there were more significant strength gains, with UCS increases of 4.70, 6.96, 8.40, and 7.74 times the control value for the same curing periods. The most significant improvements were observed with 8% of cement addition, where UCS values increased by factors of 6.22, 9.49, 11.56, and 11.17 for the respective curing durations. As the curing time increases and the cement content decreases, the negative impact of salt phases on strength development becomes more evident. For example, with 2% of SRC incorporation, the UCS dropped by 3.86%

at 14 days and by 27.14% at 28 days. Furthermore, after 28 days of curing, samples with 8% SRC addition exhibited only a 3.14% decrease in UCS, while those with 2% SRC showed a 27.14% reduction in strength. This result is consistent with that of **Zhang et al. (2014a)** indicating that the negative impact of salt concentration becomes more apparent as the curing time increases. However, this effect on the strength of cement-stabilized clays with high cement content at 15% and 20% is relatively minor. Saline soils hinder the development of soil strength as Cl<sup>-</sup> reduces the peak of CSH gels and forms a 3CaO.Al<sub>3</sub>O<sub>3</sub>.3CaCl<sub>3</sub>.32H<sub>2</sub>O compound without gelatinization. Additionally, SO<sub>4</sub><sup>2-</sup> can generate ettringite with expansion properties. As expansion reaches a certain level, the soil cement starts to crack, leading to a decrease in the strength of the cement soil. In this context, there was a slight negative impact of high salinity (ECe=23.2 dS.m<sup>-1</sup>) after treatment with 8% of SRC, where the UCS of stabilized Sebkha soil showed a gentle decrease (3.14% loss) after 28 days of curing.

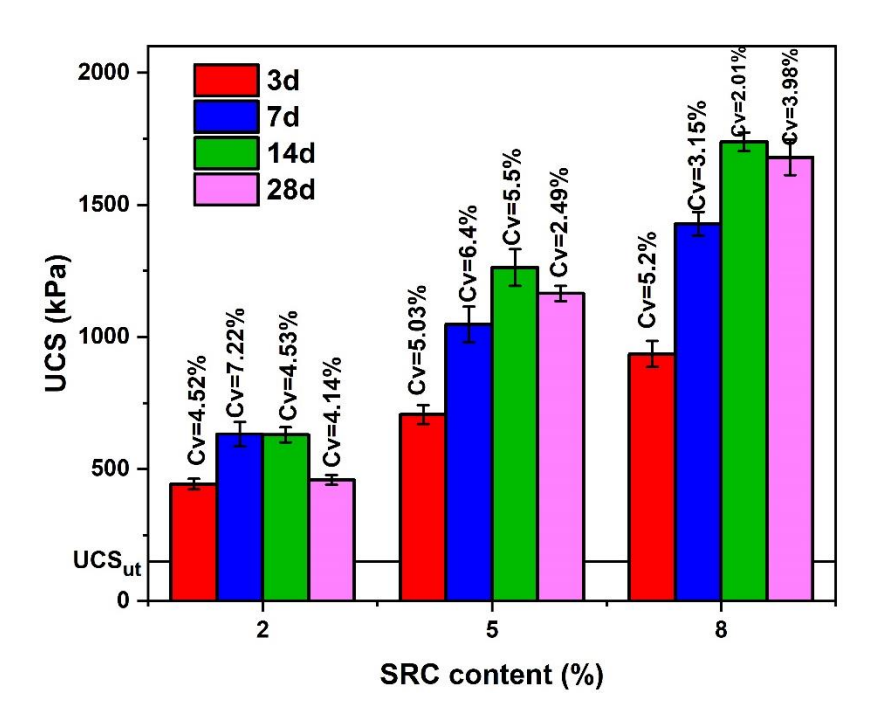


Fig 4-8. UCS histograms of treated Sebkha soil.

## 4.3.2. Effect of curing time on the physic-chemical behavior

# 4.3.2.1. XRD of SRC-treated Sebkha at different curing conditions

Fig 4-9. shows the evolution of the mineralogical phases of untreated soil and 8% of SRC-treated Sebkha soil using XRD analysis. The 14-day curing period was chosen because it typically achieved 90% of maximum strength, as most CSH gels formed during this time (Rahimi et al., 2023). Additionally, this period demonstrates the formation of Friedel's salt (Fs) in the early stage of curing, indicating competition between CSH gels and Fs during this stage (Cheng et al., 2017). The mineralogical analysis showed that the natural soil contains gypsum, with peaks at  $2\theta$ = 11.76° and 23.38°, and halite with peaks at  $2\theta = 31.74^{\circ}$  and 45.46° as the main saline mineral phases. This finding is consistent with the results of Hafhouf et al. (2022), who analyzed soil samples from the same location (Ain M'lila Sebkha). After a 14-day curing period, new minor peaks at  $2\theta = 29.06^{\circ}$  and  $50.14^{\circ}$  were observed, corresponding to the Calcium Silicate Hydrate (CSH) cementitious phase. This result is in line with previous research on cement-treated soils (Haji and Mir, 2023; Zhang et al., 2014b). Additionally, the intensities of halite peaks decreased, and a new hydration product, calcium aluminate chloride hydrate (Friedel's salt or Fs), appeared with relatively low peak intensities at  $2\theta = 11.27^{\circ}$  and  $40.74^{\circ}$  (Cheng et al., 2017; Jiang et al., 2024; Liu et al., 2018; Shi et al., 2017). According to Cheng et al. (2017), the precipitation of Fs within the soil matrix improved early strength by reducing porosity through its expansion up to 1.8 times, which is one of the main mechanisms for strength enhancement. However, this salt mineral phase has lower strength compared to cement hydrates (Al-Amoudi et al., 1995b). This is confirmed by Jiang et al. (2024), who conducted an experimental study using high alumina cement (A), ordinary Portland cement (C), and lime (L) binders to stabilize chlorine soil. Their discoveries indicate that the chloride fixation effect (more fixation, higher Fs formation) of C3L3 is inferior to that of A3L3, but its CBR value is higher. This implies that although Fs enhances the strength of the soil, the primary provider of mixture strength should be cementitious hydration products such as C-S-H. In the current study, the Sebkha soil is classified as chloride-saline (Loyer, 1991) soil with Cl<sup>-</sup>/SO<sub>4</sub><sup>2</sup>=1.23. Halite is approximately 10 times more soluble than gypsum (Babel and Schreiber, 2014), which results in a higher concentration of Cl<sup>-</sup> than SO<sub>4</sub><sup>2-</sup> ions in soil pore water. These Cl<sup>-</sup>ions can react with Ca(OH)<sub>2</sub>, C<sub>3</sub>A, and alumina (from cement and clay minerals) to form 3CaO·Al<sub>2</sub>O<sub>3</sub>·CaCl<sub>2</sub>·10 H<sub>2</sub>O (calcium aluminate chloride hydrate),known as Fs (Jiang et

al., 2024). According to **Zibara** (2001) the latter formation was observed to be involved in the following chemical reactions:

$$Ca(OH)_2 + 2NaCl = CaCl_2 + 2Na^+ + 2OH^-$$
 (1)

$$C_3A + CaCl_2 + 10H_2O = C_3A. CaCl_2. 10H_2O$$
 (2)

It is evident that some of the C<sub>3</sub>A and Ca(OH)<sub>2</sub> reacted with chloride, resulting in a reduction in pozzolanic reactions. This led to a decrease in the strength of stabilized Sebkha soil, not only due to the formation of Fs with weaker cementing properties, but also because of the diminished production of CSH gels. In simpler terms, over time, the rate of CSH formation from pozzolanic reaction decreased due to the continuous formation of weakening cementing phase Fs. Consequently, during the initial curing stage, the Fs precipitation, which expanded up to 1.8 times in the soil, was accommodated within soil voids. Conversely, at a later stage, when the treated soil had a more rigid structure with less space due to the formation of CSH cementitious compounds, the additional precipitation of Fs with high expansion properties exerted a more significant pressure than before, leading to reduced strength.

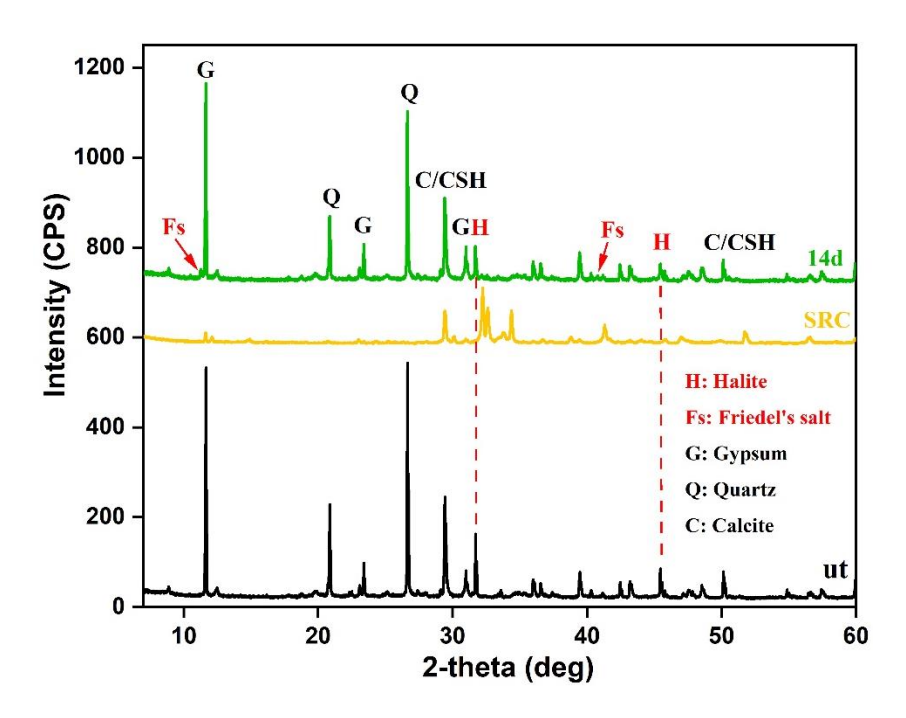


Fig 4-9. XRD diagrams of untreated and treated Sebkha soil.

### 4.3.2.2. TGA and FTIR of SRC-treated Sebkha at different curing conditions

Fig 4-10 shows the thermogravimetric analysis (TGA) curves and their derivative for untreated soil and 8% of SRC-treated soil. It is worth mentioning that the 8% SRC dosage was selected because it produces higher CSH gels than the 2% and 5% dosages. Indeed, on the one hand, higher cement dosage provided greater cementitious compounds (CAH and CSH), increasing network cementitious bridges within soil fabric, resulting in a denser structure that inhibits dissolution and movement of salts and thus limits their adverse effects on soil strength. On the other hand, higher cement content leads to an increased production of calcium hydroxide (Ca(OH)<sub>2</sub>), commonly known as portlandite, during the hydration process. This compound has the ability to react with NaCl (halite) to form a new hydration product called Fs (Friedel's salt), which has cementitious properties. The higher concentration of Ca(OH)<sub>2</sub> in the interstitial pore solution enhances the likelihood of NaCl participating in reactions that form Fs, thereby increasing the fixation of NaCl. Therefore, as cement content increases, the concentration of soluble salts (NaCl) decreases in the matrix, mitigating their harmful effects. The curves after 14 days and 28 days of treatment are not similar to those of natural soil, indicating the formation of hydrated compounds. In the untreated soil, mass loss peaks occurred at 120°C, 711°C, and 1000°C, corresponding to gypsum dehydration, calcite decarbonization/decomposition, and halite melting (Fatah et al., 2024; Hafhouf and Abbeche, 2023). However, after 14 days of curing in the treated soil, a mass loss peak appeared at 75°C, corresponding to the dehydration of the CSH gel (Chou et al., 2024; Wan et al., 2024). This peak remained consistent after 28 days, indicating rapid precipitation of hydration products such as CSH after adding cement to the soil-water mixture. Meanwhile, a major peak in the temperature range of 180–450°C, corresponding to the thermal decomposition of Fs, was observed (Shi et al., 2017). The mass loss of Fs increased up to 28 days of curing, which is inversely proportional to NaCl mass loss. According to equations (1) and (2), Ca(OH)<sub>2</sub>, C<sub>3</sub>A, and NaCl reactions produced Fs, confirming the contribution of NaCl in forming the new hydrates phase (i.e., Fs). To this end, the formation of CSH is limited in the first stage of curing. Meanwhile, the precipitation of Fs continues due to the presence of Ca(OH)<sub>2</sub>, C<sub>3</sub>A, alumina (from clay minerals), and NaCl in the system (Jiang et al., 2024). In terms of resistance, reducing the amount of NaCl is closely associated with the formation of Fs in cement-treated Sebkha soil. Fs contributes to filling the pores in stabilized soil, thereby densifying the structure and increasing the strength of the final product. Fs can act as a good filler within the soil matrix during the early curing period

because of its expansive nature, enhancing initial strength. However, as the curing period develops, the structure becomes more rigid, and fewer voids are present due to CSH gels filling and coating the soil particles. At the same time, Fs continues to precipitate and expand up to 1.8 times its original volume within this rigid structure. When the internal pressures created by this expansion exceed the restraining forces of the matrix, it potentially leads to inadequate strength development and, thus, strength loss.

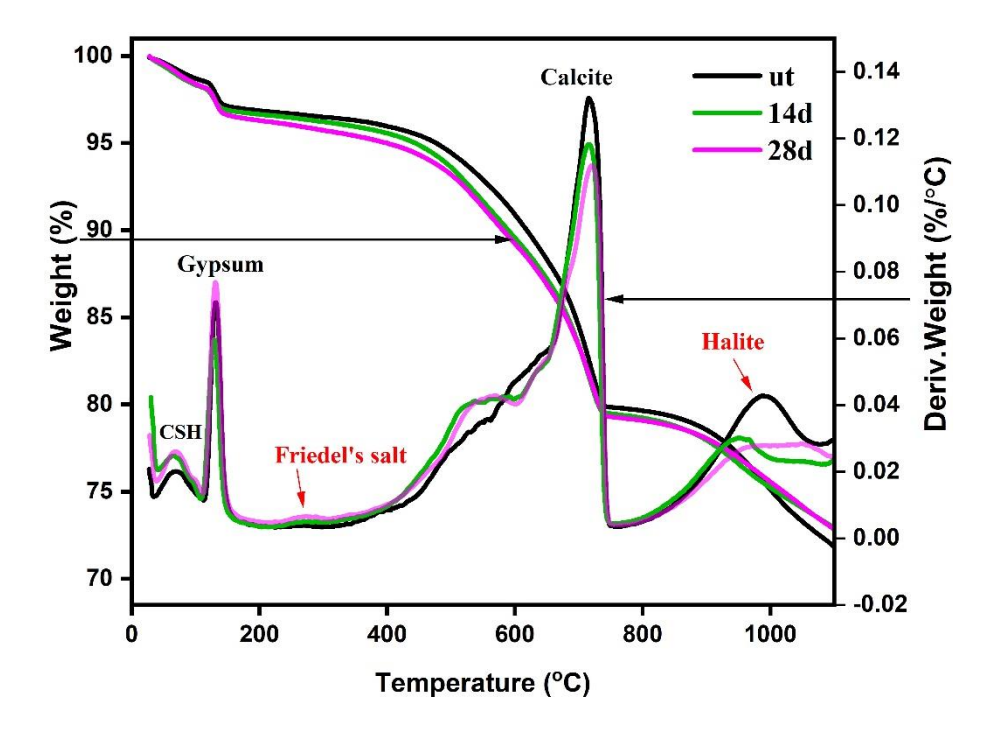


Fig 4-10. TGA curves of untreated and treated Sebkha soil.

The chemical banding and functional groups were identified using FTIR for the untreated and treated samples with 8% of SRC after 14 and 28 days of curing (Fig 4-11). Each bond possesses a distinct absorption band that corresponds to a unique vibration wavelength. Table 05 provides the functional group and mineralogical interpretation for each absorption wavenumber. The FTIR spectrum of treated soil seems a little different than the one of untread soil. This indicates that the cement incorporation has affected the functional group to some degree. For the untreated soil, the spectral bands at 3696 cm<sup>-1</sup> and 3446 cm<sup>-1</sup> are attributed to the vibrations of clay minerals such as kaolinite and montmorillonite (Xing et al., 2021). The band at 1454 cm<sup>-1</sup> corresponds to the stretching vibration of O-C-O, indicating the presence of carbonates in the soil (Zhou et al., 2021). The bands at 871 cm<sup>-1</sup> and 713 cm<sup>-1</sup> associated to characteristic peaks of calcite (Gao et al., 2005).

The peaks at 796 cm<sup>-1</sup> suggests to the symmetric stretching of Si-O in quartz (Mimboe et al., 2020). The peak at 695 cm<sup>-1</sup> indicates the presence of quartz minerals in a crystalline form with a relatively high degree of crystallinity (Chandrasekaran et al., 2015). With cement addition, bands at 3696 cm<sup>-1</sup> and 3446 cm<sup>-1</sup> corresponds to clay minerals being diminished over time. This proposes that clay minerals participate in hydration reactions. Meanwhile, the emergence of Fs is observed, with small peaks at 425 cm<sup>-1</sup> and 785 cm<sup>-1</sup> corresponding to the stretching vibration of Al-OH, and a small peak at 3628 cm<sup>-1</sup> could be the OH stretching region associated with the water stretching vibration and the M(metal)-OH stretching mode of the hydroxide layer (Birnin-Yauri and Glasser, 1998; Yue et al., 2018). The spectral peak observed between 2200 and 2400 cm<sup>-1</sup> is attributed to interference from atmospheric CO<sub>2</sub> (Demyan et al., 2013). It should be noted that Cl<sup>-</sup> does not absorb in the range 400-4000 cm<sup>-1</sup> due to the ionic nature of chloride bonding (Birnin-Yauri and Glasser, 1998). This finding is coherent with previous XRD and TGA results, where Fs formation is also noticed in cement-stabilized Sebkha soil.

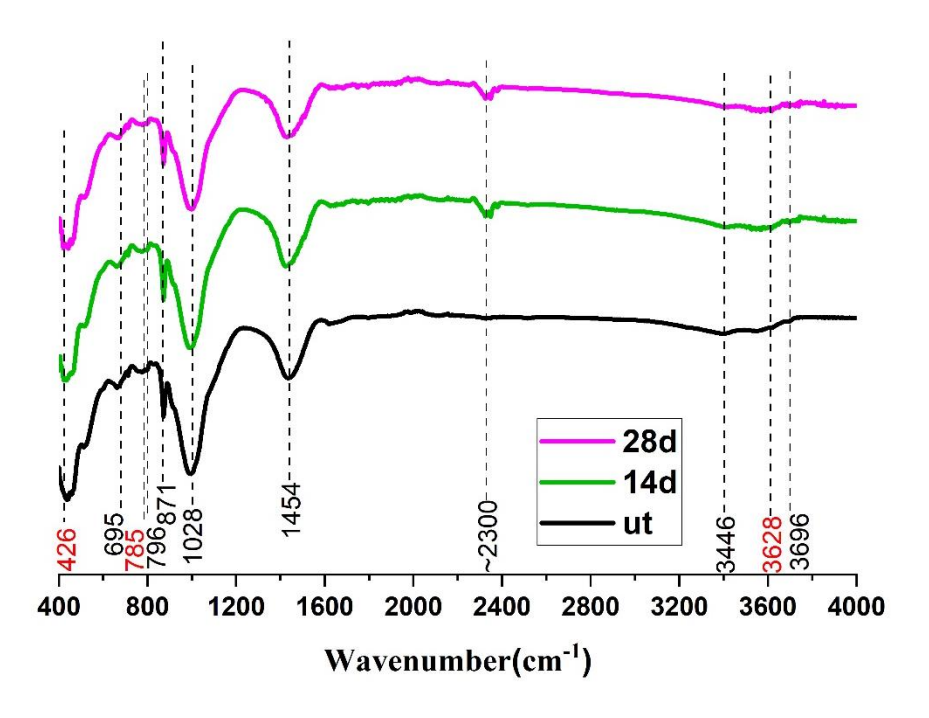


Fig 4-11. The FTIR of untreated and treated Sebkha soil.

### 4.3.2.3. pH value and Electrical Conductivity (mS/cm)

Fig 4-12a and b present the results of pH and EC tests on untreated and treated samples with different SRC dosages during various curing periods. For the 3-day treatment, the pH levels

increased to 9.89, 12.2, and 12.76 for 2%, 5%, and 8% SRC, respectively. This rise is attributed to the release of Ca<sup>2+</sup> basic ions after the dissolution of cement compounds during the initial 1-3 days of curing, creating an alkaline environment (Bouras et al., 2022). A higher cement content provides more Ca<sup>2+</sup>, resulting in higher pH, which aligns with the previously mentioned findings. Increased cement content leads to higher alkalinity, which helps mitigate the negative effects of salts. This higher alkalinity, associated with a larger amount of cement, facilitates the dissolution of alumina from clay minerals (Ying et al., 2022). Consequently, this process promotes the formation of Fs, which reduces NaCl content (participation of NaCl to form a new hydrate Fs). Over a 7-day curing period, the pH decreased to 9.34, 11.63, and 12.25 for 2%, 5%, and 8% of SRC, respectively. As cement dissolution is a rapid process primarily occurring within the first 3 days, hydration reactions proceed gradually and attain their maximum after 14 days of curing (Rahimi et al., 2023). These reactions consume Ca<sup>2+</sup> ions to produce the predominant cementitious products, C-S-H gels, thereby reducing environmental alkalinity. For 14 and 28 days of curing, the pH levels increased to 9.73 and 9.77 for 2% SRC, 12.2 and 12.33 for 5% SRC, and 12.7 and 12.93 for 8% SRC, respectively. This pH increase suggests a rise in alkaline ions, particularly hydroxide ions (OH<sup>-</sup>), after most C-S-H gels have formed. This study confirms the formation of Fs by XRD, TGA, and FTIR analyses. According to equation (1), the precipitation of Fs releases OH<sup>-</sup> ions, increasing pH. It should be noted that ettringite formation typically decreases pH significantly due to OH ions consumption (Gartner et al., 2002). However, in this case, it can be concluded that despite the relatively high gypsum content (i.e., chloride-sulfate soil), ettringite formation is inhibited due to Fs precipitation in the presence of halite. This indicates that halite has a more significant effect than gypsum on the strength development of cement-stabilized Sebkha soil. Consequently, Fs formation contributes significantly to strength enhancement through two mechanisms: Reducing voids within the soil fabric by precipitation and inhibiting ettringite formation, which could otherwise lead to expansive damage.

EC of extracted soil pore water measures the solution ability to conduct electricity, which is typically expressed in (dS/m). The untreated soil, as mentioned previously, is classified as high saline soil (i.e., 23.2 dS.m<sup>-1</sup>>16 dS.m<sup>-1</sup>). With cement stabilized Sebkha soil, for each cement content, EC decreases up to 7d. This decrease is significant at higher cement dosage. For instance, EC decreases to 17 and 16.5 for 2% of SRC and 8% of SRC, respectively. This finding agrees with that of **Zhang et al. (2014b)**, showing that EC decreases with the increase in cement content.

Ions such as K<sup>+</sup>, Na<sup>+</sup>, Ca<sup>2+</sup>, OH<sup>-</sup>, SO<sub>4</sub><sup>2-</sup>, Fe<sup>3+</sup>, and Mg<sup>2+</sup> from the cement dissolved into the water in the pores, creating an electrolytic solution that makes the soil matrix more conductive. However, the formation of hydration products consumes a significant portion of these ions, balancing the process. As the cement content increases, the EC decreases, showing a competition between the release of ions and their consumption in the formation of hydration (**Zhang et al., 2014a**). However, at 14days and 28days of curing EC starts to increase. This increase is more pronounced for higher cement content. It was noted previously that the precipitation of Fs was continuous up to 28days of curing, while that of hydration products was marginal after 14days of curing. So, variation in soil pore water ions is strongly related to Fs formation. Indeed, Fs precipitation releases more OH<sup>-</sup> and Na<sup>+</sup> ions (equation 1), which explains the increase in the EC of soil pore water.

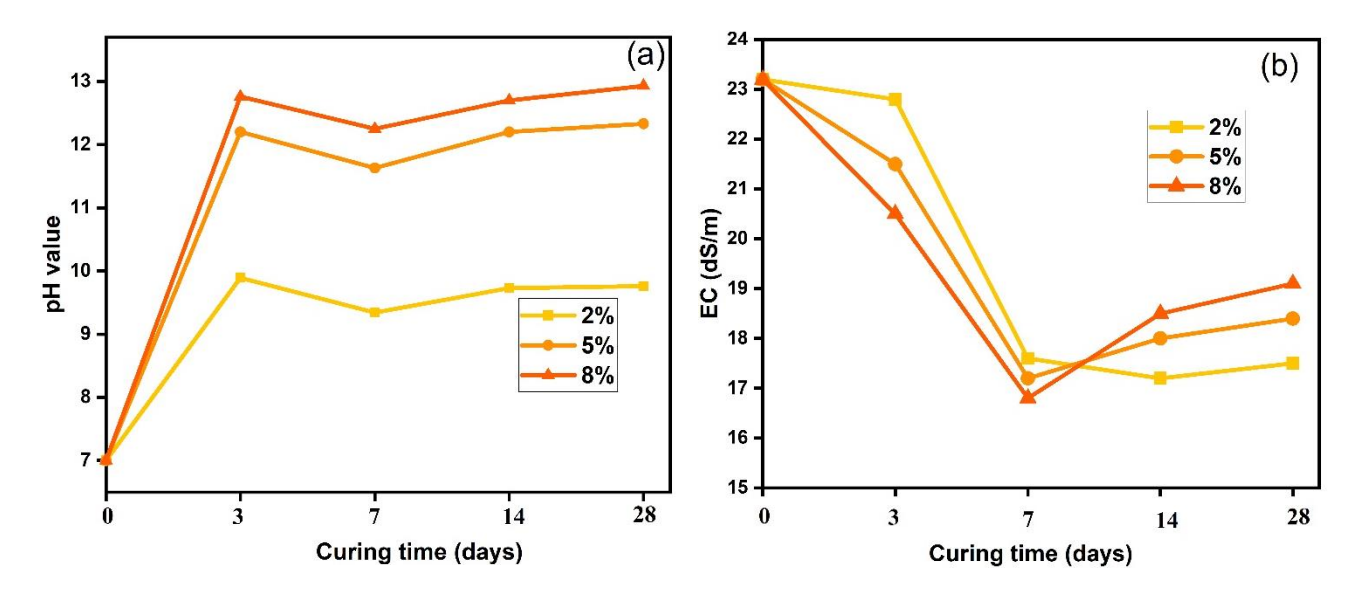


Fig 4-12. pH value (a) and the Electrical conductivity (EC) (b) of the untreated and treated Sebkha soil.

## 4.3.3. Application of Stabilized Sebkha Soil in Pavement Design

## 4.3.3.1. Design of Flexible Pavement

The design of a flexible pavement structure is outlined in the "Catalogue de dimensionnement des Chaussées Neuves" provided by the Algerian Ministry of Public Works (Alger, 2001). The basic data for pavement design include the following: 1. Determine the type of network: Roads that carry more than 1500 vehicles per day (V/d) are referred to as RP1, while roads with less than 1500 V/d

are named RP2. 2. Determine the class of traffic: The traffic class (TPLi) is expressed in terms of the number of heavy vehicles per day and per direction (PL/j/carriageway) on the most heavily trafficked road in the year of service . 3. Determine the bearing capacity of the pavement subgrade: Soil bearing classes range from S4 to S0 (refer to **Table 4-5**). This classification is used for pavement subgrade.

Table 4-5. Traffic class (TPLi) for the principal network (RP1) and subgrade bearing capacity classes (Si)

PL/d/carriageway	150-300	300-600	600-1500	1500-3000	3000-6000
TPLi	TPL3	TPL4	TPL5	TPL6	TPL7
CBR	<5	5-10	10-25	25-40	>40
Portance (Si)	S4	S3	S2	S1	S0

The data collected by a state consulting company (SETS) on the traffic in Oum El Bouaghi province, particularly in relation to the national road RN03, reveals that 7724 V/d and 1940 PL/d/carriageway were recorded in this region. This data classifies the type of network as RP1 (7724 V/d> 1500 V/d) and the class of traffic as TPL6 (1500-3000 PL/d/carriageway).

The formula proposed by **Black 1962** and **Black 1961** was used to correlate the UCS with CBR:

$$CBR = \frac{UCS (kPa)}{70}$$
 (3)

It should be mentioned that if the network type is RP1, then the untreated subgrade soil should have a bearing capacity of at least S2 (i.e., CBR value range between 10-25). If not, a subgrade improvement layer/capping layer should be added to achieve the required importance (at least S2) (Table 4-6)

Table 4-6. Material thickness of capping layer for low subgrade bearing (i.e., S4 and S3)

Capping layer	Material thickness of	Subgrade
material	capping layer (cm)	portance target
UGMs <sup>∆</sup>	50 (into 2 layers)	S3
UGMs	35	S3
UGMs	60 (into 2 layers)	S2
UGMs	40 (into 2 layers)	S2
	material  UGMs <sup>∆</sup> UGMs  UGMs	materialcapping layer (cm) $UGMs^{\Delta}$ 50 (into 2 layers) $UGMs$ 35 $UGMs$ 60 (into 2 layers)

S3 UGMs 70 (into 2 layers) S1

 $UGMs^{\Delta}$ : unbounded gravel materials

Based on the French guide (chaussées (France) and France. Service d'études sur les transports, 2000), the subgrade improvement layer thickness should be added after hydraulic binder addition, which is 35 cm. Table 4-7 shows the total structural thickness design guided by the Algerian catalog for the modified and unmodified soil.

It is clear that the thickness of the pavement structure for 8% SRC-stabilized Sebkha soil is notably less than that of naturally compacted Sebkha soil, representing a 30% reduction. This decrease is attributed to the addition of cement, which creates CSH gels. These gels coat and bind the soil particles, increasing the soil's strength and CBR.

Table 4-7. Pavement structure design as per the Algerian catalog

Particulars	Selected sebkha soil mixes			
	Sebkha soil +0%SRC	Sebkha soil+8%SRC		
Soaked CBR	2.14	20		
Category as per the Algerian catalog	RP1, TPL6, S4	RP1, TPL6, S2		
Pavement thickness (cm)	83	58		
Surface course (cm)	$AC^*$ 8	AC 8		
Base course (cm)	AG# 12	AG 12		
Subbase course (cm)	AG 13	AG 13		
Subgrade improved layer (cm)	$UGMs^{\Delta}$ 60	TS <sup>♥</sup> 35		

 $AC^*$ : asphalt concrete;  $AG^{\#}$ : asphalt gravel;  $TS^{\nabla}$ : treated sebkha soil

### 3.3.2. Assessment of raw material and construction costs

The economic cost is one of the main factors that should be calculated when applying road pavement streuture. In this regard, two stages were considered. The raw material stage comprises manufacturing/exploitation and transport, while the construction stage comprises earthwork machines (EWM). It is worth mentioning that there is a thickness difference only on the subgrade improvement layer (60 cm for the unmodified subgrade while 35 cm for the treated subgrade). Thus, the cost analysis is focused on this layer (subgrade improvement layer). The cost of raw materials and the earthmoving machine was calculated using the unit price and features provided by the state consulting company (SETS) and Barbieri et al. 2022. For a 2 x2 roadway, the width

of the subgrade is assumed to be 20 m, and the calculation is performed for a road length of 1 km. From Table 4-8. The cost of raw materials for the SRC-Sebkha soil mixture decreases by a factor of 4.9 compared to the cost of unbonded gravel materials (UGMs). Additionally, the construction costs for the treated subgrade increase by a factor of 1.5 compared to the untreated subgrade. Despite this increase in construction costs, the overall total cost for the treated subgrade is reduced by a factor of 3.8 when compared to the untreated subgrade. This highlights a significant reduction in economic costs due to the addition of cement, demonstrating the economic advantage of using treated Sebkha soils in subgrade pavement.

**Table 4-8.** Raw materials and constructions costs.

Raw materials cost	s				
Raw material	Unit price (EUR/t)	Transport price (EUR/t/h)	Nearest site (h)	Total weight(t/km)	Total cost (EUR/km)
SRC	68	10	2.5	20x0.35x1000	83328
				x1.6 x 0.08= <b>896</b>	
UGMs	6	7.5	1.5	20x0.6x1000x2=	414000
				24000	

		1 •	
Harth	WARZ	machines	COCTC
Laiu	WUIN	macmines	CUSIS

	Untreated subgrade		Treated subgr	ade
Machine	Productivity (m <sup>3</sup> /h)	Unit price (EUR/h)	Productivity (m <sup>3</sup> /h)	Unit price (EUR/h)
Dozer	200	250	/	/
Spreader	/	/	150	250
Mixer	/	/	200	450
Roller	500	200	500	200
Grader	2000	200	2000	200
Total construction cost (EUR/km)	21000		30917	
Overall total cost (EUR/km)	435000		114245	
Overall total cost (DA/km)	65250000		17136750	

# 4.4. Conclusion

In this research, an experimental study was performed to assess how curing time and SRC content affect the mechanical and physicochemical properties of locally high-saline soil. Untreated and CRS-treated chloride-sulfate soil samples experienced tests for UCS, XRD, TGA, FTIR, pH, and CE determination. The study indicates that in addition to cementitious hydration products such as CSH gels, a new hydrate product named Friedel's salt (Fs), consisting of calcium aluminate chloride hydrate, also contributes to the enhancement of soil strength, and thus limits the presence of ettringite hydrate. Based on this analysis, the following conclusion can be drawn:

- (1) Increasing curing time and SRC content stiffens the material and reduces axial strain in stress-strain curves. Untreated Sebkha soil exhibits strain-softening behavior during initial axial loading, indicating a plastic failure mode. With SRC incorporation, strain-softening behavior occurs before the occurrence of peak strength, showing double cone cracks and surface detachment, indicating a more brittle behavior.
- (2) Compared to untreated soil, the UCS increased by 4.18 and 11.56 times by adding 2% and 8% SRC after 14 days of curing. Moreover, the strength loss decreased significantly from 27.14% with 2% SRC to just 3.14% with 8% SRC after 28 days of curing. This indicates that addition of 8% cement significantly reduced the strength loss than 2% cement-treated samples at 28 days curing period. After incorporating 8% of SRC, XRD, and TGA, results showed a decrease in the NaCl phase associated with the formation of a new hydrate (C<sub>3</sub>A. CaCl<sub>2</sub>. 10H<sub>2</sub>O) named Freidel's salt (Fs), as confirmed by the FTIR spectrum. This hydrate can expand 1.8 times, and its formation within the soil matrix leads to a reduction in voids, making the structure denser and increasing the strength of the soil. However, after 28days of curing, there is a slight strength loss of 3.14% due to competition between the CSH gels and Fs phase. The higher pressures exerted by Fs phase compared to the restraining forces (from CSH gels) lead to strength loss.
- (3) pH significantly increases after 3 days of curing due to cement compound dissolution, then slightly decreases over the next 7 days due to hydroxide (OH<sup>-</sup>) ions consumption during the hydration reactions progress. After 14 and 28 days, the pH increases again, which is associated with Fs formation releasing more OH<sup>-</sup> and slightly increasing pH value. The EC decreases significantly up to 7 days of curing due to competition between ion release and consumption in

hydration reactions. However, it slightly increases after 28 days due to Fs precipitation, releasing more OH<sup>-</sup> and Na<sup>+</sup> ions.

(4) Based on the Algerian catalog, the design for the flexible pavement structure resulted in a 30% reduction in total thickness for the modified subgrade compared to the unmodified subgrade. Additionally, the overall total cost for the treated subgrade is reduced by a factor of 3.8 when compared to the untreated subgrade.

This study confirmed that using 8% of SRC is sufficient to stabilize Sebkha soil for use as a foundation for flexible pavement. However, for practical projects, it is important to investigate the long-term effects, including a more extended curing period, due to the complex chemical reactions within the soil matrix. This includes considering the continuous precipitation of Fs over time in the soil fabric. Additionally, assessing the durability of the improved soil under harmful climatic conditions, such as wet-dry cycles, is relevant in these areas and should be taken into account.

# References

- AFNOR, N., 2014. P94-093: Soils: recognition and tests-Determination of the compaction references of material-Normal Proctor test-Modified Proctor test.
- Al-Amoudi, O.S.B., Asi, I.M., EI-Naggar, Z.R., 1995a. Stabilization of an arid, saline sabkha soil using additives. Q. J. Eng. Geol. 28, 369–379.
- Al-Amoudi, O.S.B., Maslehuddin, M., Abdul-Al, Y.A., 1995b. Role of chloride ions on expansion and strength reduction in plain and blended cements in sulfate environments. Constr. Build. Mater. 9, 25–33.
- Aldaood, A., Bouasker, M., Al-Mukhtar, M., 2014. Geotechnical properties of lime-treated gypseous soils. Appl. Clay Sci. 88, 39–48.
- Alger, C., 2001. Catalogue de Dimensionnement des Chaussées neuves. Org. Natl. Contrô Tech. Trav. Publics Algér.
- Babel, M., Schreiber, B.C., 2014. 9.17-Geochemistry of evaporites and evolution of seawater. Treatise Geochem. 483–560.
- Bahmyari, H., Ajdari, M., Vakili, A., Ahmadi, M.H., 2021. The Role of the Cement, Lime, and Natural Pozzolan Stabilizations on the Mechanical Response of a Collapsible Soil. Transp. Infrastruct. Geotechnol. 8, 452–472. https://doi.org/10.1007/s40515-020-00146-3
- Barbieri, D.M., Lou, B., Dyke, R.J., Wang, X., Chen, H., Shu, B., Gazder, U., Horpibulsuk, S., Tingle, J.S., Hoff, I., 2022. Design and sustainability analyses of road base layers stabilized with traditional and nontraditional additives. J. Clean. Prod. 372, 133752. https://doi.org/10.1016/j.jclepro.2022.133752
- Benmebarek, S., Berrabah, F., Benmebarek, N., Belounar, L., 2015. Effect of Geosynthetic on the Performance of Road Embankment over Sabkha Soils in Algeria: Case Study. Int. J. Geosynth. Ground Eng. 1, 35. https://doi.org/10.1007/s40891-015-0040-4
- Birnin-Yauri, U.A., Glasser, F.P., 1998. Friedel's salt, Ca2Al (OH) 6 (Cl, OH) 2H2O: its solid solutions and their role in chloride binding. Cem. Concr. Res. 28, 1713-1723.
- Black, W.P.M., 1962. A Method of Estimating the California Bearing Ratio of Cohesive Soils from Plasticity Data. Géotechnique 12, 271–282. https://doi.org/10.1680/geot.1962.12.4.271
- Black, W.P.M., 1961. The Calculation of Laboratory and In-situ Values of California Bearing Ratio from Bearing Capacity Data. Géotechnique 11, 14–21. https://doi.org/10.1680/geot.1961.11.1.14
- Bouras, F., Al-Mukhtar, M., Tapsoba, N., Belayachi, N., Sabio, S., Beck, K., Martin, M., 2022.
  Geotechnical Behavior and Physico-Chemical Changes of Lime-Treated and Cement-Treated
  Silty Soil. Geotech. Geol. Eng. 40, 2033–2049. https://doi.org/10.1007/s10706-021-02008-2

- Caliendo, C., 2012. Local Calibration and Implementation of the Mechanistic-Empirical Pavement Design Guide for Flexible Pavement Design. J. Transp. Eng. 138, 348–360. https://doi.org/10.1061/(ASCE)TE.1943-5436.0000328
- Calvello, M., Lasco, M., Vassallo, R., Di Maio, C., 2005. Compressibility and residual shear strength of smectitic clays: influence of pore aqueous solutions and organic solvents. Ital. Geotech. J. 1, 34– 46.
- Carteret, R.D., Buzzi, O., Fityus, S., Liu, X., 2014. Effect of Naturally Occurring Salts on Tensile and Shear Strength of Sealed Granular Road Pavements. J. Mater. Civ. Eng. 26, 04014010. https://doi.org/10.1061/(ASCE)MT.1943-5533.0000938
- Chandrasekaran, A., Ravisankar, R., Rajalakshmi, A., Eswaran, P., Vijayagopal, P., Venkatraman, B., 2015. Assessment of natural radioactivity and function of minerals in soils of Yelagiri hills, Tamilnadu, India by Gamma Ray spectroscopic and Fourier Transform Infrared (FTIR) techniques with statistical approach. Spectrochim. Acta. A. Mol. Biomol. Spectrosc. 136, 1734– 1744.
- chaussées (France), L. central des ponts et, France. Service d'études sur les transports, les routes et leurs aménagements, 2000. Traitement des sols à la chaux et-ou aux liants hydrauliques: application à la réalisation des remblais et des couches de forme. Laboratoire central des ponts et chaussées.
- Chen, Q., Xiong, Z., Tao, G., Nimbalkar, S., Wang, C., 2024. Laboratory investigation on static and dynamic properties, durability, and microscopic structure of Nano-SiO2 and polypropylene fiber cemented soil under coupled seawater corrosion and cyclic loading. Constr. Build. Mater. 440, 137449. https://doi.org/10.1016/j.conbuildmat.2024.137449
- Cheng, Y., Li, Z., Huang, X., Bai, X., 2017. Effect of Friedel's salt on strength enhancement of stabilized chloride saline soil. J. Cent. South Univ. 24, 937–946. https://doi.org/10.1007/s11771-017-3496-7
- Chikhaoui, M., Nechnech, A., Hoxha, D., Moussa, K., 2015. Contribution to the Behavior Study and Collapse Risk of Underground Cavities in Highly Saline Geological Formations, in: Lollino, G., Giordan, D., Thuro, K., Carranza-Torres, C., Wu, F., Marinos, P., Delgado, C. (Eds.), Engineering Geology for Society and Territory - Volume 6. Springer International Publishing, Cham, pp. 393– 397. https://doi.org/10.1007/978-3-319-09060-3 68
- Chou, Y., Zhang, P., Yang, W., Zhang, Y., Li, D., 2024. Study on salt-frost heave characteristics, improvement effect, and curing mechanism of loess-like sulphate soil. Cold Reg. Sci. Technol. 104241.

- Demyan, M.S., Rasche, F., Schütt, M., Smirnova, N., Schulz, E., Cadisch, G., 2013. Combining a coupled FTIR-EGA system and in situ DRIFTS for studying soil organic matter in arable soils. Biogeosciences 10, 2897–2913.
- Dingwen, Z., Libin, F., Songyu, L., Yongfeng, D., 2013. Experimental Investigation of Unconfined Compression Strength and Stiffness of Cement Treated Salt-Rich Clay. Mar. Georesources Geotechnol. 31, 360–374. https://doi.org/10.1080/1064119X.2012.690826
- Estabragh, A.R., Soltannajad, K., Javadi, A.A., 2014. Improving piping resistance using randomly distributed fibers. Geotext. Geomembr. 42, 15–24. https://doi.org/10.1016/j.geotexmem.2013.12.005
- Fatah, A., Al-Yaseri, A., Theravalappil, R., Radwan, O.A., Amao, A., Al-Qasim, A.S., 2024. Geochemical reactions and pore structure analysis of anhydrite/gypsum/halite bearing reservoirs relevant to subsurface hydrogen storage in salt caverns. Fuel 371, 131857. https://doi.org/10.1016/j.fuel.2024.131857
- Fattah, M.Y., al-Musawi, H.H.M., Salman, F.A., 2012. Treatment of Collapsibility of Gypseous Soils by Dynamic Compaction. Geotech. Geol. Eng. 30, 1369–1387. https://doi.org/10.1007/s10706-012-9552-z
- Gao, B.-Y., Chu, Y.-B., Yue, Q.-Y., Wang, B.-J., Wang, S.-G., 2005. Characterization and coagulation of a polyaluminum chloride (PAC) coagulant with high Al13 content. J. Environ. Manage. 76, 143– 147.
- Gartner, E.M., Young, J.F., Damidot, D.A., Jawed, I., 2002. Hydration of Portland cement. Struct. Perform. Cem. 2, 57–113.
- Hafhouf, I., Abbeche, K., 2023. Impact of drying-wetting cycles on shear properties, suction, and collapse of sebkha soils. Heliyon 9.
- Hafhouf, I., Bahloul, O., Abbeche, K., 2022. Effects of drying-wetting cycles on the salinity and the mechanical behavior of sebkha soils. A case study from Ain M'Lila, Algeria. Catena 212, 106099.
- Haji, T.R., Mir, B.A., 2023. Effect of nano-gypsum on mechanical properties cement admixed marginal silty soil. Constr. Build. Mater. 408, 133639.
- Hammad, M.A., Mohamedzein, Y., Al-Aghbari, M., 2023. Improving the Properties of Saline Soil Using a Deep Soil Mixing Technique. CivilEng 4, 1052–1070.
- Heurteaux, P., Servant, J., 1979. Transferts et stockage de l'eau et des sels dans le profil pédologique des sols halomorphes camarguais. Rev. DÉcologie 51-91.
- Horpibulsuk, S., Phojan, W., Suddeepong, A., Chinkulkijniwat, A., Liu, M.D., 2012. Strength development in blended cement admixed saline clay. Appl. Clay Sci. 55, 44–52.

- Hossain, K.M.A., Mol, L., 2011. Some engineering properties of stabilized clayey soils incorporating natural pozzolans and industrial wastes. Constr. Build. Mater. 25, 3495–3501.
- Jefferson, I., Rogers, C., Evstatiev, D., Karastanev, D., 2005. Treatment of metastable loess soils: Lessons from Eastern Europe, in: Elsevier Geo-Engineering Book Series. Elsevier, pp. 723–762.
- Jiang, Y., Dai, H., Fisonga, M., Li, C., Hong, Z., Xia, C., Deng, Y., 2024. Feasibility and mechanism of high alumina cement-modified chlorine saline soil as subgrade material. Constr. Build. Mater. 429, 136411.
- Kalipcilar, I., Mardani-Aghabaglou, A., Sezer, A., Altun, S., Inan Sezer, G., 2018. Sustainability of cement-stabilised clay: sulfate resistance. Proc. Inst. Civ. Eng. - Eng. Sustain. 171, 254–274. https://doi.org/10.1680/jensu.16.00005
- Kalipcilar, İ., Mardani-Aghabaglou, A., Sezer, G.İ., Altun, S., Sezer, A., 2016. Assessment of the effect of sulfate attack on cement stabilized montmorillonite. Geomech. Eng. 10, 807–826.
- Laboratory (US), R.S., 1954. Diagnosis and improvement of saline and alkali soils. US Department of Agriculture.
- Li, S., Zhang, C., Zhang, T., Li, W., Jia, P., 2023. Experimental study on the strength, collapsibility, and microstructure of cement and micro-silica-stabilized saline soil under freeze-thaw cycles. Case Stud. Constr. Mater. 19, e02518. https://doi.org/10.1016/j.cscm.2023.e02518
- Liu, J., Zha, F., Xu, L., Yang, C., Chu, C., Tan, X., 2018. Effect of chloride attack on strength and leaching properties of solidified/stabilized heavy metal contaminated soils. Eng. Geol. 246, 28– 35.
- Loyer, J.-Y., 1991. Classification des sols salés: les sols Salic. Cah. ORSTOM Sér. Pédologie 51-61.
- Lv, Q., Jiang, L., Ma, B., Zhao, B., Huo, Z., 2018. A study on the effect of the salt content on the solidification of sulfate saline soil solidified with an alkali-activated geopolymer. Constr. Build. Mater. 176, 68–74.
- Mimboe, A.G., Abo, M.T., Djobo, J.N.Y., Tome, S., Kaze, R.C., Deutou, J.G.N., 2020. Lateritic soil based-compressed earth bricks stabilized with phosphate binder. J. Build. Eng. 31, 101465.
- Moayed, R.Z., Izadi, E., Heidari, S., 2012. Stabilization of saline silty sand using lime and micro silica. J. Cent. South Univ. 19, 3006–3011. https://doi.org/10.1007/s11771-012-1370-1
- Nan, J., Liu, J., Chang, D., Li, X., 2022. Mechanical characteristics and microstructure study of saline soil stabilized by quicklime after curing and freeze-thaw cycle. Cold Reg. Sci. Technol. 201, 103625.
- NF P94-077, 1997. Uniaxial compressive test. AFNOR., n.d.
- Pansu, M., Gautheyrou, J., 2006. Handbook of Soil Analysis. Springer Berlin Heidelberg, Berlin, Heidelberg. https://doi.org/10.1007/978-3-540-31211-6

- Pei, W., Shouxi, C., 2011. Laboratory and in-situ tests on solidified saline soils for highway fillings. 工程 地质学报 19, 440-446.
- Pereira, P., Pais, J., 2017. Main flexible pavement and mix design methods in Europe and challenges for the development of an European method. J. Traffic Transp. Eng. Engl. Ed. 4, 316–346.
- Rahimi, M.Z., Zhao, R., Sadozai, S., Zhu, F., Ji, N., Xu, L., 2023. Research on the influence of curing strategies on the compressive strength and hardening behaviour of concrete prepared with Ordinary Portland Cement. Case Stud. Constr. Mater. 18, e02045. https://doi.org/10.1016/j.cscm.2023.e02045
- Razeghi, H.R., Ghadir, P., Javadi, A.A., 2022. Mechanical strength of saline sandy soils stabilized with alkali-activated cements. Sustainability 14, 13669.
- Rhoades, J.D., 1982. Soluble Salts, in: Page, A.L. (Ed.), Agronomy Monographs. Wiley, pp. 167–179. https://doi.org/10.2134/agronmonogr9.2.2ed.c10
- Rica, H.C., Saussaye, L., Boutouil, M., Leleyter, L., Baraud, F., 2016. Stabilization of a silty soil: Effects of disruptive salts. Eng. Geol. 208, 191–197. https://doi.org/10.1016/j.enggeo.2016.04.032
- Rouchy, J.-M., Blanc-Valleron, M.-M., 2006. Les évaporites: matériaux singuliers, milieux extrèmes. Vuibert-SGF.
- Saussaye, L., Cuadrado Rica, H., Boutouil, M., Baraud, F., Leleyter, L., 2020. Influence of salt-forming anions on the geotechnical properties of a soil stabilised with hydraulic binders: effect of cation type. Road Mater. Pavement Des. 21, 1439–1453. https://doi.org/10.1080/14680629.2018.1553729
- Shi, Z., Geiker, M.R., Lothenbach, B., De Weerdt, K., Garzón, S.F., Enemark-Rasmussen, K., Skibsted, J., 2017. Friedel's salt profiles from thermogravimetric analysis and thermodynamic modelling of Portland cement-based mortars exposed to sodium chloride solution. Cem. Concr. Compos. 78, 73-83.
- Shuja, D., Rollakanti, C., Poloju, K., Joe, A., 2022. An experimental investigation on -stabilization of sabkha soils with cement and Cement Kiln Dust (CKD) in Sultanate of Oman. Mater. Today Proc. 65. https://doi.org/10.1016/j.matpr.2022.04.127
- Tumwiine, H., Aziz, M., Ali, U., Al-Amoudi, O.S., Saleem, M.A., Zami, M.S., Mazher, K.M., Hanif, A., 2024. Pore fluid salinity effects on post-stabilization performance of cement-treated Marl. Case Stud. Constr. Mater. 20, e03193.
- Uzielli, M., Lacasse, S., Nadim, F., Phoon, K.K., 2007. Soil variability analysis for geotechnical practice. Characterisation Eng. Prop. Nat. Soils 3, 1653–1752.

- Wan, X., Ding, J., Mou, C., Gao, M., Jiao, N., 2024. Role of Bayer red mud and phosphogypsum in cement-stabilized dredged soil with different water and cement contents. Constr. Build. Mater. 418, 135396. https://doi.org/10.1016/j.conbuildmat.2024.135396
- Wei, L., Chai, S., Guo, Q., Wang, P., Li, F., 2020. Mechanical properties and stabilizing mechanism of stabilized saline soils with four stabilizers. Bull. Eng. Geol. Environ. 79, 5341–5354. https://doi.org/10.1007/s10064-020-01885-w
- Xing, H., Yang, X., Xu, C., Ye, G., 2009. Strength characteristics and mechanisms of salt-rich soil cement. Eng. Geol. 103, 33–38.
- Xing, Z., Du, C., Shen, Y., Ma, F., Zhou, J., 2021. A method combining FTIR-ATR and Raman spectroscopy to determine soil organic matter: Improvement of prediction accuracy using competitive adaptive reweighted sampling (CARS). Comput. Electron. Agric. 191, 106549.
- Yang, B., Qin, Z., Zhou, Q., Li, H., Li, L., Yang, X., 2020. Pavement damage behaviour of urban roads in seasonally frozen saline ground regions. Cold Reg. Sci. Technol. 174, 103035.
- Ying, Z., Cui, Y.-J., Duc, M., Benahmed, N., 2022. Effect of salt solution on the optimum lime contents of bentonite and silt. Acta Geotech. 17, 3731–3745. https://doi.org/10.1007/s11440-022-01488-7
- Yue, Y., Wang, J.J., Basheer, P.M., Bai, Y., 2018. Raman spectroscopic investigation of Friedel's salt. Cem. Concr. Compos. 86, 306–314.
- Zhang, D., Cao, Z., Fan, L., Liu, S., Liu, W., 2014a. Evaluation of the influence of salt concentration on cement stabilized clay by electrical resistivity measurement method. Eng. Geol. 170, 80–88.
- Zhang, D., Cao, Z., Fan, L., Liu, S., Liu, W., 2014b. Evaluation of the influence of salt concentration on cement stabilized clay by electrical resistivity measurement method. Eng. Geol. 170, 80–88. https://doi.org/10.1016/j.enggeo.2013.12.010
- Zhang, P.C., Dong, Z.X., 2003. Damage mechanism of Dunhuang civil airport foundation and management measures. Hydrogeol Eng Geol 3, 78–80.
- Zhang, S., Yang, X., Xie, S., Yin, P., 2020. Experimental study on improving the engineering properties of coarse grain sulphate saline soils with inorganic materials. Cold Reg. Sci. Technol. 170, 102909.
- Zhao, X., Shen, A., Guo, Y., Li, P., Lv, Z., 2017. Pavement mechanic response of sulfate saline soil subgrade section based on fluid-structure interaction model. Int. J. Pavement Res. Technol. 10, 497–506.
- Zhou, S., Li, J., Rong, L., Xiao, J., Liu, Y., Duan, Y., Chu, L., Li, Q., Yang, L., 2021. Immobilization of uranium soils with alkali-activated coal gangue-based geopolymer. J. Radioanal. Nucl. Chem. 329, 1155–1166. https://doi.org/10.1007/s10967-021-07812-x
- Zibara, H., 2001. Binding of external chlorides by cement pastes (PhD Thesis).

# **General conclusion**

This study first investigated the effectiveness of lime treatment on Ain M'lila Sebkha soil at three salinity levels, investigating the physic-chemical and mechanical properties over different curing times. Subsequently, the study investigated the potential stabilization of Sebkha soil with sulphate-resistant cement (SRC) for use as a flexible pavement subgrade. Physical, mechanical, chemical and mineralogical analyses including UCS, granulometry, carbonation, X-ray diffraction (XRD), thermogravimetric analysis (TGA) and fourier transform infrared spectroscopy (FTIR) tests were carried out. The following conclusions can be made:

- (1) Geotechnical, chemical, and mineralogical characterization revealed that Ain M'lila Sebkha soil exhibits high salinity with an electrical conductivity of 23.2 dS/m. The soil's ionic composition is predominantly characterized by Cl<sup>-</sup> and SO<sub>4</sub><sup>2-</sup> ions, classifying it as a neutral chloride-sulfate soil, with halite (NaCl) and gypsum (CaSO<sub>4</sub>·2H<sub>2</sub>O) as the primary salt minerals contributing to its salinity. Based on the Casagrande diagram and technical road guide (GTR) classification, the soil is classified as less plastic clay and type A2 (fine clayey sands, silts), respectively.
- (2) Variations in salinity significantly influenced the soil's particle size distribution, particularly in the silt range. The reduction in salinity from ECe3 (23.2 dS/m) to ECe1 (2.32 dS/m) resulted in an 18% increase in fine particles below 20 μm diameter, with ECe1 and ECe3 soils containing 56% and 38% fine particles, respectively. This inverse relationship between salinity and fine particle content is attributed to the disappearance of NaCl and reduction in CaSO<sub>4</sub>·2H<sub>2</sub>O content in ECe1 soil. In ECe3 soil, these mineral phases create binding bridges between particles, promoting cementation and formation of larger agglomerates, thereby reducing the proportion of finer particles.
- (3) Salinity exhibited opposing effects on CaCO<sub>3</sub> precipitation between untreated and treated soils. In untreated soil, increasing salinity reduced CaCO<sub>3</sub> content, particularly in ECe3 soil where abundant CaSO<sub>4</sub>.2H<sub>2</sub>O caused Ca<sup>2+</sup> ions to bind preferentially with SO<sub>4</sub><sup>2-</sup> rather than form CaCO<sub>3</sub>. Conversely, treated ECe3 soil showed enhanced CaCO<sub>3</sub> precipitation compared to ECe2 and ECe1 soils, attributed to the reaction between HCO<sup>3-</sup>, Ca<sup>2+</sup>, and OH<sup>-</sup> ions.
- (4) Salinity demonstrated a negative impact on the unconfined compressive strength (UCS) of both untreated and lime-treated samples. Thermogravimetric analysis (TGA) revealed higher portlandite content in ECe1 soil compared to ECe3 soil, despite ECe3 containing more lime. This inverse relationship between salinity and portlandite formation, even with higher lime content in ECe3 soil, confirms the detrimental effect of soluble salts on the strength development of lime-treated Ain M'lila Sebkha soil.

- (5) Sebkha soil treatment with sulfate-resistant cement (SRC) significantly enhanced its unconfined compressive strength (UCS), showing 4.18 and 11.56-fold increases with 2% and 8% SRC addition respectively after 14 days of curing. XRD, TGA, and FTIR analyses of 8% SRC-treated soil revealed a reduction in NaCl phase accompanied by the formation of Friedel's salt (Fs), a hydrate capable of 1.8 times expansion. This Fs formation densified the soil matrix by filling voids, thereby increasing strength. However, extended curing to 28 days resulted in a minor strength reduction of 3.14%, attributed to the competition between CSH gels and Fs phase, where the expansive pressure from Fs exceeded the restraining forces of CSH gels
- (6) The use of SRC-stabilized Sebkha soil as subgrade reduced both pavement thickness by 30% and overall costs by 3.8 times compared to untreated soil, demonstrating its economic viability for pavement construction.